Neue Ansätze zur Produktion Kollagen-basierter Biomaterialien

DISSERTATION

zur Erlangung des akademischen Grades eines
Doktors der Naturwissenschaften (Dr. rer. nat.)
in der Bayreuther Graduiertenschule für Mathematik und
Naturwissenschaften (BayNAT)
der Universität Bayreuth

vorgelegt von

Adrian V. Golser
aus Salzburg
Bayreuth, 2019

Mit tiefstem Dank an all jene,
die mir während dieses prägenden Lebensabschnittes
zur Seite gestanden sind.

Die vorliegende Arbeit wurde in der Zeit von September 2009 bis April 2018 in Bayreuth am Lehrstuhl Biomaterialien unter Betreuung von Herrn Professor Dr. Thomas Scheibel angefertigt.

Vollständiger Abdruck der von der Bayreuther Graduiertenschule für Mathematik und Naturwissenschaften (BayNAT) der Universität Bayreuth genehmigten Dissertation zur Erlangung des akademischen Grades einer Doktorin/ eines Doktors der Naturwissenschaften (Dr. rer. nat.).

Dissertation eingereicht am:	22.02.2019
Zulassung durch das Leitungsgremium:	27.02.2019
Wissenschaftliches Kolloquium:	29.07.2019

Amtierender Direktor: Prof. Dr. Dirk Schüler

Prüfungsausschuss:

Prof. Dr. Thomas Scheibel	(Gutachter/in)
Prof. Dr. Stephan Schwarzinger	(Gutachter/in)
Prof. Dr. Andreas Möglich	(Vorsitz)
PD. Dr. Ralf Braun	

1 Kurzzusammenfassung

Kollagen ist ein zentraler Bestandteil der extrazellulären Matrix und damit eines der am häufigsten vorkommenden Proteine im Tierreich, welches somit maßgeblich für die Struktur, Form und Mechanik des darauf basierenden Gewebes verantwortlich ist.

Die biomedizinische Verwendbarkeit von Kollagen wurde bereits früh erkannt, nachdem festgestellt wurde, dass sich gereinigte Kollagenfasern, die aus der Submucosa des Dünndarms von Tieren gewonnen wurden, als resorbierbares Nahtmaterial eignen, welches seither als *Catgut* bekannt ist. Trotz möglicher unerwünschter Nebenreaktionen, wie z.B. der Möglichkeit einer allergischen Reaktion auf derartige Xenotransplantate, wird Kollagen heutzutage in vielfältige Morphologien prozessiert und findet besonders als Barriere- und Füllsubstanz bei der Geweberekonstruktion Verwendung als Biomaterial.

Natürliches Kollagen ist eine hierarchisch assemblierte Struktur, die in ihrer Proteinsequenz klar definiert ist: Da sich Kollagen aus drei α-Ketten in eine schlanke, rechtsdrehende Tripelhelix faltet, bestehen sterische Einschränkungen, die dazu führen, dass an jeder dritten Position der α-Kette nur Glycin als Aminosäure in Frage kommt. Das führt dazu, dass Kollagen-codierende Gene oft anhand der repetitiven Konsensussequenz $(Gly\text{-}X\text{-}Y)_n$ erkannt werden können.

Tierische Kollagene zeichnen sich außerdem dadurch aus, dass die Positionen X und Y des Konsensusmotivs oft mit Prolin bzw. Hydroxyprolin besetzt sind, da diese Aminosäuren durch die Ausbildung von intermolekularen Wasserstoffbrücken und die energetisch im Gegensatz zu anderen Aminosäuren günstigere trans-Konfirmation einen stabilisierenden Effekt auf die Tripelhelix ausüben. Die gezielte Hydroxylierung von Prolin zu 4-Hydroxyprolin und der damit verbundene Stabilitätsgewinn führen im Umkehrschluss dazu, dass nicht korrekt hydroxyliertes Kollagen oftmals eine verhältnismäßig instabile Faltung aufweist, welche die Verwendung von solchen inkorrekt prozessierten Proteinen als Biomaterial einschränkt.

Zusätzlich zu der enzymatisch katalysierten Prolin-Hydroxylierung finden während der Synthese von fibrillärem Kollagen außerdem weitere posttranslationale Prozessierungsschritte statt, während derer die Grundlage für die weitere Assemblierung der einzelnen Tropokollagenmoleküle in Kollagenfibrillen bis hin zu ganzen Kollagenfaserbündeln geschaffen wird. Trotz der einfachen Primärstruktur handelt es sich bei tierischem Kollagen also um eine hochkomplexe, hierarchische Struktur, welche nicht ohne weiteres *in vitro* nachgebaut werden kann. Vereinfacht wäre die Struktur-Funktionsanalyse durch ausreichende Mengen nicht prozessierten Kollagens, welches aber nur mittels rekombinanter Techniken bereit gestellt werden kann. Bislang konnte jedoch trotz zahlreicher Bemühungen zur Herstellung von geeigneten Expressionssystemen auf Basis von Bakterien und Hefen biotechnologisch Kollagen nur durch die Kultivierung von Fibroblasten produziert werden.

Im Zuge dieser Arbeit wurde deshalb versucht, den Anspruch eines rekombinanten Kollagens an das Expressionssystem besonders in Hinsicht auf die Notwendigkeit von Sekundärmodifikationen zu verringern. Als ein möglicher Kandidat in diesem Zusammenhang wurde das Muschelbyssuskollagen preColD gewählt und erfolgreich in *P. pastoris* produziert.

Bei preColD handelt es sich um einen zentrales Strukturprotein des Muschelbyssusfadens, welches mitunter für dessen ausgezeichnete mechanische Eigenschaften verantwortlich ist. Zusätzlich zu einer zentralen Kollagendomäne enthält preColD Alanin-reiche, flankierende Domänen, die während der Assemblierung des Proteins β-kristalline Strukturen ausbilden, sowie Histidin-reiche Termini, die im natürlichen Faden zusätzlich DOPA enthalten, welches Metallkomplexierung und Adhäsion vermittelt. Obwohl das natürliche preColD während der Biosynthese sowohl in der Kollagendomäne Hydroxyprolin und in den terminalen Domänen DOPA als posttranslationale Modifikation enthält, konnte das Protein rekombinant ohne diese Sekundärmodifikationen produziert werden und selbst aus dem vollständig denaturierten Zustand in Fibrillen assemblieren, sowie seidenähnliche, β-kristalline Strukturen in entsprechenden Domänen ausbilden.

Es konnte gezeigt werden, dass die Selbstassemblierung von preColD möglich ist, da flankierende Domänen vorhanden sind, die die Entstehung von Gelatine-artigen Netzwerken verhindern, indem sie eine Erstassemblierung ermöglichen, die als Keim für die Ausbildung einer korrekt gefalteten Kollagen-Tripelhelix dient.

Diese Beobachtung konnte im Zuge einer zweiten Arbeit bestätigt werden, in der ein synthetisches $(GPP)_{50}$-Polymer in *E. coli* rekombinant produziert wurde. Das so genannte eCol wurde am Aminoterminus mit einem redox-schaltbaren Foldon versehen, welches unter oxidierenden Bedingungen Cystin-Brücken ausbildet und damit zur Oligomerisierung der gelösten Monomere führt.

Im Zuge von Schmelzpunktbestimmungen wurde der Einfluss der Foldon-Domäne auf das Assemblierungsverhalten der eCol-Konstrukte unterschiedlicher Länge untersucht und dabei festgestellt, dass eine derartige Domäne ausreichend ist, um eine Assemblierung von tripelhelikalem Kollagen unter physiologischen Bedingungen zu ermöglichen. Weiterhin wurde beobachtet, dass das gezeigte $(GPP)_n$-basierte Polymer überraschend stabil ist und auch ohne das Vorhandensein von Hydroxyprolin Schmelzpunkte weit jenseits derer von natürlichem Kollagen aufweist.

Außerdem konnte gezeigt werden, dass die Cytokompatibilität von eCol dahingehend gewährleistet ist, dass es im nativen Zustand keinerlei Interaktion mit Zelloberflächenrezeptoren wie z.B. Integrin zeigt und damit eine aus biologischer Sicht inerte Oberfläche bietet, an welche mehrere untersuchte Zelllinien nicht adhärierten. Wurde das langkettige eCol als Matrix für kurzkettige $(GPP)_n$-Peptide genutzt, welche zusätzlich spezifische Adhäsionsmotive tragen, fand daran die Zelladhäsion statt.

Es konnte also gezeigt werden, dass es durch rationales Design möglich ist, rekombinant produzierbare, kollagenartige Proteine herzustellen, die die Möglichkeit zur schaltbaren Selbstassemblierung besitzen und zusätzlich dazu genutzt werden können, gewünschte Funktionalitäten gezielt in das Protein einzubringen, wodurch rekombinante Kollagene in Zukunft gute Kandidaten für Anwendungen als Biomaterial sind.

2 Short summary

Collagen is an important constituent of the extracellular matrix and therefore one of the most abundant proteins in the animal kingdom. It is largely responsible for the shape, structure and mechanical properties of the tissues it helps to form.

The possible biomedical applications of collagen have been known since ancient times, with the most prominent example being absorbable suture materials called catgut, which is made from the cut and purified submucosa of sheep intestine. Even though there is a chance for unwanted immune reactions to such xenotransplants, such as allergic responses, collagen-based biomaterials for medical use have since been processed into a variety of morphologies and are currently most prominently applied as a barrier or filler material during reconstructive surgery.

Natural collagen is a hierarchical structure with a well-defined protein consensus sequence: Since collagen folds by assembling three α-chains into a slim, right-handed triple-helix, some steric hindrances arise, allowing only glycine on every third position within the α-chain. As a result, this often allows collagen-encoding genes to be identified solely by their repetitive $(Gly\text{-}X\text{-}Y)_n$ consensus sequence.

Additionally, in animal collagen, the positions X and Y of this consensus sequence are often populated by proline and 4-hydroxyproline, respectively, because these amino acids allow the formation of intermolecular hydrogen bonds and, due to their statistically higher abundance of the trans-conformation, provide an energetic benefit and hence stabilizing effect to the triple helix. Conversely, this means that when the stabilizing properties of hyrdoxyproline are missing due to improper hydroxylation, the resulting collagen will be more easily unfolded and degraded, which reduces the applicability of such a biomaterial.

In addition to the enzymatically catalyzed proline hydroxylation, additional post-translational processing steps take place during the biosynthesis of fibrillar collagen, during which the basis for the assembly of the single tropocollagen molecules into collagen fibrils and even fibers is established.

Consequently, even though the repetitive primary sequence might appear simple, animal collagen is a highly complex, hierarchical structure that cannot be easily replicated *in vitro*.

In order to analyze the structure-function-relationship of these proteins, sufficiently large quantities of unprocessed collagen are required, which can only be provided with recombinant expression systems. Even though several attempts have been made to find such systems utilizing bacteria and yeast, the only currently viable, biotechnological strategy for the production of collagen is the cultivation of fibroblasts.

One of the goals of this thesis was therefore to reduce the requirements of the recombinant collagen towards the expression host, especially with regards to the necessity of secondary modifications. One candidate to fulfill this prerequisite was found with the mussel byssus protein preColD, which could be successfully produced in the yeast *P. pastoris*.

preColD is a major structural protein within the byssus thread and strongly impacts the overall mechanical performance of this tough fiber. In addition to a central collagen-like core domain, preColD contains alanin-rich flanking domains that form silk-like β-sheet rich crystals during the fiber assembly, as well as histidine-rich terminal domains that, in the natural byssus, also contain DOPA. Both of these amino acids can form metal ion complexes, which mediate intermolecular adhesion and provide a mechanism for a remarkable form of energy dissipation and subsequent self-healing. Although the natural preCol proteins contain secondary modifications such as hydroxyproline within the collagen domain, as well as DOPA within the terminal domains, this protein could be successfully produced recombinantly without these posttranslational modifications, and still has the ability to correctly form both fibrillar and silk-like crystalline structures from unfolded monomers.

It could be shown that the self-assembly of preColD was possible because of the presence of flanking domains that assembled before the collagen-like domain and thereby provided a nucleation site for the growth of single, correctly folded collagen triple-helix instead of an unstructured gelatin-like network.

The same observation could be made when a synthetic $(GPP)_{50}$-polymer was expressed in *E. coli*. The amino-terminus of this so called eCol protein was fitted with redox-switchable foldon domain that, under oxidizing conditions, would form cystein bridges between other eCol-monomers and thereby lead to the formation of oligomers.

The influence of this foldon domain on the folding and assembly properties was investigated during melting-point determination experiments for eCol-constructs of varying lengths. It was found that the domain was sufficient to promote the formation of collagen-like secondary structures under physiological conditions. Furthermore, it could be shown that even without hydroxylation, $(GPP)_n$-based polymers are remarkably stable and, depending on their length, can have melting points far beyond those of natural collagen.

Furthermore, it could be shown that eCols are cytocompatible in that they do not show interaction with cell surface proteins such as integrins in their native state, thereby offering an inert surface that does not show adhesion for several tested cell types. However, when using a long-chain eCol as a matrix for short $(GPP)_n$-peptides, specific functionalities such as adhesion motifs can be integrated into the structure and in the case of RGD-motifs, cell adhesion could be observed.

In conclusion, this thesis shows that with rational design, it is possible to recombinantly produce collagen like proteins that contain features which allow a switchable self-assembly and furthermore possess the ability to quickly integrate specific functional groups, which should allow these recombinant collagens to be promising candidates for future biomaterials based thereon.

3 Inhaltsverzeichnis

4 Einleitung

Bei Kollagen handelt es sich um eines der mengenmäßig am häufigsten vorkommenden Proteine im Tierreich [1]. Bereits einfache mehrzellige Organismen wie z.B. Schwämme und Nesseltierchen nutzen Varianten von Kollagen, um daraus ihre extrazelluläre Matrix aufzubauen, deren mechanische Eigenschaften zu prägen und eine kompatible Umgebung für die Zellen des jeweiligen Gewebes zu schaffen [2].

Zusätzlich zu eukaryontischem Kollagen sind auch manche Prokaryoten in der Lage Proteine herzustellen, die eine Kollagen-typische, tripelhelikale Faltung annehmen, welche nach der Verankerung in der Zellwand des Bakteriums dazu dienen, es im Gewebe zu adhärieren und vor der Immunantwort des Wirts zu schützen [3]. Bei bakteriellem Kollagen handelt es sich deshalb in erster Linie um einen Virulenzfaktor und weniger um ein Strukturprotein [4].

Besonders in Hinblick auf biomedizinische Anwendungen sind fibrilläre Formen von Kollagen seit langem ein attraktives Material, da es durch seine klar definierte molekulare Struktur, seine morphologische Variabilität und sein beinahe ubiquitäres Vorkommen auch über Speziesgrenzen hinweg Anwendungsmöglichkeiten bietet [5].

Die ersten resorbierbaren Nahtmaterialien wurden beispielsweise aus dem gereinigten Dünndarm von Schafen gefertigt („*Catgut*“) und sind seit jeher neben der Seide von *B. mori* in diesem Zusammenhang eines der bekanntesten proteinergen Biomaterialien, welches zur Zeit jedoch aufgrund seiner schwachen mechanischen Festigkeit nur für die Vereinigung von weichem Gewebe verwendet werden kann [6], [7].

Neue Verfahren zur Prozessierung von gelöstem Kollagen, darunter insbesondere der Einsatz von Mikrofluidik-basierten Nassspinnverfahren [8], führte in den letzten Jahren zu mechanisch leistungsfähigeren Kollagenfasern, die der Festigkeit von Sehnen gleichen und demnach für die Herstellung und Reparatur von Biomaterialien mit ähnlichen Charakteristika geeignet sein sollten.

Im Zuge der plastischen und rekonstruktiven Chirurgie sind seit den 80er Jahren des letzten Jahrhunderts nicht-fibrilläre, gereinigte Präparationen von Typ 1 Kollagen aus Rinderhaut (z.B. Zyderm® und Zyplast®) als Implantate und Füllstoffe verfügbar, welche jedoch in bis zu 5% aller Patienten aufgrund von allergischen Reaktionen nicht verwendet werden können und in manchen Fällen trotz nicht bestehender Allergie nach der Implantation verzögert Immunreaktionen und Kreuzreaktionen zu anderen Kollagenen hervorrufen können [9], [10]. Aus diesen Gründen wurden die genannten Produkte in den letzten Jahren zunehmend von Produkten auf Basis von anderen Polymeren, wie z.B. Hyaluronsäure, und biotechnologisch produziertem, humanen Kollagen (z.B. Cosmoderm® und Cosmoplast®) verdrängt [11].

Durch die Entwicklung neuer Technologien, wie der eben genannten biotechnologischen Proteinproduktion, Gen- und Festphasenproteinsynthese sowie biomimetischer Prozessierung steht seit einigen Jahren der Weg hin zu neuen Kollagenen und kollagenmimetischen Produkten offen, welche in Zukunft die Möglichkeit bieten werden, die soeben beispielhaft genannten Probleme zu umgehen [12], [13].

Diese Arbeit setzt sich aus mehreren Teilarbeiten zusammen, welche die momentane Rolle von Kollagen als Biomaterial diskutieren und die Möglichkeit der Produktion von Kollagen-ähnlichen Proteinen unterschiedlicher Herkunft demonstrieren, die Ansätze zur Lösung der genannten Probleme bieten können.

4.1 Die molekulare Struktur und Assemblierung von Kollagen

Bei fibrillärem Kollagen, welches den Hauptanteil der extrazellulären Matrix ausmacht und besonders von den Typen I, II, III, V und XI vertreten wird [14], handelt es sich um hierarchisch aufgebaute Strukturen, deren Primärsequenz bereits zur korrekten Identifikation als Kollagen dienen kann. Fibrilläre Kollagene durchlaufen im Zuge ihrer Assemblierung jedoch mehrere Schritte, um ihre endgültige Struktur und mechanischen Eigenschaften auszubilden.

Die grundlegende Eigenschaft aller Kollagene ist die Faltung in Form in einer rechtshändigen Tripelhelix, bestehend aus drei linkshändigen α-Proteinketten, welche einen geringen Durchmesser von 1,6 nm aufweist und etwa alle drei Aminosäuren eine Windung vollendet (s. Abb. 1). Als Folge dieser räumlichen Vorgabe ist es nötig, dass alle Aminosäuren, deren Seitenketten die Ausbildung der Helix aus sterischen Gründen stören würden, durch Glycin ersetzt wurden, was zu einer repetitiven Konsensussequenz mit dem Motiv $(Gly\text{-}X\text{-}Y)_n$ führt [15].

Die Positionen X und Y des Konsensusmotivs werden in typischem Tierkollagen oft von Prolin (X) und 4-Hydroxyprolin (Y) besetzt, da für diese Aminosäuren die für die Tripelhelix nötige trans-Konformation energetisch günstiger ist als für andere Aminosäuren [16], [17]. Außerdem können diese Aminosäuren, besonders Hydroxyprolin in der Y-Position, die Stabilität und damit den Schmelzpunkt der Tripelhelix durch die Ausbildung von intermolekularen Wasserstoffbrücken erhöhen [18].

Da die genannte cis-trans-Isomerisierung von Prolin bei der Ausbildung der Kollagen-Helix den zentralen ratenlimitierenden Schritt darstellt, ist es zur korrekten Faltung von Tropokollagen aus den α-Ketten nötig, dass eine gezielte Nukleation der zukünftigen Helix stattfindet [19], weil es ansonsten durch die spontane Ausbildung von zufällig verteilten, tripelhelikalen Abschnitten zwischen den einzelnen Monomeren zum Entstehen von gelatineartigen Netzwerken kommt. Aus diesem Grund nutzen beinahe alle Kollagene spezielle Trimerisierungsdomänen (s. Abb. 2), welche die Faltung von Prokollagen aus den monomeren α-Ketten begünstigen [20]. Erst nach der proteolytischen Spaltung dieser Domänen handelt es sich um Tropokollagen, welches durch weitere Selbstassemblierung zur Bildung von Kollagenfibrillen in der Lage ist.

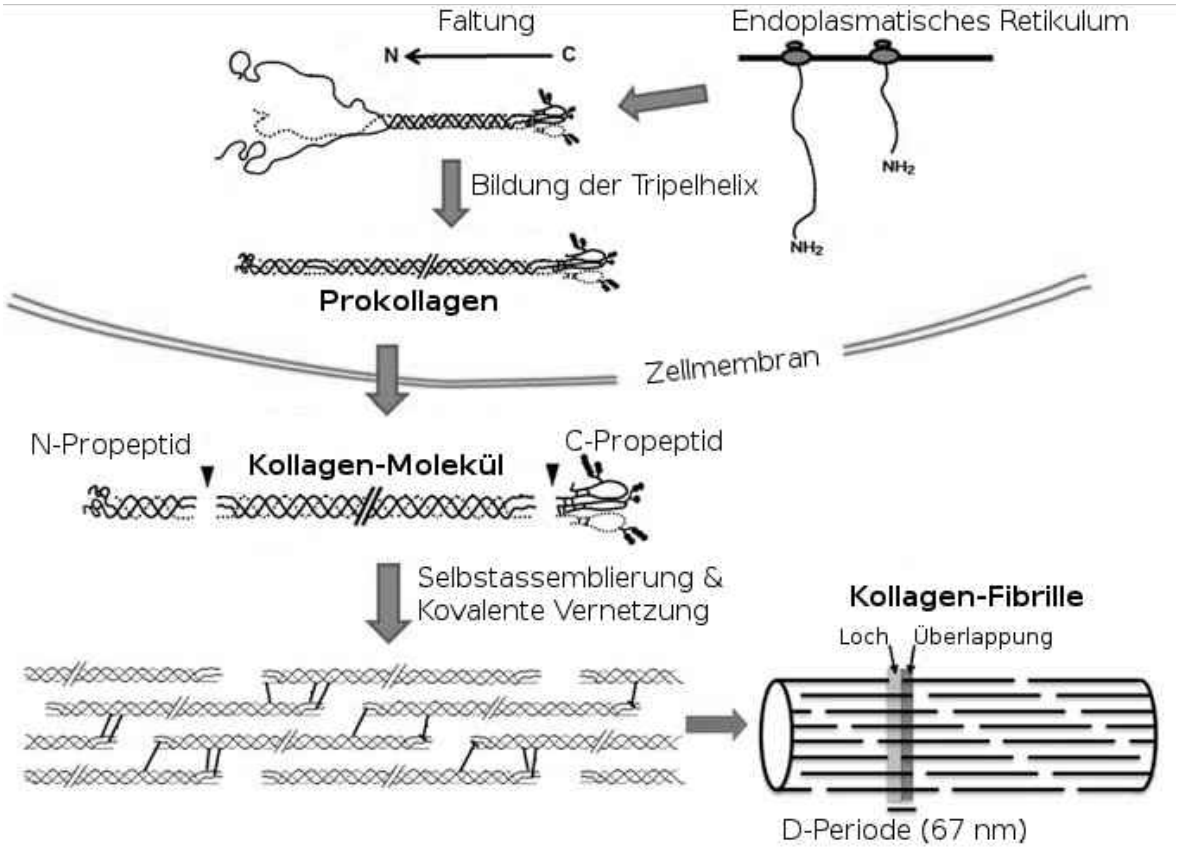

Abbildung 1: Die löslichen α-Ketten werden im Endoplasmatischen Retikulum (ER) posttranslationalen Modifikationen unterzogen und falten dann, induziert durch die Nukleation ausgehend von einer Trimerisierungsdomäne, in ein tripelhelikales Prokollagen. Im Zuge weiterer Prozessierung kommt es während oder kurz nach der Sekretion zu einer proteolytischen Spaltung der terminalen Propeptide und damit zur Bildung von Tropokollagen. Je nach Kollagentyp findet nun im Extrazellulären Raum eine weitere Assemblierung (hier: Fibrillisierung) statt, welche mit zunehmender Alterung des Kollagens durch die Knüpfung von kovalenten Bindungen stabilisiert wird. Modifiziert nach [21] mit Erlaubnis des Verlags (© The Authors Journal compilation © 2012 Biochemical Society).

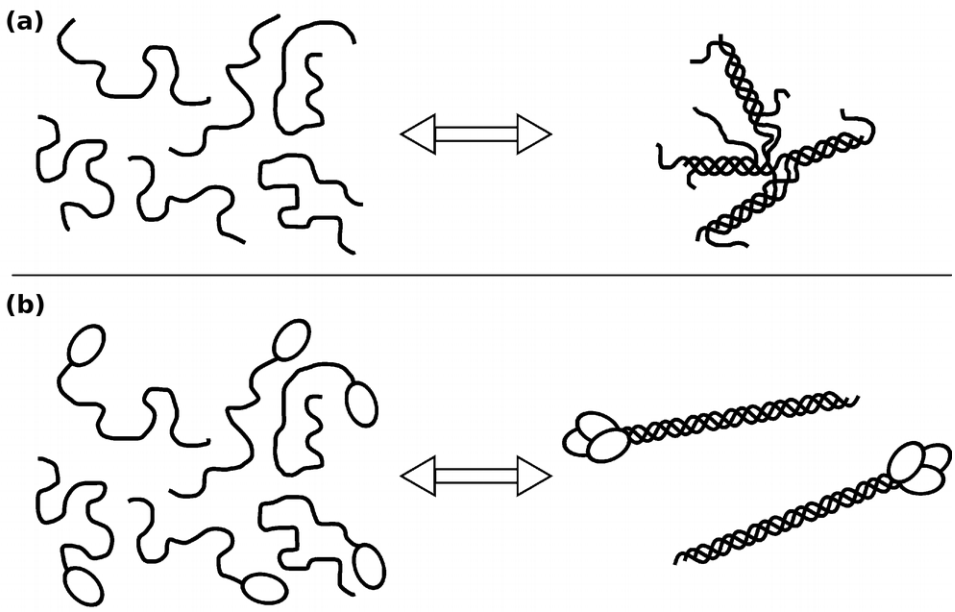

Abbildung 2: Beispielhafte Darstellung der Funktion von Trimerisierungsdomänen während der Faltung von Kollagen: **(a)** Geschmolzenes Kollagen ohne Trimerisierungsdomäne bildet bei der Assembrierung aus ungefalteten Monomeren eine quervernetzte, Gelatine-artige Struktur aus. **(b)** Ist eine Trimerisierungsdomäne vorhanden, welche vor der Ausbildung der Helix assembliert, dann dient diese Struktur als Keim für die Faltung von klar definiertem Prokollagen. Übernommen aus [20] mit Erlaubnis des Verlags (© Elsevier Ltd.).

4.2 Fibrilläre Kollagene in der extrazellulären Matrix

Die extrazelluläre Matrix (ECM) füllt im Wesentlichen den extrazellulären Raum eines Gewebes aus und ist somit maßgeblich für dessen biochemische und physikalische Eigenschaften verantwortlich. Die typischen Hauptkomponenten der ECM sind Polysaccharide (Glucosaminoglycan, Hyaluronsäure), Proteine (Kollagen, Elastin, Keratin) und Glycoproteine (Proteoglycan, Fibronectin), welche untereinander vernetzt sind [22], [23].

Der Übergang zwischen Protein, Glycoprotein und Proteoglycan ist abhängig vom Grad und Art der Glycosylierung fließend, sodass die Einteilung der ECM-Komponenten in diese Klassen hauptsächlich historisch begründet ist (s. Tab. 1).

Während die ECM in erster Näherung in manchen Geweben als simple Gerüststruktur für die Verankerung der darin enthaltenen Zellen verstanden werden kann, sind besonders mechanisch stark belastete Gewebe wie Haut, Sehnen und Knochen vorwiegend von den mechanischen Eigenschaften der zugrundeliegenden Polymere geprägt. Fibrilläres Kollagen ist in diesem Zusammenhang besonders wichtig, da es spontan zur Ausbildung von stabilen Fibrillen aus einzelnen Tropokollagen-Tripelhelices in der Lage ist, welche weiterhin zu mechanisch belastbaren makroskopischen Fasern assemblieren können und demnach diese Rolle im Körper vorwiegend übernehmen [24].

Zellen interagieren mittels verschiedener Oberflächenrezeptoren, insbesondere Integrin, mit den unterschiedlichen Bestandteilen der ECM und können sich so einerseits mechanisch verankern, als auch andererseits die über diese Membranproteine transduzierten Signale zur Regulation des eigenen Stoffwechsels nutzen, um z.B. Differenzierung, Migration, Apoptose oder Auf- und Abbau der ECM einzuleiten [25], [26].

Da es sich bei der ECM also nicht um ein inertes, statisches Gebilde handelt, welches lediglich die darin beherbergten Zellen fixiert, sondern alle Bestandteile miteinander interagieren und einem ständigen Umbau unterlegen sind, ist es unter diesem Gesichtspunkt sinnvoll, bei der Manipulation von bestehenden Geweben im Zuge von medizinischen Behandlungen die Kompatibilität zu der bereits vorhandenen ECM als wichtiges Merkmal des dazu verwendeten Biomaterials in Betracht zu ziehen.

Fibrilläres Kollagen, insbesondere das beinahe ubiquitär vorkommende Typ I Kollagen, sind aus diesem Grund für die meisten Anwendungen ein gut geeignetes Biomaterial, besonders dann, wenn im Zuge von regenerativer Medizin eine hohe Kompatibilität zu bestehenden ECMs und deren darin residierenden Zellen gewünscht ist [27].

Tabelle 1: Bestandteile der extrazellulären Matrix

Stoffklasse	Familie	Bemerkung	
Protein	**Kollagen**	Zahlreiche Varianten, je nach Typ Homo- und Heterotrimere möglich. Hauptprotein der extrazellulären Matrix. Typenspezifische Interaktion mit anderen Bestandteilen der ECM und Zellrezeptoren.	Fibrillär (Typ I, II, III, V, XI)
			Fibrillenassoziiert (Typ IX, XII, XIV)
			Netzbildend (Typ IV, VIII, X)
			Andere
	Elastin	Elastischer, weniger fest als Kollagen. Hauptbestandteil von weichen Geweben, insb. Blutgefäße, Lunge, Haut.	
	Keratin	Als Bestandteil von Keratinozyten; Heterodimer; stark über Disulfide quervernetzt.	
Glycoprotein	**Fibronectin**	Cystein-verknüpftes Dimer. Zahlreiche Funktionen, darunter Quervernetzung von anderen Matrix-Bestandteilen, Interaktion mit Signalrezeptoren, Wundheilung.	
	Laminin	Heterotrimer, 15 bekannte Klassen. Hauptbestandteil der Basallamina. Bildet zusammen mit Typ IV-Kollagen ein Vlies aus vernetzten Fibrillen.	
Proteoglycan	**Heparan-sulfat**	Strukturell verwandt mit Heparin. Langkettiges, unverzweigtes Poly-Disaccharid, häufigste Untereinheiten: Glucuronsäure und N-Acetylglucosamin bzw. deren Sulfate. Interagiert mit Integrinen, Perlecan, Agrin, Kollagen XVIII.	
	Chondroitin-sulfat	Unverzweigtes Poly-Disaccharid (N-Acetylgalactosamin und Glucuronsäure bzw. Sulfate). Wichtiger Bestandteil von Knorpeln.	
	Dermatan-sulfat	Poly-Disaccharid, Bestandteil von Haut, Blutgefäßen, Lunge, Sehnen.	
	Keratan-sulfat	Poly-Disaccharid. Bestandteil von Cornea, Knorpel, Sehnen und Knochen.	
Glucosamino-glykan	**Hyaluronsäure**	Polysaccharid aus Glucuronsäure und N-Acetyl-Glucosamin. Nicht sulfatiert und nicht an Protein gebunden. Generelle Funktion als „Schmierstoff“, zusätzlich zahlreiche Aufgaben während Zellmigration, Wundheilung, Regulation von Entzündung.	

4.3 Limitationen von Kollagen als Biomaterial

Biomaterialien sind Materialien, die für einen medizinischen Zweck mit einem Organismus interagieren und sich dabei durch hohe Biokompatibilität auszeichnen. Das bedeutet, dass das Material weder toxisch noch immunogen sein darf und sich in seinen weiteren Eigenschaften dahingehend auszeichnet, dass es eine spezifische Aufgabe mit einer angemessenen Wirtsantwort erfüllt.

Die genannte Definition von Biokompatibilität nach Williams [28] ist besonders realitätsnah, da sie die geforderte Funktionalität des Biomaterials als Kompromiss den möglicherweise unerwünschten Reaktionen des Wirts gegenüberstellt. Somit sind auch körperfremde Materialien wie z.B. Titan für gewisse Aufgaben der Definition nach biokompatibel, nämlich dann, wenn die (mechanischen) Anforderungen nur durch solche Stoffe erfüllt werden können. Als Umkehrschluss dessen wird außerdem klar, warum Kollagen-basierte Materialien trotz ihrer Rolle als zentraler Bestandteil der ECM und der damit gegebenen Cytokompatibilität nicht in weitaus höherem Ausmaß zur Anwendung kommen:

Die heutzutage verwendeten, medizinischen Produkte, welche aus extrahierten und gereinigten Kollagenen hergestellt werden, beschränken sich größtenteils auf Filme und sonstige Barrieren, Schwämme, Füllstoffe, Gele und Nanopartikel, welche sich allesamt nicht durch hohe mechanische Festigkeit auszeichnen [29]. Trotz der nachweislich hohen mechanischen Leistungsfähigkeit von vielmals stark belasteten, kollagenbasierten Strukturen im Körper, wie z.B. Knochen, Haut und Sehnen [30], ist es heutzutage nicht möglich, diese Eigenschaften mit den derzeit üblichen Verarbeitungsmethoden *ex vivo* im kommerziellen Maßstab zu reproduzieren.

Ein weiterer Nachteil von Kollagen ist die potentielle Immunogenität, die, wie bereits zuvor erwähnt, bei der Verwendung von xenogenen Transplantaten auftreten kann und somit die Biokompatibilität von tierischem Kollagen generell in Frage stellt. Vor der Anwendung von bovinem Kollagen ist es z.B. üblich, einen Allergietest auf das Material durchzuführen, der in etwa 5% aller Fälle positiv ausfällt [11].

Da allogene Kollagenquellen nur begrenzt verfügbar sind, ist die biotechnologische Produktion von humanidentischem Kollagen oder hypoimmunogenen Mimetika deshalb ein zentraler Punkt der derzeitigen Kollagenforschung – der momentane Stand der Technik bedient sich hier der Kultivierung von humanen Fibroblasten, welche mit vergleichsweise hohen Kosten verbunden ist. Auch pflanzlich produzierte, rekombinante Kollagene sind bereits kommerziell verfügbar, jedoch ist es auch hier nicht möglich, fibrilläre Formen mit hoher mechanischer Festigkeit zu produzieren.

Zusammenfassend lässt sich deshalb sagen, dass die derzeitig verfügbaren, Kollagen-basierten Biomaterialien teuer, nicht ausreichend biokompatibel und/oder mechanisch schwach sind, und dass neue Wege zur Eliminierung dieser Nachteile erstrebenswert sind.

4.4 Muschelbyssuskollagene

Der Byssus z.B. einer Miesmuschel (*Mytilus galloprovincialis*) ist eine aus zahlreichen Fasern bestehende Haltestruktur, mit der sich der Organismus am Untergrund fixiert (s. Abb. 3). Da Miesmuscheln die Gezeitenzone besiedeln, muss der Byssus starken Strömungen und unterschiedlichen chemischen Bedingungen auf längere Zeit standhalten können.

Am proximalen, d.h. dem muschelseitigen Ende entspring ein Byssusfaden dem Byssusstamm, welcher wiederum über einen Retraktormuskel mit dem Schalengelenk und dem Muschelfuß verbunden ist. Am distalen Ende des Fadens geht dieser in einen zementartigen Plaque über, welcher mittels spezieller Klebeproteine die Haftung an den jeweiligen Untergrund vermittelt [31].

Weil es sich bei dieser Haltestruktur und dem damit verbundenen Untergrund um mechanisch und chemisch stark unterschiedliche Stoffe handelt ist es wichtig, dass das Elastizitätsmodul des Fadens dem des damit verbundenen Materials entspricht, da es sonst bei der Deformation in Folge von mechanischer Belastung zu Brüchen zwischen diesen Übergängen kommen kann [32]. Da die Muschel aus verhältnismäßig weichem Gewebe besteht (E = 10 – 50 MPa), sich jedoch mit harten Untergründen (E = 500 MPa – 50 GPa) verbinden muss, wurde das Problem der radialen Belastung bei derartigen Übergängen evolutionär dahingehend gelöst, dass der Faden einen mechanischen Gradienten aufweist: der distale Bereich des Fadens, welcher mit der harten Haftstruktur interagiert, ist bedeutend steifer und zugfester als der proximale Teil, der hingegen elastischer und dehnbarer ist und dem E-Modul des Molluskengewebes ähnelt (s. Abb. 3).

Auf molekularer Ebene besteht der gut untersuchte Byssus der *Mytilidae* aus einer amorphen, proteinbasierten Matrix, in die kollagenartige Fibrillen eingebettet sind, die zusätzlich zu einer zentralen Kollagendomäne auch weitere Funktionalitäten besitzen, welche die mechanischen Eigenschaften der Faser ebenfalls prägen (s. Abb. 4) [33]:

Das im proximalen Byssusfaden vorrangig vorkommende preColP enthält Elastin-ähnliche Domänen, welche diesem Abschnitt des Fadens eine hohe Elastizität verleihen [34]. Im Zuge eines Proteingradienten, welcher makroskopisch als

morphologische und mechanische Varianz im Faden beobachtet werden kann, nimmt der Gehalt an preColP zugunsten eines höheren Anteils an preColD im distalen Bereich der Faser ab.

preColD, welches, anstelle der elastinähnlichen Domänen von preColP, Alanin-reiche, seidenähnliche Domänen besitzt, verleiht dem Byssusfaden im distalen Bereich eine bedeutend höhere Steifigkeit und Zugfestigkeit, was es dem Faden erlaubt, hohe Mengen an mechanischer Energie umzusetzen, bevor der Byssus und die daran befestigte Muschel Schaden nehmen [35].

preColNG, das Strukturmotive enthält, die denen von Pflanzenzellwandproteinen ähneln, ist im Byssus mit beinahe konstanter Verteilung zu finden und übernimmt die Rolle eines „Mediators“ zwischen den anderen Muschelbyssuskollagenen [36].

Neben den elastin- und seidenähnlichen Domänen besitzen alle preCols außerdem terminale Domänen, die einen hohen Anteil an Histidin, sowie durch enzymatisch katalysierte Oxidation von Tyrosin gewonnenes DOPA (3,4-Dihydroxyphenylalanin) aufweisen [37], [38]. Diese Aminosäuren komplexieren Metallionen und sind so in der Lage, sowohl die Ende-zu-Ende-Assemblierung der preCol-Fibrillen, als auch die intermolekulare Interaktion mit Matrixproteinen und die Adhäsion an verschiedene Oberflächen zu vermitteln.

Da die genannten Domänen nicht wie bei anderen Kollagenen proteolytisch vor der Sekretion aus der produzierenden Zelle gespalten werden, ist außerdem davon auszugehen, dass sie vor der Trimerisierung der Kollagen-Domäne eine Rolle als Nukleationskeim spielen und demnach an der Bildung von korrekt gefalteten Homotrimeren beteiligt sind [39].

Abbildung 3: (links) Der Byssus einer mediterranen Miesmuschel (*Mytilus galloprovincialis*) ist nach dem Ablösen der Muschel vom Untergrund als Bündel von ca. 50 Fäden erkennbar. Durch das Schließen der Schale ist hauptsächlich der mechanisch belastbarere, distale Teil des Byssusfadens exponiert. **(rechts)** Um der mechanischen Belastung durch die Gezeiten zu widerstehen, muss die Muschel das weiche Muskelgewebe mit dem harten Untergrund verbinden. Damit dies möglich ist, nimmt die Steifigkeit des Byssus im distalen Bereich um bis zu eine Größenordnung zu. Auf molekularer Ebene lässt sich diese Eigenschaft durch einen Konzentrationsgradienten von preColP hin zu preColD und eine Verringerung des Anteils an Matrixproteinen erklären. Modifiziert nach [40] mit Erlaubnis des Verlags (© Taylor & Francis).

Eine sowohl aus mechanischer als auch chemischer Hinsicht beachtliche Besonderheit der His/DOPA-Domänen und der von ihnen gebildeten Metallkomplexe ist außerdem die Eigenschaft, auf molekularer Ebene als nichtkovalente Sollbruchstellen zu fungieren, welche sich beim Überschreiten der entsprechenden Dehnungsgrenze reversibel öffnen, bevor eine Entfaltung der anderen Domänen des preCol-Proteins stattfindet. Aus makroskopischer Sicht äußert sich dieser Mechanismus als eine Form der Selbstheilung [41]:

Wenn der Faden im distalen Bereich über seine Dehnungsgrenze hinaus beansprucht wurde, ist innerhalb von wenigen Minuten eine Rückbildung des ursprünglichen Zug-/Dehnungsverhaltens zu beobachten, bis hin zu der kompletten Wiederherstellung der Dämpfungseigenschaft des Byssusfadens, ohne dass dazu eine metabolisch aufwändige Reparatur nötig ist.

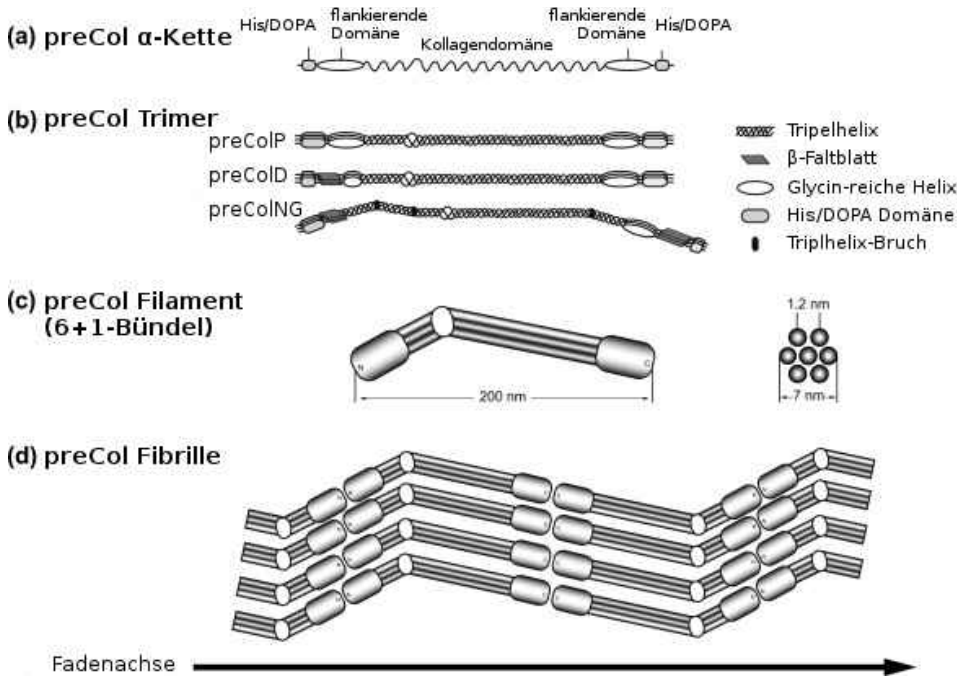

Abbildung 4: Der hierarchische Aufbau von preCols im Byssusfaden beginnt mit der Faltung von Kollagen-Homotrimeren und führt über die Bildung von Filament-Bündeln im Zuge einer Ende-an-Ende-Assemblierung zu Nanofibrillen, welche in die amorphe Matrix des Byssusfadens eingebettet sind. Modifiziert nach [42] mit Erlaubnis des Verlags (© Elsevier Ltd.).

Aus Sicht des rationalen Proteindesigns bieten die preCol-Proteine eine ausgezeichnete Grundlage für die Produktion von Kollagen-Mimetika, da der blockweise Aufbau der preCols es erlaubt, gezielt verschiedene Funktionalitäten einzubringen und bestehende Sequenzen so zu modifizieren, dass diese die gewünschten Eigenschaften aufweisen bzw. unerwünschte Charakteristika verlieren [43].

Außerdem besitzen die preCols im Gegensatz zu den Kollagenen der ECM die Eigenschaft, auch nach vollständiger Denaturierung unter geeigneten Bedingungen alle Schritte der in Abbildung 4 gezeigten Assemblierung zu durchlaufen und Fasern mit zum natürlichen Byssus vergleichbaren mechanischen Eigenschaften zu bilden. Damit sind preCols und preCol-basierte Proteine gute Kandidaten für die Herstellung von mechanisch hoch belastbaren und dennoch biokompatiblen Biomaterialien, die mittels einfacher Methoden versponnen werden können.

4.5 preColD: Seide, Kollagen oder beides?

Im Zuge dieser Arbeit wurde besonders das Hauptkollagen des distalen Muschelbyssus genauer betrachtet. Da dieses Protein etwa 90% des Gesamtproteins im distalen Bereich des Byssusfadens ausmacht [44], muss davon ausgegangen werden, dass die mechanischen Eigenschaften des distalen Muschelbyssus größtenteils von preColD geprägt werden.

preColD besitzt, wie die anderen Muschelbyssuskollagene auch, klar voneinander abgrenzbare Domänen und kann in seiner assemblierten Form (s. Abb. 4) als Block-Copolymer verstanden werden. Die Alanin-reichen, flankierenden Domänen wurden bereits in Abschnitt 4.4 erwähnt, jedoch ist nicht klar, ob es sich bei preColD um ein Kollagen mit seidenähnlichen Eigenschaften, oder um eine seidenähnliche Struktur mit kollagenartigen Domänen handelt.

Seiden, darunter auch die mechanisch äußerst belastbaren Spinnenseiden, zeichnen sich dadurch aus, dass sie kristalline Domänen in einer amorphen Matrix einbetten und damit ein partikelverstärktes Kompositmaterial ausbilden. Bei den genannten Partikeln handelt es sich um Kristalle aus Alanin-reichen β-Faltblättern, die während des Spinnprozesses durch Scherkräfte in der Spinndrüse ausgerichtet werden und deren korrekte Orientierung einen großen Einfluss auf die Mechanik des Fadens haben [45]. Unter Anbetracht des Aufbaus von Seiden kann deshalb auch preColD als eine Seidenart verstanden werden, da gezeigt werden konnte, dass auch hier orientierte β-Faltblätter vorhanden sind, die bereits bei geringer Deformation des natürlichen Byssus lasttragend sind und somit die mechanischen Eingenschaften des Fadens prägen [35].

Der zentrale Unterschied zwischen Seidenproteinen und Byssuskollagenen ist jedoch die Eigenschaft, dass Byssusproteine dazu in der Lage sind, ohne einen genau kontrollierten Spinnprozess aus vollständig gelösten Vorläufern fibrilläre Strukturen und sogar Fasern zu bilden [39].

Diese Charakteristik beruht auf der Eigenschaft der zentralen Kollagendomäne, bereits im frühen Stadium der Assemblierung von preCols eine axiale Orientierung zu ermöglichen, wodurch im weiteren Verlauf eine Selbstassemblierung ähnlich der von fibrillärem Typ I Kollagen stattfindet.

Da die dargestellte Selbstassemblierung eine zentrale Eigenschaft von fibrillärem Kollagen ist, wird preColD deshalb in dieser Arbeit als Kollagen betrachtet, wobei nicht auszuschließen ist, dass die seidenähnliche Domäne unter bestimmten Bedingungen einen größeren Einfluss auf die Gesamtfaltung des Proteins hat als die Kollagen-artige Domäne.

4.6 Biotechnologische Produktion von Kollagen und Kollagenmimetika

Obwohl bereits gezeigt werden konnte, dass die biotechnologische Produktion von humanem Kollagen die zuvor genannten Probleme der Immunogenität von tierischen Kollagenprodukten umgehen kann, wird nach wie vor ein Großteil des heutzutage verwendeten Kollagens aus tierischem Gewebe gewonnen [46].

Hierbei kommen unterschiedliche Extraktionsmethoden zum Einsatz, bei denen, je nach Bedarf die Ausbeute, die Homogenität und der Grad an Denaturierung des Endmaterials gegeneinander abgewogen werden. Sofern kein lösliches Kollagen benötigt wird bzw. die Struktur eines Gewebes erhalten werden soll, wie es z.B. bei der Herstellung von *scaffolds* der Fall ist, wird in der Regel eine schonende Dezellularisierung durchgeführt, die die bestehende Kollagenstruktur und deren Quervernetzungen weitestgehend intakt lässt [47].

Zur Gewinnung von löslichem Kollagen werden hingegen zum einen verdünnte organische Säuren eingesetzt, welche sehr geringe Ausbeuten liefern, oder zum anderen mittels Pepsin oder weiteren Proteasen der Abbau von nicht-tripelhelikalen, quervernetzten Domänen induziert, was zwar die Ausbeute erhöht, aber gleichzeitig die Funktionalität dieser Bereiche zerstört [48].

Der Grund für den Mangel an Alternativen war für lange Zeit der mit entsprechenden hohen Kosten verbundene Aufwand der Kultivierung von humanen Fibroblasten, was wiederum nötig ist, da einfacher zu handhabende Expressionssysteme typischerweise nicht das notwendige enzymatische Repertoire zur korrekten Prozessierung von Kollagen während der Biosynthese besitzen.

Auch in letzter Zeit etablierte und bereits kommerziell verfügbare, pflanzenbasierte Expressionssysteme für humanidentisches Kollagen leiden unter der schweren Handhabbarkeit von Tropokollagen im Downstream-Prozess, was die Reinigung des Proteins erschwert (s. Tab. 2).

Neben der bereits in Abbildung 1 skizzierten Faltung, Sekretion und Proteolyse unter Zuhilfenahme von spezifischen Chaperonen und Proteasen ist vor allem die korrekte Hydroxylierung von Prolin durch die Prolyl-4-Hydroxylase (P4H) ein zentraler Schritt der Kollagensynthese, da ein zu geringer Anteil an 4-Hydroxyprolin die Stabilität der Kollagen-Tripelhelix bis hin zum kompletten Verlust der Faltung unter physiologischen Bedingungen verringert [49].

Da es sich bei der P4H um einen ER-ständigen und vergleichsweise großen $\alpha_2\beta_2$-Komplex handelt, ist die Koexpression in geeigneten Expressionswirten wie *P. pastoris* [50], [51] oder *E. coli*-Stämmen mit oxidierendem Cytosol (z.B. Origami) zwar möglich, führt jedoch aufgrund der geringen Löslichkeit des Tetramers letztendlich oftmals nicht zu dem gewünschten Grad an Hydroxylierung und damit geringen Ausbeuten und inhomogenem Produkt [52].

Als weitere Hindernisse bei der rekombinanten Produktion von Kollagen seien außerdem die hohen Molekulargewichte der monomeren α-Ketten von 100-200 kDa zu nennen, sowie die oftmals vorhandene Notwendigkeit der Ausbildung von Heterotrimeren, die Limitationen beim *downstream-processing* hinsichtlich der Verwendbarkeit von Denaturierungsmitteln (die Tripelhelix darf nicht zerstört werden) und die Notwendigkeit von weiteren Sekundärmodifikationen, wie z.B. Lysin-Oxidation und Glycosylierung.

Obwohl es mehreren Gruppen bereits gelungen ist, ein oder mehrere der genannten Hindernisse zu überwinden, ist bislang keine Methode bekannt, mit der humanidentisches Kollagen mittels rekombinanter Proteinsynthese in Bakterien- oder Hefesystemen im Fermentermaßstab hergestellt werden kann.

Tabelle 2: Beispiele für biotechnologisch produzierte Kollagene

	Epressionssystem	**Besonderheit**	**Nachteile**
Humanes Typ I Kollagen [11]	Fibroblasten-Zellkultur	Humanidentisch	Benötigt stetige Quelle junger, humaner Fibroblasten für jede neue Charge; teuer; Nur Typ I Kollagen
Rekombinantes humanes Kollagen bzw. Prokollagen	Säugetierzellen (kommerzieller Anbieter) [53]	Rekombinante Volllängen-α-Ketten der Gene COL1A1, COL2A1, COL3A1	Teures Expressionssystem; Inhomogenes Endprodukt (Telopeptide teilw. gespalten)
	Pichia Pastoris [54]	Koexpression von P4H ermöglicht Hydroxylierung	Niedrige Ausbeuten; keine vollständige Hydroxylierung
	S. cerevisiae [55]		
	Pflanzen (Tabak, Mais, Gerste) [56]		Etablierung des Expressionssystems langwierig; Aufwändige Reinigung
Kurzkettige Human-basierte „*collagen-like*“ Sequenzen (hydroxyliert) [52]	*E. coli*	Koexpression von P4H; fibrillär, hydroxyliert	Größenlimitierung des Expressionssystems
Kurzkettige Human-basierte Sequenzen (keine posttr. Modifikation) [57]		Hohe Ausbeuten, homogenes Endprodukt	Instabil, nicht als Biomaterial geeignet
Kurzkettige Fragmente voll- bzw. teilsynthetische Sequenzen	Peptidsynthese [12], [58]–[60]	Zahlreiche Ansätze Vollständige Flexibilität bez. Sequenz und nicht-kanonischer Aminosäuren	Stark größenlimitiert (30-50 Aminosäuren)
Tierische Kollagene	*E. coli* (Pflanzenwespen-seide) [61]	Nativ kein Hydroxyprolin Hohe Ausbeuten	nicht-humane Sequenz, Biokompatibilität nicht etabliert *in vitro* Assemblierung nicht etabliert
	P. pastoris (Muschelbyssus-kollagen) [62]	Hydroxylierung möglich (noch nicht etabliert) Nach Optimierung hohe Ausbeuten möglich	nicht-humane Sequenz, Biokompatibilität nicht etabliert
Bakterielle Kollagene [63]	*E. coli*	Von *S. pyogenes* abgeleitet Hohe Ausbeuten Keine Sekundär-modifikation nötig	Nicht fibrillär Möglicherweise immunogen
Synthetische Kollagene [64]	*E. coli* (Engineered Collagen)	Synthetische Sequenz Biokompatibel Hohe Ausbeuten Keine Sekundär-modifikation nötig	Trimerisierungsdomäne für Fibrillisierung nötig

4.7 Zielsetzung der Arbeit

Kollagenähnliche Biomaterialen der Zukunft sollen mechanisch eine Festigkeit vergleichbar mit der von Sehnen aufweisen und damit den möglichen Einsatzbereich von Kollagen als Biomaterial vergrößern, dabei keine Immunogenität besitzen und mit hoher Ausbeute in skalierbaren Fermentationsprozessen kostengünstig produzierbar sein.

Aufgrund der einzigartigen Eigenschaften von Muschelbyssuskollagen, *in vitro* aus vollständig entfalteten preCols tripelhelikale, fibrilläre Strukturen auszubilden, ohne dabei gelatinöse Netzwerke zu formen, wurde im Zuge dieser Arbeit versucht, das Byssuskollagen preColD rekombinant herzustellen und daraus biokompatible Materialen zu gewinnen.

Zusätzlich zu der eben genannten Herangehensweise wurden außerdem Bemühungen unternommen, synthetische Kollagenmimetika, sogenannte eCols, zu designen und rekombinant zu produzieren. Hierbei wurde davon ausgegangen, dass die Fähigkeit von gelösten α-Kollagenen, im Zuge der Synthese von fibrillärem Kollagen Tropokollagen zu bilden und dabei gleichzeitig eine ungezielte Quervernetzung zu vermeiden, größtenteils davon abhängig zu sein scheint, dass eine gezielte Nukleation durch eine Trimerisierungsdomäne eingeleitet wird, welche die Bildung von einzelnen Kollagen-Trimeren kinetisch begünstigt, nicht jedoch die Entstehung von quervernetzten Gelatine-ähnlichen Strukturen.

Außerdem wurde, basierend auf Beobachtungen anderer Gruppen, die mit synthetischen $(GPP)_n$-Peptiden gemacht wurden, angenommen, dass die Schmelztemperatur von Kollagenmimetika mit großem Prolin-Anteil auch ohne das Vorhandensein von nicht-kanonischen Aminosäuren, wie z.B. Hydroxyprolin, hoch genug sein kann, um unter physiologischen Bedingungen stabil gefaltet zu bleiben. Diese Hypothese schien naheliegend, da diese Eigenschaft auch bei bakteriellen Kollagenen beobachtet werden kann, welche ebenfalls kein Hydroxyprolin besitzen.

5 Synopsis

Bei den hier präsentierten Teilarbeiten handelt es sich um Publikationen, in welchen die Möglichkeit der rekombinante Produktion von verschiedenen kollagenartigen Proteinen demonstriert wird.

Die zugrundeliegende Problematik der Gewinnung von mechanisch leistungsfähigen und dennoch biokompatiblen Materialien auf Kollagenbasis wurde bereits in der Einleitung behandelt und wird im Zuge einer Übersichtsarbeit (Teilarbeit Kapitel 11) vertieft behandelt, welche außerdem die zuvor publizierte Primärliteratur sowie den momentanen Stand der Forschung in Kontext setzt.

5.1 Biotechnologische Produktion des Muschelbyssuskollagens preColD

Teilarbeit 1: s. Kapitel 9 und Ref. [62]

preColD ist ein homotrimeres, kollagenbasiertes Strukturprotein, das im mechanisch stark beanspruchten distalen Teil des Muschelbyssus bis zu 90% des Gewichtsanteils des Fadens ausmacht. Es ist somit naheliegend, dass preColD maßgeblich für die hohe Festigkeit des Byssus verantwortlich ist.

Durch den blockweisen Aufbau von preColD können verschiedene Attribute des Proteins den einzelnen Domänen zugeschrieben werden: Die zentrale Kollagendomäne sorgt dafür, dass das Protein Fibrillen bilden kann, welche sich im Byssusfaden axial in Zugrichtung anordnen (s. Abb. 4). Die terminalen, His-DOPA-reichen Domänen sorgen über die darin gebildeten Metallkomplexe für die intermolekulare Verknüpfung der einzelnen Fibrillen und dienen bei Überschreiten der elastischen Zugphase des Byssusfadens als selbsheilende, energieabsorbierende mechanische Dämpfer.

Die Alanin-reichen *flanks* ähneln in ihrer Primärstruktur der von Seidenprotein und bilden im Zuge der Faltung des Proteins β-kristalline Strukturen aus, die dazu führen, dass der preColD-reiche Abschnitt des Byssusfadens sich wie ein partikelverstärktes, fibrilläres Kompositmaterial verhält.

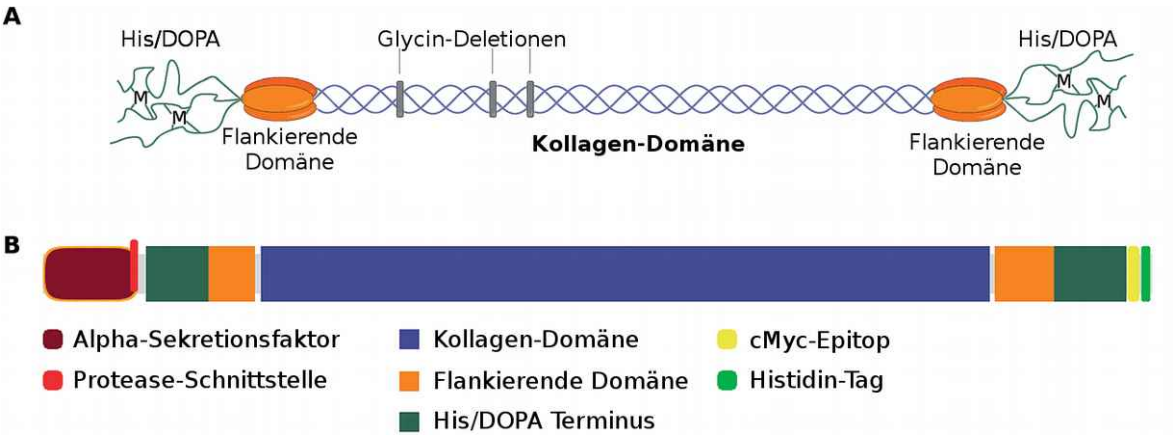

Abbildung 5: (A) Schematischer Aufbau eines trimeren preColD und das Blockdiagramm **(B)** des rekombinanten Proteins, wie es in *P. pastoris* hergestellt wurde. Der α-Sekretionsfaktor wird nach der Translokation in das ER proteolytisch abgespalten. Modifiziert aus [62] mit Erlaubnis des Verlags (© The Royal Chemical Society of Chemistry).

Im Zuge der Teilarbeit wurde preColD in der Hefe *Pichia pastoris* hergestellt. Auf die Koexpression von P4H und Tyrosinase wurde verzichtet, da in entsprechenden Vorversuchen nur unbefriedigende Resultate erzielt werden konnten, sodass das rekombinante Protein keine Sekundärmodifikationen aufweist. Trotz des Vorhandenseins eines α-Sekretionsfaktors wurde bei der Fermentation keine erfolgreiche Sekretion beobachtet, sodass davon ausgegangen werden muss, dass das Protein im ER aggregiert oder durch andere Mechanismen von dem Weitertransport in den sekretorischen Golgi-Apparat der Hefezelle abgehalten wird. Die Reinigung des Proteins erfolgte deshalb aus dem Zellpellet mittels Nickel-Affinitätschromatographie unter denaturierenden Bedingungen.

Das so gewonnene Protein wurde unter verschiedenen Bedingungen zur Aufklärung der Sekundärstruktur sowohl mittels Zirkulardichroismus- (CD) als auch Fouriertransformierter Infrarotspektroskopie (FTIR) untersucht. Dabei konnte festgestellt werden, dass die Alanin-reichen *flanks* besonders in Lösung einen großen Einfluss auf die mittels CD messbare Sekundärstruktur des Proteins haben und äußerst stabil gefaltet zu sein scheinen, da selbst unter denaturierenden Bedingungen in 4 M Harnstoff noch starke β-Faltblatt-Anteile in den jeweiligen Spektren zu beobachten sind (s. Fig. 2, Teilarbeit 1). Wird das Denaturierungsmittel in Lösung entfernt, scheint sich das CD-Spektrum zusätzlich mit dem Signal einer Kollagen-Tripelhelix zu überlagern.

Wird das Protein in Ameisensäure gelöst und aus dieser Lösung durch Abdampfen des Lösungsmittels ein Film hergestellt, bilden sich unmittelbar nach der Trocknung β-kristalline Strukturen, die zusammen mit unstrukturierten Bereichen des Proteins ein Mischsignal in der Amid-I-Bande des FTIR-Spektrums erkennen lassen. Das CD-Spektrum des so hergestellten Films ist vergleichbar mit dem von preColD in 4 M Harnstoff, was nahelegt, dass sich die kristallinen Strukturen innerhalb von kurzer Zeit während der Trocknung aus Ameisensäure formen, während hingegen die Ausbildung der Kollagenhelix zu langsam verläuft, als dass sie in diesem kurzen Zeitraum stattfinden kann.

Wird eine niedrig konzentrierte Lösung von preColD mittels Gelfiltrationschromatographie in einen nicht-denaturierenden Acetatpuffer (pH 5,5) transferiert, bilden sich nach Erhöhung des pH-Werts in dieser Lösung Fibrillen, welche in gewissem Ausmaß an den Termini interagieren und zusätzlich nicht-fibrilläre Strukturen zeigen (s. Abb. 6 bzw. Fig. 3, Teilarbeit 1). Dies legt nahe, dass in den His-DOPA-reichen Termini die Deprotonierung von Histidin als pH-abhängiger Schalter wirken kann, welche daraufhin zu einer intermolekularen Assemblierung führt und die Faltung der Kollagendomäne nukleiert.

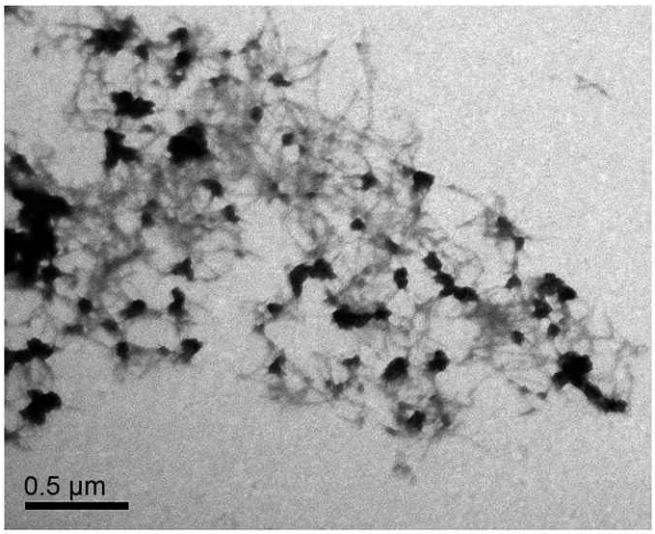

Abbildung 6: Transmissionselektronenmikroskopische (TEM) Aufnahme von rekombinanten preColD-Fibrillen, welche sich nach pH-Erhöhung in Lösung bilden. Die einzelnen Fibrillen bilden Bündel aus, die an den Termini zu interagieren scheinen. Diese Interaktion wird vermutlich durch die terminalen Domänen (His-DOPA) vermittelt. Übernommen aus [62] mit Erlaubnis des Verlags (© The Royal Chemical Society of Chemistry).

5.2 *Engineered Collagen* – Ein Redox-schaltbares Grundgerüst zur steuerbaren Assemblierung und Produktion von biokompatiblen Oberflächen

Teilarbeit 2: s. Kapitel 10 und Ref. [64]

Tierisches Typ 1 Kollagen besitzt eine stark prozessierte und hierarchisch assemblierte Struktur, die jedoch letztendlich auf einfachen, repetitiven Sequenzen beruht. Da bereits mit der rekombinanten Produktion von preColD in *P. pastoris* (s. Kapitel 5.1) gezeigt werden konnte, dass selbst ohne die Prolin-Hydroxylierung in manchen Fällen ein Großteil der Funktionalität von Kollagensequenzen erhalten bleibt, wurde in dieser Arbeit untersucht, ob ein einfaches $(GPP)_{50}$-Biopolymer dazu in der Lage ist, korrekt gefaltete Tripelhelices auszubilden, welche im Zuge weiterer Entwicklung in Zukunft als Biomaterial nutzbar sind.

Da bekannt ist, dass langkettige, vollständig denaturierte Kollagene in Abwesenheit von gezielter Nukleation gelatineartige Netzwerke ausbilden, aber im Gegensatz dazu selbst verhältnismäßig instabile Kollagene, wie z.B. die zuvor erwähnten bakteriellen Kollagene, nach Nukleation durch spezielle Trimerisierungsdomänen stabile, lösliche Tripelhelices formen können, wurden die hier verwendeten Konstrukte mit einer redox-schaltbaren Nukleationsdomäne versehen.

Bei dem WC_2-genannten Foldon handelt es sich um eine kurze Sequenz, welche mittels zweier Cysteine die oxidationsabhängige Verknüpfung am Aminoterminus des Polymers erlaubt. Es wurden mehrere Konstrukte unterschiedlicher Länge hergestellt, um den Einfluss des genannten Foldons auf Konstrukte unterschiedlicher Stabilität einschätzen zu können.

Zwei kurze Peptide, eCol-WC_2-$(GPP)_3$ und eCol-WC_2-$(GPP)_7$ wurden mittels Festphasensynthese am *Laboratory for Organic Synthesis of Functional Systems, Department of Chemistry*, Humboldt-Universität zu Berlin gewonnen, während eCol-WC2-$(GPP)_{50}$ erfolgreich in *E. coli* produziert und mittels einer modifizierten Nickel-Affinitäts Reinigungsstrategie aufgearbeitet werden konnte.

Hierbei wurde beobachtet, dass das genannte Konstrukt nur unter denaturierenden Bedingungen löslich ist, weshalb viele der folgenden Messungen in Gegenwart von 4 M Guanidinhydrochlorid (GdmCl) durchgeführt werden mussten.

Zur Untersuchung der Faltung wurden temperaturabhängige CD-Messungen durchgeführt (s. Abb. 7 bzw. Fig. 3, Teilarbeit 2), bei denen festgestellt wurde, dass alle Konstrukte in der Lage sind, tripelhelikale Sekundärstrukturen auszubilden. Das kürzeste Peptid eCol-WC_2-$(GPP)_3$ formte nur unter oxidierenden Bedingungen und Inkubation bei unter 10 °C Tripelhelices, konnte diese aber auch nach Hitzedenaturierung so schnell wieder ausbilden, dass keine Hysterese zwischen Heizen und Kühlen zu erkennen war. Wurde das zuvor unter oxidierenden Bedingungen trimerisierte eCol-WC_2-$(GPP)_3$ reduziert, behielt das Konstrukt die tripelhelikale Faltung vorerst, entfaltete aber nach Überschreiten des Schmelzpunktes und konnte danach trotz erneutem Abkühlen keine Helix mehr ausbilden (s. Abb. 7A bzw. Fig. 3A, Teilarbeit 2).

Das Peptid eCol-WC_2-$(GPP)_7$ konnte sowohl unter oxidierenden als auch unter reduzierenden Bedingungen lösliche Kollagenhelices formen, benötigte in der reduzierten Form hierzu aber eine mehrstündige Inkubation bei 2 °C. Dieses Verhalten wurde auch im zyklischen Schmelzexperiment beobachtet; im oxidierten Zustand konnte sich die Tripelhelix bereits während der Abkühlphase mit geringer Hysterese wieder falten, während das reduzierte Protein nach Überschreiten des Schmelzpunktes bis zum Abschluss des Experiments kein kollagentypisches Signal mehr zeigte (s. Abb. 7B bzw. Fig. 3B, Teilarbeit 2).

Das lange eCol-WC_2-$(GPP)_{50}$-Konstrukt war nur in Gegenwart von 4 M GdmCl löslich und aggregierte auch hier langsam unter reduzierenden Bedingungen. Unter oxidierenden Bedingungen konnte ein ähnliches Verhalten zu den kurzen Peptiden beobachtet werden, nämlich dass sich die thermisch denaturierte

Kollagenfaltung bei Vorhandensein von Cysteinverknüpfungen im WC_2-Foldon noch während der Abkühlphase wieder ausbildet, während dieselbe Probe nach Reduktion unter denselben Bedingungen erst die Faltung verliert und danach während der Abkühlphase unspezifisch aggregiert (s. Abb. 7C bzw. Fig. 3C, Teilarbeit 2).

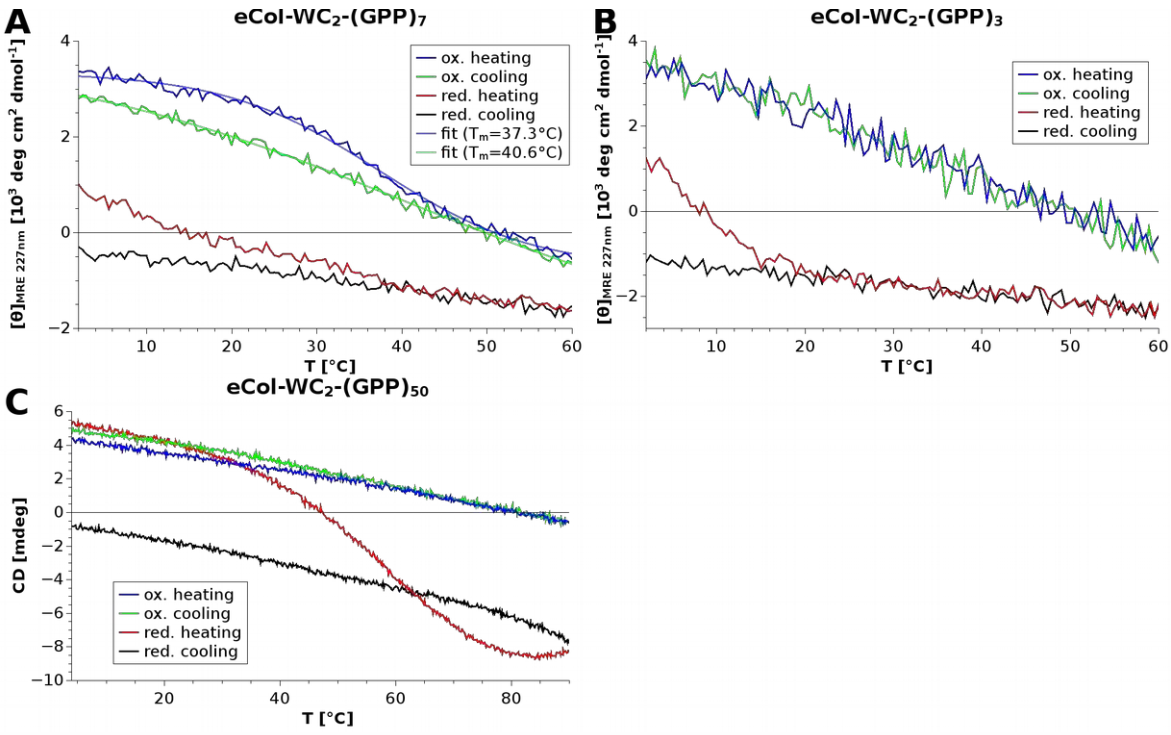

Abbildung 7: Schmelzkurven der drei untersuchten Konstrukte eCol-WC_2-$(GPP)_{3/7/50}$ unter reduzierenden und oxidierenden Bedingungen. In allen Fällen wird deutlich, dass die korrekt gefalteten Konstrukte unter oxidierenden Bedingungen ihre tripelhelikale Faltung nach dem Schmelzen wieder einnehmen, während die thermische Denaturierung unter reduzierenden Bedingungen irreversibel ist. Übernommen aus [64] mit Erlaubnis des Verlags (© American Chemical Society).

Die gezeigten Experimente verdeutlichen, dass die Nukleation der Tripelhelix einen großen Einfluss auf die korrekte Faltung von den hier gezeigten Kollagenmimetika hat. Es wird vermutet, dass besonders bei längeren Konstrukten die Erstnukleation ein entropisch ungünstiger Schritt ist, der aufgrund seiner Seltenheit die Ausbildung von unspezifischen Aggregaten und gelatineähnlichen Netzwerken begünstigt, sofern diese Charakteristik nicht durch spezifische Funktionalitäten im Protein bereits gegeben ist.

Um das Oligomerisierungsverhalten des WC_2-Foldons zu untersuchen, wurden das reduzierte und das oxidierte eCol-WC_2-$(GPP)_3$-Peptid per SEC/MALS (*size exclusion chromatography / multi-angle light scattering*) untersucht (s. Fig. 4, Teilarbeit 2). Da die Messung bei Raumtemperatur und damit oberhalb des Schmelzpunktes der Kollagendomäne durchgeführt wurde, sind sämtliche Oligomerisierungen auf die Auswirkung des Foldons zurückzuführen.

Es wurde festgestellt, dass das Peptid in reduzierter Form wie erwartet monomer ist. Außerdem wurde beobachtet, dass das Peptid in für in dieser Arbeit relevanten Konzentrationen nach der Oxidation tatsächlich größtenteils Monomere, Dimere und Trimere ausbildet. Damit ist sicher gestellt, dass das Foldon nicht alleine für die Ausbildung von hochmolekularen Netzwerken verantwortlich ist, sondern lediglich einen ratenlimitierenden Schritt bei der Faltung von Kollagen-Trimeren beschleunigt.

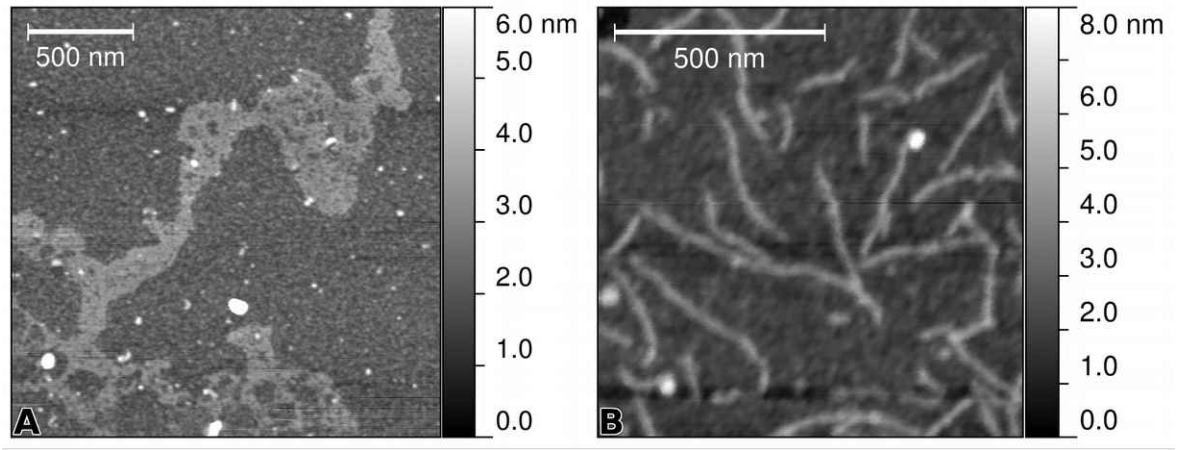

Abbildung 8: AFM-Aufnahmen von **(A)** eCol-WC_2-$(GPP)_{50}$ unter oxidierenden Bedingungen, präpariert aus 4 M GdmCl. Es sind längliche, offene Strukturen erkennbar, die das Vorhandensein von fibrillären Anteilen erkennen lassen. **(B)** eCol-WC_2-$(GPP)_7$ bildet unter reduzierenden Bedingungen Fibrillen, die durch eine Überlappung der Monomere in Längsrichtung die Gesamtlänge der einzelnen Peptide um mehrere Größenordnungen überschreitet. Es ist keine Interaktion der Fibrillen untereinander zu beobachten. Die WC_2-Domäne scheint die Faltung nicht zu stören. Übernommen aus [64] mit Erlaubnis des Verlags (© American Chemical Society).

Zur morphologischen Untersuchung von eCol-WC_2-$(GPP)_7$ und eCol-WC_2-$(GPP)_{50}$ wurde Rasterkraftmikroskopie (AFM) eingesetzt (s. Abb. 8 bzw. Fig. 5, Teilarbeit 2). Das $(GPP)_{50}$-Konstrukt bildete unter oxidierenden Bedingungen in 4 M GdmCl längliche, schwammartige Strukturen, welche jedoch eine fibrilläre Grundstruktur erahnen lassen. Das $(GPP)_7$-Peptid formte unter oxidierenden Bedingungen eine raue Oberfläche aus, was vermuten lässt, dass in Lösung eine ungeordnete Ansammlung von Fibrillen vorliegt, welche unspezifisch mit der Glimmeroberfläche interagieren. Im reduzierten Zustand bildete $(GPP)_7$ dagegen einzeln unterscheidbare Fibrillen aus, deren Durchmesser als der einer einzelnen Kollagen-Tripelhelix gemessen werden konnte. Während eCol-WC_2-$(GPP)_7$ somit zwar in der Lage ist, eine axiale Überlappung der Monomere im reduzierten Zustand zu erlauben, ist eine gerichtete Assemblierung nach Oxidation für eCol-WC_2-$(GPP)_7$ nicht zu beobachten. eCol-WC_2-$(GPP)_{50}$ hingegen lässt zumindest ansatzweise vermuten, dass eine Interaktion der einzelnen Fibrillen untereinander stattfinden kann, was nahelegen würde, dass das Protein zur Ausbildung von größeren, fibrillären Strukturen in der Lage ist.

Um das Potential als Biomaterial zu testen, wurde eCol-WC_2-$(GPP)_{50}$ in Ameisensäure gelöst und zu Filmen gegossen, welche als Substratum für BALB-3T3-Fibroblasten und die neuronalen Zelllinien B50 und RN22 eingesetzt wurden. Da eCol keinerlei Strukturmotive für Integrin-basierte Adhäsion aufweist, ist es nicht verwunderlich, dass für keine der getesteten Zelllinien eine Adhäsion beobachtet werden konnte.

Wird jedoch ein Film aus einer Mischung aus eCol-WC_2-$(GPP)_{50}$ und 10% (w/w) des mit einem carboxyteminalen RGD-Motiv versehenen eCol-WC_2-$(GPP)_7$-RGD eingesetzt, findet eine signifikante Adhäsion von Fibroblasten und die damit verbundene morphologische Veränderung (Spreiten) statt. Somit konnte gezeigt werden, dass eCol-basierte Materialien Zellen gegenüber inert sind, sofern sie nicht gezielt mit den gewünschten Funktionalitäten ausgestattet werden (s. Fig. 6, Teilarbeit 2).

Die Vermischung mit kurzkettigen Peptiden erlaubt in diesem Zusammenhang somit eine elegante Möglichkeit, eine Vielzahl von Peptiden unter diesem Aspekt auf unkompliziertem Weg zu untersuchen, jedoch liegt eine weitere Stärke des Systems in der Möglichkeit, die gewünschte Funktionalität direkt durch gentechnische Methoden in das rekombinant produzierte eCol-Protein einbringen zu können.

Es konnte mit den durchgeführten Experimenten gezeigt werden, dass eCol zur Ausbildung von kollagenartigen Strukturen in der Lage ist und gezielt durch die redox-schaltbare WC_2-Domäne in seiner Assemblierung gesteuert werden kann. Da die Interaktion mit Zellen nur gegeben ist, wenn dazu eine spezifische Integrin-bindende Domäne eingebracht wird, dient das Konstrukt außerdem als Grundgerüst für weiteres rationales Design, um Stoffe mit maßgeschneiderten Funktionalitäten auf unkomplizierte Art und Weise herstellen zu können.

5.3 Wege hin zu neuen kollagenbasierten Materialien

Teilarbeit 3: s. Kapitel 11 und Ref. [65]

Kollagen ist als Hauptbestandteil der ECM ein wichtiges Strukturprotein, welches seit längerem Anwendung als Biomaterial findet. Die molekulare Struktur von Tropokollagen ist in seiner tripelhelikalen Faltung gut definiert und führt dazu, dass die Kollagen-Tripelhelix unabhängig von der Primärsequenz in der Regel nicht vom Immunsystem erkannt wird [66].

Dieser Umstand wird von einigen Bakterienspezies, darunter insbesondere *Streptococcus pyogenes* ausgenutzt, indem es Kollagen-ähnliche Proteine auf seiner Oberfläche präsentiert, welche als Virulenzfaktor zur Ausbildung von Biofilmen, zur Adhäsion an Wirtszellen und der eben genannten Maskierung vor Immunrezeptoren beitragen [3]. Eine Besonderheit der bakteriellen Kollagene ist die Eigenschaft, keine Sekundärmodifikationen wie z.B. das in der Einleitung behandelte 4-Hydroxyprolin zu besitzen, sondern die Tripelhelix stattdessen durch die Ausbildung von intermolekularen Salzbrücken zu stabilisieren [63].

Ein weiteres, kürzlich entdecktes Kollagen wird von Pflanzenwespen als Kokonseide versponnen und benutzt ebenfalls die genannte Form der Ladungsstabilisierung [61]. Sowohl bakterielle als auch Seidenkollagene sind aufgrund ihrer vergleichsweise geringen Größe und den einfachen Ansprüchen an das Expressionssystem gute Beispiele für kollagenartige Proteine, welche kaum sekundäre Proteinmodifikationen aufweisen [67].

Die beiden genannten Beispiele sollen zeigen, dass eine Vereinfachung der Struktur von Kollagenen und kollagenartigen Proteinen prinzipiell möglich ist, und dass die genannten Vorbilder eine Herangehensweise zur Gewinnung von neuen Materialien liefern, welche möglicherweise in Zukunft als Biomaterialien genutzt werden können.

Weitere Ansätze zur Produktion von kollagenbasierten Materialien werden derzeit von verschiedenen Arbeitsgruppen mit unterschiedlichen Herangehensweisen verfolgt. Obwohl in letzter Zeit die meisten Neuerungen auf diesem Gebiet durch biotechnologische Methoden und Peptidsynthese zustande kommen (s. Tab. 2), werden die meisten kommerziell genutzten Kollagene derzeit nach wie vor durch Extraktion aus tierischem Gewebe gewonnen.

Soll die Grundstruktur des Gewebes erhalten bleiben, z.B. bei der Herstellung von *Catgut* oder biologischen Herzklappen- oder Sehnenersätzen, werden Lösungsmittel und proteolytische Enzyme benutzt, die die nicht-kollagenen Bestandteile des Gewebes und Zellen entfernen, um die Exposition von immunogenen Strukturen zu minimieren und damit die Abstoßung durch den Wirt zu vermeiden [68].

Bei der Extraktion von löslichem Kollagen erhält man Tropokollagen, welches zu mehreren Morphologien prozessiert werden kann, aber häufig die mechanische Festigkeit des Ausgangsgewebes verliert. Besonders in der Prozessierung von löslichem Typ I Kollagen wurden in den letzten Jahren jedoch erhebliche Fortschritte erzielt, so ist es z.B. seit kurzem möglich, mittels mikrofluidischer Spinntechniken Fasern herzustellen, die mechanische Eigenschaften ähnlich denen von Sehnen besitzen [8].

Synthetische, kollagenmimetische Peptide, welche ursprünglich zur Strukturaufklärung und zur Bestimmung der Schmelzpunkte und Faltungskinetiken von Kollagen eingesetzt wurden [19], [60], [69], sind nach wie vor durch die maximale Größe von mittels Festphasenpeptidsynthese herstellbaren Molekülen limitiert. Dennoch zeichnet sich diese Methode durch eine hohe chemische Flexibilität hinsichtlich der verwendeten Aminosäuren aus und wird deshalb unter anderem zur Herstellung von diagnostischen Sonden und Markern auf Kollagenbasis angewendet. Die biotechnologische Produktion von natürlichem, humanidentischem Kollagen ist derzeit nur unter Verwendung von komplexen und damit teuren Systemen auf Basis von Fibroblasten-Zellkultur möglich. Da sich die Produktion von weniger komplexen kollagenbasierten Proteinen jedoch als zielführend herausgestellt hat, ist die rekombinante Proteinproduktion für diese Konstrukte die Methode der Wahl [70].

Sowohl bakterielles als auch Seidenkollagen können ohne große Modifikationen mit großen Ausbeuten in *E. coli* hergestellt werden und werden derzeit auf ihre Eignung als Biomaterial untersucht. *Engineered Collagen* (eCol), ein $(GPP)_{50}$-Polymer, lässt sich ebenfalls in *E. coli* produzieren und wird als Teil dieser Arbeit genauer in Kapitel 11 beschrieben.

Kollagenbasierte Block-Copolymere und darauf basierende Hybride, welche z.B. in *P. pastoris* erfolgreich exprimiert wurden, formen Hydrogele, Mizellen und Fibrillen und sind als Beispiele für die Verwerdbarkeit von kollagenartigen Sequenzen im Zuge des rationalen Proteindesigns zu nennen. preColD, bei dem es sich ebenfalls um ein Block-Copolymer handelt, konnte genauso in *P. pastoris* hergestellt werden und wird in Abschnitt 10 genauer behandelt.

6 Literatur

[1] J. P. Bentley, „Excelsior: A Retrospective View Of Collagen“, *J. Invest. Dermatol.*, Bd. 67, Nr. 1, S. 119–123, Juli 1976.

[2] J.-Y. Exposito, C. Cluzel, R. Garrone, und C. Lethias, „Evolution of collagens“, *Anat. Rec.*, Bd. 268, Nr. 3, S. 302–316, Nov. 2002.

[3] S. Lukomski *u. a.*, „Identification and characterization of the scl gene encoding a group A Streptococcus extracellular protein virulence factor with similarity to human collagen.“, *Infect Immun*, Bd. 68, Nr. 12, S. 6542–6553, Dez. 2000.

[4] D. H. McNitt *u. a.*, „Surface-exposed loops and an acidic patch in the Scl1 protein of group A Streptococcus enable Scl1 binding to wound-associated fibronectin“, *J. Biol. Chem.*, Bd. 293, Nr. 20, S. 7796–7810, Mai 2018.

[5] J. Philip McCoy *u. a.*, „Connective tissue diseases and bovine collagen implants“, *J. Am. Acad. Dermatol.*, Bd. 16, Nr. 2, S. 315–318, Feb. 1987.

[6] T. Gibson, „Evolution of catgut ligatures: the endeavours and success of Joseph Lister and William Macewen“, *Br. J. Surg.*, Bd. 77, Nr. 7, S. 824–825, Juli 1990.

[7] M. O. Othman, W. Qassem, und A. B. Shahalam, „The mechanical properties of catgut in holding and bonding fractured bones“, *Med. Eng. Phys.*, Bd. 18, Nr. 7, S. 584–590, Okt. 1996.

[8] C. Haynl, E. Hofmann, K. Pawar, S. Förster, und T. Scheibel, „Microfluidics-Produced Collagen Fibers Show Extraordinary Mechanical Properties“, *Nano Lett.*, Bd. 16, Nr. 9, S. 5917–5922, Sep. 2016.

[9] H. Nowack, E. Hahn, und R. Timpl, „Specificity of the antibody response in inbred mice to bovine type I and type II collagen“, *Immunology*, Bd. 29, Nr. 4, S. 621–628, Okt. 1975.

[10] D. A. Zeide, „Adverse reactions to collagen implants“, *Clin. Dermatol.*, Bd. 4, Nr. 1, S. 176–182, Jan. 1986.

[11] L. Bauman, „CosmoDerm/CosmoPlast (Human Bioengineered Collagen) for the Aging Face“, *Facial Plast. Surg.*, Bd. 20, Nr. 02, S. 125–128, Mai 2004.

[12] C. M. Yamazaki, S. Asada, K. Kitagawa, und T. Koide, „Artificial collagen gels via self-assembly of de novo designed peptides.“, *Biopolymers*, Bd. 90, Nr. 6, S. 816–823, 2008.

[13] J.-D. Malcor *u. a.*, „The synthesis and coupling of photoreactive collagen-based peptides to restore integrin reactivity to an inert substrate, chemically-crosslinked collagen“, *Biomaterials*, Bd. 85, S. 65–77, Apr. 2016.

[14] J. Bella und D. J. S. Hulmes, „Fibrillar Collagens“, in *Fibrous Proteins: Structures and Mechanisms*, Bd. 82, D. A. D. Parry und J. M. Squire, Hrsg. Cham: Springer International Publishing, 2017, S. 457–490.

[15] A. Bhattacharjee und M. Bansal, „Collagen Structure: The Madras Triple Helix and the Current Scenario“, *IUBMB Life Int. Union Biochem. Mol. Biol. Life*, Bd. 57, Nr. 3, S. 161–172, März 2005.

[16] N. Dai und F. A. Etzkorn, „Cis-trans proline isomerization effects on collagen triple-helix stability are limited“, *J. Am. Chem. Soc.*, Bd. 131, Nr. 38, S. 13728–13732, Sep. 2009.

[17] A. Bachmann, T. Kiefhaber, S. Boudko, J. Engel, und H. P. Bächinger, „Collagen triple-helix formation in all-trans chains proceeds by a nucleation/growth mechanism with a purely entropic barrier.“, *Proc Natl Acad Sci U A*, Bd. 102, Nr. 39, S. 13897–13902, Sep. 2005.

[18] A. V. Persikov, Y. Xu, und B. Brodsky, „Equilibrium thermal transitions of collagen model peptides.“, *Protein Sci*, Bd. 13, Nr. 4, S. 893–902, Apr. 2004.

[19] S. Boudko *u. a.*, „Nucleation and propagation of the collagen triple helix in single-chain and trimerized peptides: transition from third to first order kinetics.“, *J Mol Biol*, Bd. 317, Nr. 3, S. 459–470, März 2002.

[20] S. P. Boudko, J. Engel, und H. P. Bächinger, „The crucial role of trimerization domains in collagen folding“, *Int. J. Biochem. Cell Biol.*, Bd. 44, Nr. 1, S. 21–32, Jan. 2012.

[21] M. Yamauchi und M. Sricholpech, „Lysine post-translational modifications of collagen“, *Essays Biochem.*, Bd. 52, S. 113–133, Mai 2012.

[22] K. A. Piez und A. H. Reddi, Hrsg., *Extracellular Matrix Biochemistry*. New York: Elsevier Science Ltd, 1984.
[23] A. D. Theocharis, S. S. Skandalis, C. Gialeli, und N. K. Karamanos, „Extracellular matrix structure“, *Adv. Drug Deliv. Rev.*, Bd. 97, S. 4–27, Feb. 2016.
[24] K. Gelse, E. Pöschl, und T. Aigner, „Collagens—structure, function, and biosynthesis“, *Adv. Drug Deliv. Rev.*, Bd. 55, Nr. 12, S. 1531–1546, Nov. 2003.
[25] S. Hamaia und R. W. Farndale, „Integrin recognition motifs in the human collagens“, *Adv. Exp. Med. Biol.*, Bd. 819, S. 127–142, 2014.
[26] C. Zeltz, J. Orgel, und D. Gullberg, „Molecular composition and function of integrin-based collagen glues-introducing COLINBRIs“, *Biochim. Biophys. Acta*, Bd. 1840, Nr. 8, S. 2533–2548, Aug. 2014.
[27] S. Chattopadhyay und R. T. Raines, „Review collagen-based biomaterials for wound healing: Collagen-Based Biomaterials“, *Biopolymers*, Bd. 101, Nr. 8, S. 821–833, Aug. 2014.
[28] D. F. Williams, *Williams Dictionary of Biomaterials*, 1. Aufl. Liverpool University Press, 1999.
[29] R. Khan und M. H. Khan, „Use of collagen as a biomaterial: An update“, *J. Indian Soc. Periodontol.*, Bd. 17, Nr. 4, S. 539–542, 2013.
[30] Y.-C. Fung, *Biomechanics*. New York, NY: Springer New York, 1993.
[31] J. E. Smeathers und J. F. V. Vincent, „Mechanical properties of mussel byssus threads“, *J. Molluscan Stud.*, Bd. 45, Nr. 2, S. 219–230, Aug. 1979.
[32] X. X. Qin, K. J. Coyne, und J. H. Waite, „Tough tendons. Mussel byssus has collagen with silk-like domains“, *J. Biol. Chem.*, Bd. 272, Nr. 51, S. 32623–32627, Dez. 1997.
[33] J. H. Waite, X. X. Qin, und K. J. Coyne, „The peculiar collagens of mussel byssus“, *Matrix Biol. J. Int. Soc. Matrix Biol.*, Bd. 17, Nr. 2, S. 93–106, Juni 1998.
[34] M. H. Suhre, T. Scheibel, C. Steegborn, und M. Gertz, „Crystallization and preliminary X-ray diffraction analysis of proximal thread matrix protein 1 (PTMP1) from Mytilus galloprovincialis“, *Acta Crystallogr. Sect. F Struct. Biol. Commun.*, Bd. 70, Nr. Pt 6, S. 769–772, Juni 2014.
[35] A. Hagenau, P. Papadopoulos, F. Kremer, und T. Scheibel, „Mussel collagen molecules with silk-like domains as load-bearing elements in distal byssal threads.“, *J Struct Biol*, Bd. 175, Nr. 3, S. 339–347, Sep. 2011.
[36] X.-X. Qin und J. H. Waite, „A potential mediator of collagenous block copolymer gradients in mussel byssal threads“, *Proc. Natl. Acad. Sci.*, Bd. 95, Nr. 18, S. 10517–10522, Sep. 1998.
[37] M. H. Ravindranath und K. Ramalingam, „Histochemical identification of dopa, dopamine and catechol in the phenol gland and the mode of tanning of byssus threads of Mytilus edulis“, *Acta Histochem.*, Bd. 42, Nr. 1, S. 87–94, 1972.
[38] W. Wei, J. Yu, C. Broomell, J. N. Israelachvili, und J. H. Waite, „Hydrophobic Enhancement of Dopa-Mediated Adhesion in a Mussel Foot Protein“, *J. Am. Chem. Soc.*, Bd. 135, Nr. 1, S. 377–383, Jan. 2013.
[39] M. J. Harrington und J. H. Waite, „pH-Dependent Locking of Giant Mesogens in Fibers Drawn from Mussel Byssal Collagens“, *Biomacromolecules*, Bd. 9, Nr. 5, S. 1480–1486, Mai 2008.
[40] A. Hagenau und T. Scheibel, „Towards the Recombinant Production of Mussel Byssal Collagens“, *J. Adhes.*, Bd. 86, Nr. 1, S. 10–24, Jan. 2010.
[41] A. Reinecke, L. Bertinetti, P. Fratzl, und M. J. Harrington, „Cooperative behavior of a sacrificial bond network and elastic framework in providing self-healing capacity in mussel byssal threads“, *J. Struct. Biol.*, Bd. 196, Nr. 3, S. 329–339, Dez. 2016.
[42] A. Hagenau, M. H. Suhre, und T. R. Scheibel, „Nature as a blueprint for polymer material concepts: Protein fiber-reinforced composites as holdfasts of mussels“, *Prog. Polym. Sci.*, Bd. 39, Nr. 8, S. 1564–1583, Aug. 2014.
[43] K. J. Coyne, X. X. Qin, und J. H. Waite, „Extensible collagen in mussel byssus: a natural block copolymer“, *Science*, Bd. 277, Nr. 5333, S. 1830–1832, Sep. 1997.
[44] J. M. Lucas, E. Vaccaro, und J. H. Waite, „A molecular, morphometric and mechanical comparison of the structural elements of byssus from Mytilus edulis and Mytilus galloprovincialis“, *J. Exp. Biol.*, Bd. 205, Nr. Pt 12, S. 1807–1817, Juni 2002.
[45] A. M. Anton, A. Heidebrecht, N. Mahmood, M. Beiner, T. Scheibel, und F. Kremer, „Foundation of the Outstanding Toughness in Biomimetic and Natural Spider Silk“, *Biomacromolecules*, Bd. 18, Nr. 12, S. 3954–3962, Dez. 2017.

[46] S. R. Chowdhury *u. a.*, „Collagen Type I: A Versatile Biomaterial“, *Adv. Exp. Med. Biol.*, Bd. 1077, S. 389–414, 2018.
[47] G. Mattei, C. Magliaro, A. Pirone, und A. Ahluwalia, „Bioinspired liver scaffold design criteria“, *Organogenesis*, Bd. 14, Nr. 3, S. 129–146, 2018.
[48] E. Mocan, O. Tagadiuc, und V. Nacu, „Aspects of Collagen Isolation Procedure“, *Curiecul Med.*, Bd. 2, S. 320, 2011.
[49] W. B. Van Robertson, „The effect of ascorbic acid deficiency on the collagen concentration of newly induced fibrous tissue“, *J. Biol. Chem.*, Bd. 196, Nr. 1, S. 403–408, Mai 1952.
[50] M. Nokelainen, H. Tu, A. Vuorela, H. Notbohm, K. I. Kivirikko, und J. Myllyharju, „High-level production of human type I collagen in the yeast Pichia pastoris“, *Yeast Chichester Engl.*, Bd. 18, Nr. 9, S. 797–806, Juni 2001.
[51] O. Pakkanen, A. Pirskanen, und J. Myllyharju, „Selective expression of nonsecreted triple-helical and secreted single-chain recombinant collagen fragments in the yeast Pichia pastoris.“, *J Biotechnol*, Bd. 123, Nr. 2, S. 248–256, Mai 2006.
[52] Y. Tang *u. a.*, „Efficient Production of Hydroxylated Human-Like Collagen Via the Co-Expression of Three Key Genes in Escherichia coli Origami (DE3)“, *Appl. Biochem. Biotechnol.*, Bd. 178, Nr. 7, S. 1458–1470, Apr. 2016.
[53] „Recombinant Human Collagens and Associated Reagents: R&D Systems“. [Online]. Verfügbar unter: https://www.rndsystems.com/resources/posters/recombinant-human-collagens-and-associated-reagents. [Zugegriffen: 09-Okt-2018].
[54] J. Myllyharju, M. Nokelainen, A. Vuorela, und K. I. Kivirikko, „Expression of recombinant human type I-III collagens in the yeast pichia pastoris“, *Biochem. Soc. Trans.*, Bd. 28, Nr. 4, S. 353–357, 2000.
[55] P. D. Toman *u. a.*, „Production of Recombinant Human Type I Procollagen Trimers Using a Four-gene Expression System in the Yeast Saccharomyces cerevisiae“, *J. Biol. Chem.*, Bd. 275, Nr. 30, S. 23303–23309, Juli 2000.
[56] X. Xu *u. a.*, „Hydroxylation of recombinant human collagen type I α 1 in transgenic maize co-expressed with a recombinant human prolyl 4-hydroxylase“, *BMC Biotechnol.*, Nr. 11, Juni 2011.
[57] I. Goldberg, A. J. Salerno, T. Patterson, und J. I. Williams, „Cloning and expression of a collagen-analog-encoding synthetic gene in Escherichia coli.“, *Gene*, Bd. 80, Nr. 2, S. 305–314, Aug. 1989.
[58] M. A. Cejas *u. a.*, „Collagen-related peptides: self-assembly of short, single strands into a functional biomaterial of micrometer scale.“, *J Am Chem Soc*, Bd. 129, Nr. 8, S. 2202–2203, Feb. 2007.
[59] J. Ottl, H. J. Musiol, und L. Moroder, „Heterotrimeric collagen peptides containing functional epitopes. Synthesis of single-stranded collagen type I peptides related to the collagenase cleavage site.“, *J Pept Sci*, Bd. 5, Nr. 2, S. 103–110, Feb. 1999.
[60] S. E. Paramonov, V. Gauba, und J. D. Hartgerink, „Synthesis of Collagen-like Peptide Polymers by Native Chemical Ligation“, *Macromolecules*, Bd. 38, Nr. 18, S. 7555–7561, Sep. 2005.
[61] T. D. Sutherland *u. a.*, „A new class of animal collagen masquerading as an insect silk.“, *Sci Rep*, Bd. 3, S. 2864, 2013.
[62] A. V. Golser und T. Scheibel, „Biotechnological production of the mussel byssus derived collagen preColD“, *RSC Adv.*, Bd. 7, Nr. 61, S. 38273–38278, 2017.
[63] Y. Xu, D. R. Keene, J. M. Bujnicki, M. Höök, und S. Lukomski, „Streptococcal Scl1 and Scl2 proteins form collagen-like triple helices.“, *J Biol Chem*, Bd. 277, Nr. 30, S. 27312–27318, Juli 2002.
[64] A. Golser, M. Roeber, H. Boerner, und T. Scheibel, „Engineered collagen - a redox switchable framework for tunable assembly and fabrication of biocompatible surfaces“, *ACS Biomater. Sci. Eng.*, Nov. 2017.
[65] A. Golser, T. Scheibel, A. V. Golser, und T. Scheibel, „Routes towards Novel Collagen-Like Biomaterials“, *Fibers*, Bd. 6, Nr. 2, S. 21, Apr. 2018.
[66] A. K. Lynn, I. V. Yannas, und W. Bonfield, „Antigenicity and immunogenicity of collagen“, *J. Biomed. Mater. Res. B Appl. Biomater.*, Bd. 71, Nr. 2, S. 343–354, Nov. 2004.

[67] R. Han *u. a.*, „Assessment of prokaryotic collagen-like sequences derived from streptococcal Scl1 and Scl2 proteins as a source of recombinant GXY polymers.“, *Appl Microbiol Biotechnol*, Bd. 72, Nr. 1, S. 109–115, Aug. 2006.
[68] M. Bottagisio, A. F. Pellegata, F. Boschetti, M. Ferroni, M. Moretti, und A. B. Lovati, „A new strategy for the decellularisation of large equine tendons as biocompatible tendon substitutes“, *Eur. Cell. Mater.*, Bd. 32, S. 58–73, 08 2016.
[69] J. Engel, H. T. Chen, D. J. Prockop, und H. Klump, „The triple helix in equilibrium with coil conversion of collagen-like polytripeptides in aqueous and nonaqueous solvents. Comparison of the thermodynamic parameters and the binding of water to (L-Pro-L-Pro-Gly)n and (L-Pro-L-Hyp-Gly)n.“, *Biopolymers*, Bd. 16, Nr. 3, S. 601–622, März 1977.
[70] C. I. F. Silva, P. J. Skrzeszewska, M. D. Golinska, M. W. T. Werten, G. Eggink, und F. A. de Wolf, „Tuning of collagen triple-helix stability in recombinant telechelic polymers.“, *Biomacromolecules*, Bd. 13, Nr. 5, S. 1250–1258, Mai 2012.

7 Abbildungsverzeichnis

8 Tabellenverzeichnis

9 Biotechnological production of the mussel byssus derived collagen preColD

Die genannte Teilarbeit wurde von mir als Erstautor verfasst. Das Manuskript wurde dankend mit der Hilfe von Prof. Dr. Scheibel erstellt.

Die Konzeptionierung, praktische Arbeit und Datenauswertung dieses Projektes wurden von mir am Lehrstuhl Biomaterialen unter der Projektleitung von Prof. Dr. Thomas Scheibel durchgeführt.

Während der Arbeit wurde dankend die Hilfe und Inspiration von anderen Mitgliedern des Lehrstuhls Biomaterialien im Rahmen von Lehrstuhlseminaren und Gruppendiskussionen in Anspruch genommen.

[62] – Published by The Royal Chemical Society of Chemistry.

RSC Advances

PAPER

View Article Online
View Journal | View Issue

Cite this: *RSC Adv.*, 2017, **7**, 38273

Biotechnological production of the mussel byssus derived collagen preColD†

Adrian V. Golser[a] and Thomas Scheibel *[ab]

Received 21st April 2017
Accepted 25th July 2017

DOI: 10.1039/c7ra04515h

rsc.li/rsc-advances

Marine mussels adhere to substrates within the intertidal zone by means of a bundle of threads called the mussel byssus which contains several collagen-like proteins responsible for the mechanical properties of the fibers. Here, we demonstrate the biotechnological production of one of three identified byssus collagens, preColD, from *Mytilus galloprovincialis* using *Pichia pastoris* as the expression host. Previously detected structural features of natural preColD, such as collagen triple helix formation, could also be detected in the recombinant preColD, even in the absence of hydroxylation of proline or tyrosine residues.

Introduction

Several marine species produce a variety of distinct materials for underwater attachment with mechanical properties ranging from those of cement[1] to silk[2] to softer and more elastic materials.[3] These holdfasts have the ability to dissipate mechanical stress without losing their structural integrity. One of these remarkable devices is the byssus of *Mytilidae*,[4] *e.g. Mytilus galloprovincialis*, which consists of several distinct threads each comprising a mechanical gradient along the fiber axis.[5] This gradient of the material's Young's modulus allows the soft muscle (the mussel foot) to seamlessly connect to hard substrates without causing radial stress within the material.[6]

The byssus contains a variety of different proteins, including collagen-like preCols,[7] which assemble into fibrils being the byssus' main load-bearing structure located in the fiber core.[8] preCols (Fig. 1), are a class of structural proteins comprising a collagen core domain flanked by specific domains which strongly contribute to the overall mechanical properties of the byssus threads:[9] the elastic, proximal portion of a thread is rich in preColP[10] comprising elastin-like flanking domains, whilst the tougher, more rigid portion of the thread consists mostly of preColD[11] which incorporates crystalline silk-like flanking domains.

The influence of the preCol-composition on the thread's mechanics is significant: even though the preCols are embedded in a complex array of matrix proteins,[12–14] the mechanical properties of the byssus thread have been largely reproduced by spinning a fiber from matrix-free preCols extracted from the mussel foot.[15,16]

In addition to mechanical stability, all known preCols mediate various intermolecular interactions with other preCols, matrix proteins and substrates. The amino- and carboxyterminal domains of the natural preCols contain DOPA moieties for adhesion, metal binding and crosslinking, as well as histidine-based metal chelate complexes, which are likely responsible for previously detected self-healing properties of byssus threads,[15,17] since the latter are fully reversible. Like other collagens, proline residues within the natural preCols are often hydroxylated at the *Y*-position in the collagen triplet (GXY) by a mussel specific hydroxylase; it is known, however, that most types of collagen will readily form triple-helices even when the content of hydroxyproline is low, albeit at lower melting points.

In this context, the lack of DOPA-residues will also reduce the crosslinking, but it is not expected to influence the protein's folding. Therefore, recombinant production of preColD was chosen as one possible strategy to investigate individual mussel byssus collagens and their properties in greater detail.

Experimental section

Molecular cloning and microbiology

The general methodology for the handling of *P. pastoris*, as well as the molecular biology methods utilized for obtaining the preColD expression plasmid are described in the pPICZ user manual[18] and other relevant literature.[19]

***M. galloprovincialis* preColD.** The gene encoding preColD was amplified from a mussel foot cDNA-Library by PCR.[20] It was subsequently cloned (GenBank JQ837491) into the vector pPICZα (Invitrogen, Carlsbad USA), utilizing the plasmid-intrinsic α-secretion factor and the carboxyterminal cMyc- and His6-tags. The amplified PCR fragment was digested with XhoI and XbaI restriction enzymes (the cleavage sites were artificially inserted into the PCR primer), creating a fragment which allowed

[a]*Lehrstuhl Biomaterialien, Fakultät für Ingenieurwissenschaften, Universität Bayreuth, Universitätsstraße 30, 95440 Bayreuth, Germany*

[b]*Bayreuther Zentrum für Kolloide und Grenzflächen (BZKG), Bayerisches Polymerinstitut (BPI), Bayreuther Zentrum für Molekulare Biowissenschaften (BZMB), Bayreuther Materialzentrum (BayMAT), Universität Bayreuth, Universitätsstraße 30, 95440 Bayreuth, Germany. E-mail: thomas.scheibel@uni-bayreuth.de*

† Electronic supplementary information (ESI) available. See DOI: 10.1039/c7ra04515h

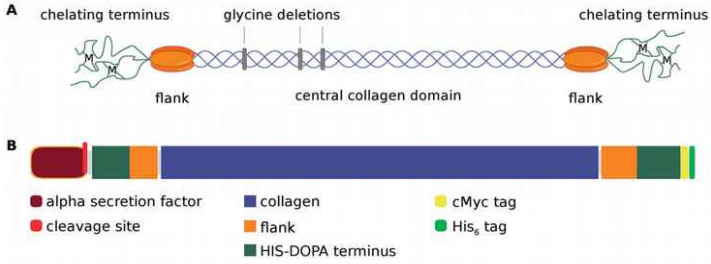

Fig. 1 (A) Schematic representation of a preColD triple helix. The central collagen sequence is based on the collagen-typical $(GXY)_n$-repeat which is interrupted by glycine deletions. The flanking regions of preColD contain poly-alanine stretches similar to those of silks and putatively form nanocrystalline beta sheets upon higher order assembly of the thread. The chelating termini of preCols contain both histidine and DOPA residues and thereby can promote a reversible, metal dependent end-to-end arrangement between fibrils that become increasingly chemically crosslinked during the maturation of the thread.[9] (B) Block schematic of the domain structure of monomeric, recombinant preColD (domain size drawn to scale).

seamless in-frame ligation into a XhoI/XbaI-digested pPICZα vector using T4 ligase. The ligated DNA was transformed into *E. coli* which were plated onto LB-agar containing Zeocin (50 μg mL^{-1}) and grown overnight. Resulting colonies were grown in a 4 mL liquid culture, plasmids were isolated using a Wizard (TM) SV Miniprep kit (Promega; Madison WI, USA) and the correct gene insertion confirmed using gene sequencing.

Transformation of *P. pastoris*. *P. pastoris* strain X33 (Invitrogen, Carlsbad USA) was transformed with 10 μg of linearized pPICZα-preColD plasmid *via* electroporation.[21,22] The transformants were selected for Zeocin-resistance (100 μg mL^{-1}) on YPD-plates and screened (8 colonies) for maximal anti-cMyc-antibody binding by western blotting. The transformant showing the strongest signal in both secreted as well as intracellular recombinant protein was chosen as production strain (see ESI Fig. S1†).

Fermentation of *Pichia pastoris*

Fermentation was carried out in a Minifors fermenter (Infors, Basel Switzerland) according to established protocols[23,24] with slight modifications. Cells were grown at 30 °C in BMGY medium (13.4 g L^{-1} YNB, 1% (v/v) glycerol, 1% (w/v) yeast extract, 2% (w/v) peptone, 100 mM potassium phosphate, pH 6.0) until the initial carbon sources were depleted and subsequently fed with 86% glycerol, 1.2% PTM1 trace salts[25] at 10 mL h^{-1} L^{-1} starting volume until the wet cell mass reached 200 g L^{-1}. Production of recombinant protein was induced with methanol (final concentration of 0.5% (v/v)). The concentration was kept stable with an automated feeding procedure controlled by a methanol sensor. The pH was held constant at 6.0, and pO_2 was kept at 40%.

Purification of recombinant preColD

Cells were harvested by centrifugation (6000 xG) and washed once with phosphate buffered saline (PBS; 137 mM NaCl, 2.7 mM KCl, 10 mM Na_2HPO_4, 1.8 mM KH_2PO_4, pH 7.4). The pellet was resuspended in an equal volume of buffer A (4 M guanidinium hydrochloride in PBS) and disrupted by 5 passes through a Microfluidics M-110S homogenizer at 80 psi inlet pressure. After centrifugation (40 000 xG), the supernatant of the extract was loaded onto a high-performance Ni-NTA IMAC column (approx. 200 mL bed volume), washed extensively with 8 M urea in PBS and eluted with 200 mL buffer A + 500 mM imidazole. The eluate was dialyzed against 10 mM ammonium bicarbonate and subsequently dried *via* lyophilization (see ESI Fig. S2† for SDS-PAGE).

Transmission electron microscopy

200 μL of preColD were desalted using a 5 mL HiTrap desalting column equilibrated with 50 mM sodium acetate, pH 5.5 and concentrated to approx. 25 mg mL^{-1} using a centricon centrifugation tube with a MW cutoff of 30 kDa.

5 μL of 50 mM TRIS/HCl pH 8.0 were applied to TEM-grids, then adding 5, 1 or 0.1 μL of preColD solution, respectively. After incubating for 1 min, the grids were washed twice with 10 μL TRIS-buffer and negatively stained with uranyl acetate. The samples were visualized using a Zeiss CEM 902 microscope at 80 kV.

CD and FTIR spectroscopy

CD spectra were recorded with a Jasco J-815 spectrometer at 20 °C (scanning speed: 50 nm min^{-1}; band width: 1.7 nm; D.I.T.: 2 s; accumulations: 5). Films were poured onto glass slides from a 5 mg mL^{-1} solution in formic acid and measured directly after the evaporation of the solvent. preColD in solution was measured in a 1 mm quartz cuvette after dialyzing the same solution against PBS and PBS containing 4 M urea at 4 °C. FTIR spectra were recorded with a Bruker Tensor 27 spectrometer, using a PIKE Miracle Ga-ATR crystal. The films were prepared directly on the freshly cleaned crystal by allowing the solvent to evaporate from 10 mg mL^{-1} solutions of protein (preColD, gelatin, spider silk protein eADF4(C16)) in formic acid. The spider silk protein, after measuring the freshly prepared film, was additionally treated with methanol to induce beta-sheet formation. The obtained spectra were smoothed, baseline-adjusted and corrected for atmospheric moisture.

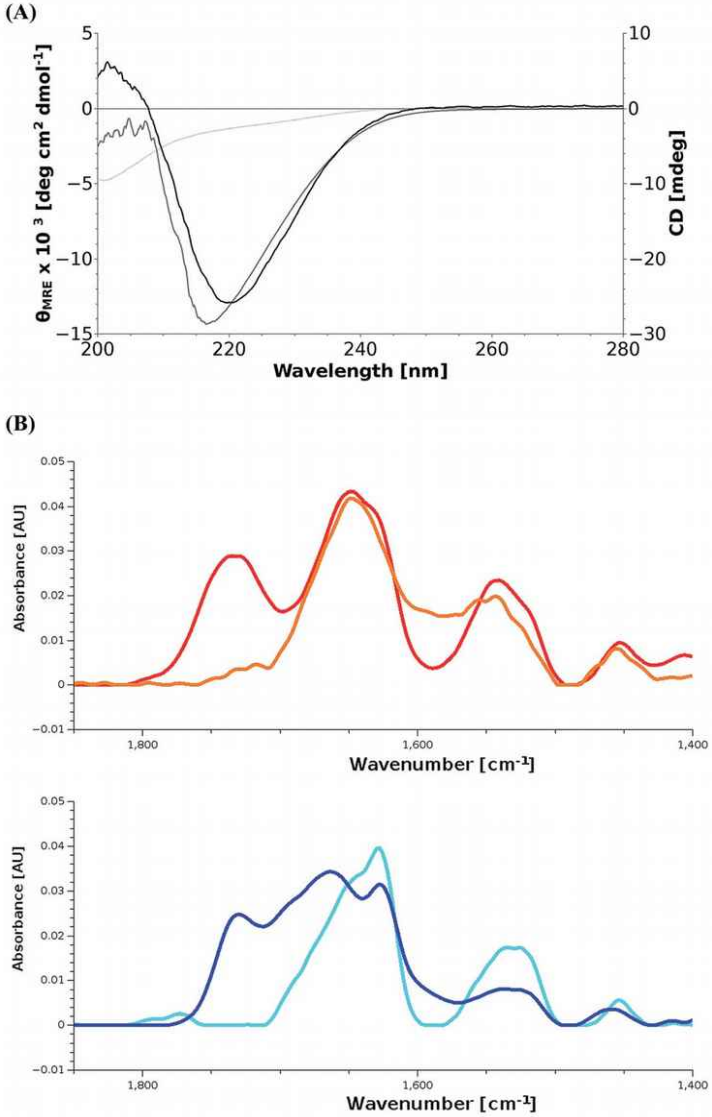

Fig. 2 (A) CD spectra of preColD film (black) and solutions (5 mg mL^{-1}) in PBS containing no urea (light gray) and 4 M urea (dark gray). The film sample shows a 2 nm redshift possibly due to the lack of solvent. All samples show minima/shoulders at 218–220 nm which correspond to β-sheets most likely forming within the silk-like flanking domains of preColD. The spectrum of the non-denatured sample seems to consist of an overlay of the aforementioned β-sheets and triplehelical collagen which typically shows a small positive peak at 220–225 nm and a larger negative peak at 200 nm. (B) FTIR-spectra of protein films. Gelatin (orange), random coil spider silk protein (red), preColD (dark blue), β-sheet-rich spider silk protein (cyan). Unstructured or helical proteins have an amide I peak at around 1650 cm^{-1}, as seen for gelatin and unstructured spider silk protein, while β-sheets have a peak at around 1635 cm^{-1} (crystalline spider silk protein). preColD shows two peaks in the amide I region, of which one corresponds to β-sheets and the other one corresponds to unstructured elements.

Results and discussion

Production and purification of preColD

P. pastoris can be a suitable host for the production of secreted proteins, which simplifies downstream processing steps during recombinant protein production. Therefore, preColD was cloned with an α-secretion factor inducing translocation into the endoplasmic reticulum (ER) and subsequent secretion *via* the Golgi apparatus. Accordingly, the selection for the highest producing *P. pastoris* expression strain was performed by

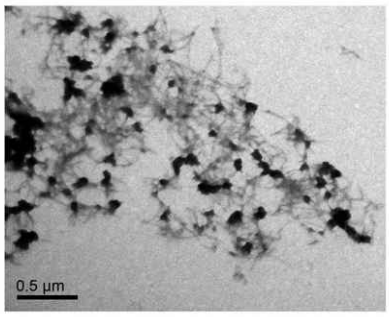

Fig. 3 TEM analysis of recombinant preColD shows fibrils with lengths of 180 nm and assemblies thereof. The single fibrils interact at the termini, sometimes forming globular aggregates and dense fibril bundles.

screening for both intracellular as well as secreted transgenic cMyc-Antigen that is present at the carboxyterminus of recombinant preColD (Fig. 1B). The screening was performed in shake flask culture, and secreted protein levels corresponded well with intracellular retention (see ESI Fig. S1†).

Nevertheless, apparently no secretion past the yeast cell wall took place during fermentation, since no recombinant protein could be detected in the medium. Therefore, the recombinant protein was purified from the cell pellet. A single band at the expected molecular weight could be detected by SDS-PAGE (ESI Fig. S2†), suggesting that the recombinant preColD was successfully translocated into the endoplasmic reticulum (ER), had its secretion factor cleaved as expected, but could not be secreted due to unknown reasons. The most likely explanation therefore is a difference in relative expression levels due to the scale-up, since the induction level is dependent on the methanol concentration, which is kept constant during fermentation but isn't monitored in shake flasks.

The yield of pure recombinant preColD from a 1 L fermentation up to 350 g L^{-1} wet cell mass was 252 mg when purified according to the protocol in the experimental section. While this is low compared to industrial processes employing *P. pastoris*,[26] this number is adequate for lab scale production using a non-optimized system.

Determination of secondary structures

The β-sheet signal observed in the CD spectra (Fig. 2A) suggest a strong influence of the silk-like flanking domains on the overall structure of preColD, as they are present even under denaturing conditions (4 M urea) and when dried from formic acid, conditions that would usually favor random coil structures.

Under physiological conditions, the signal intensity was reduced, suggesting that the negative β-sheet-peak (218 nm) is partially canceled out by the positive peak from triple-helical collagen (220 nm). The emergence of a negative peak around 200 nm, which is also expected for folded collagen, supports this hypothesis. It is known that denatured collagen mostly loses its CD-active properties (loss of positive peak at 220 nm, reduction of mean residual ellipticity at 200 nm from −30 to -5×10^3 deg cm^2 $dmol^{-1}$), while non-collagenous proteins would instead show a random-coil structure, which would interfere with the β-sheet-signal also under denaturing conditions.[27,28] The spectra of preColD in solution at 4 M and 0 M urea have been compared to reference spectra using the web-based tool K2D3,[29] showing no similarity to standard proteins present in the database, which supports the hypothesis of having mixed signals (ESI Fig. S3†).

Additional experiments suggesting the presence of β-sheets as well as unstructured collagen have been obtained for films of preColD *via* FTIR (Fig. 2B). The recombinant spider silk protein eADF4(C16) was used as a control to visualize the peak shift towards lower wavenumbers that occurs when beta sheet formation is induced in the previously unstructured film[30,31] which, in this measurement, manifests itself as a shift of the amide I peak from 1645 cm^{-1} to 1630 cm^{-1}. Commercial gelatin was used as a control to determine the signal obtained by an unstructured collagen-like protein, and corresponds to that of a random coil protein at 1645 cm^{-1}. preColD has two peaks within the amide I band, one suggesting the presence of beta-sheets (1645 cm^{-1}), the other suggesting the presence of random coil structures or helices (1660 cm^{-1}).

While no Fourier self deconvolution was performed, it is evident that a part of preColD contains structural features that can be compared to those of silk proteins under the given conditions, while another portion of the protein seems to contain structures that correspond to unstructured or alpha-helical proteins, similar to those obtained by unstructured gelatin.

We hypothesize that the silk-like flanking domains of preColD form a stable, β-sheet-rich structure under virtually all conditions, being largely responsible for the stiffness of the distal portion of the natural mussel byssus. The collagen core appears to be stable at room temperature even when not hydroxylated, but loses its folding under denaturing conditions. Additionally, the formation of the collagen triple-helix seems to be kinetically hindered,[32] since it does not appear when the denaturing solvent is removed quickly, such as during the preparation of films.

Fibrillization of preColD

Natural preCols extracted from the foot of *M. edulis* undergo fibrillization when the pH is increased above the pK_a of histidine, as this enables the chelation of metal ions by the HIS/DOPA-rich termini of the proteins which thereby promote intermolecular interactions.[17,33] Here, we analyzed the assembly of recombinant preColD under similar conditions. Preliminary experiments haven shown that the dilution of a highly concentrated solution of preColD in formic acid rapidly results in unspecific aggregation (ESI Fig. S4†), while dilute solutions of preColD undergo fibrillization within the same timescale after shifting the pH from 5.5 to 8.0 (Fig. 3). This has also been described for the natural extract of mixed preCols in ref. 33. Our recombinant fibrils also show similar properties as the natural

extract in regard to size and intermolecular arrangement and, as expected, lack any amyloid-like features such as Thioflavin T binding. The presence of globular structures, as seen here, has not been described for the natural extract and seems to be depending on the preparation of the samples. However, since these structures are only observable in the vicinity of high densities of fibrils, they likely result from higher order assembly and/or aggregation of preColD trimers, which might likely be the result of artifacts due to the sample preparation.

Conclusions

The mussel byssus collagen preColD of *M. galloprovincialis* could be recombinantly produced in *P. pastoris* and successfully purified under denaturing conditions using IMAC. It was shown that, even when no posttranslational modifications are present, preColD still has the ability to form nanofibrils under native conditions, which appeared to be similar to those obtained when subjecing natural preCols extracted from mussel feet to the same conditions.[33]

The secondary structure of soluble preColD and films made thereof showed β-sheet structures even under mild denaturing conditions, which suggests that the silk-like flanking domains are involved in early-on structure formation of preColD. Further, they might play a central role in providing physical stability and chemical resilience in the natural byssus thread, since they have been shown in silk to withstand even stronger denaturing conditions.[34–36] Furthermore, the data obtained by CD and FTIR spectroscopy suggest the presence of correctly folded collagen triplehelices. Since the formation of collagen triplehelices is kinetically hindered due to the very slow proline *cis*/*trans* isomerization, it is believed that the unique structure of the flanking regions[15,37,38] is involved in premature assembly similar to the function of pro-domains in vertebrate collagens[39] and certain foldons in bacterial collagens.[40,41] This stabilizing effect seems to be sufficient to compensate for the decrease in stability due to the absence of hydroxyprolines.

Conclusively, the deeper understanding of byssus collagens can serve as an inspiration for the development of biotechnologically produced, protein-based, highly resilient biopolymers with adjustable functions.

Acknowledgements

The authors thank Dr A. Hagenau for providing the mussel foot cDNA library as well as K. Schacht (Biomaterials, University of Bayreuth), R. Grotjahn and PD Dr S. Geimer (Electron Microscopy, University of Bayreuth) for assistance with TEM. Fig. 1B was created using DomainDraw.[42] This work was funded by DFG Grant SCHE603/14-1. A. Golser (MSc) received a scholarship from the Bayerisches Eliteförderungsgesetz (BayEFG).

References

1 R. R. Despain, K. L. De Vries, R. D. Luntz and M. L. Williams, *J. Dent. Res.*, 1973, **52**, 674–679.
2 K. Kronenberger, C. Dicko and F. Vollrath, *Naturwissenschaften*, 2012, **99**, 3–10.
3 M. E. Callow and J. E. Callow, *Biologist*, 2002, **49**, 10–14.
4 J. P. Pujol, *Nature*, 1967, **214**, 204–205.
5 J. E. Smeathers and J. F. V. Vincent, *J. Mollus. Stud.*, 1979, **45**, 219–230.
6 J. H. Waite, E. Vaccaro, C. Sun and J. M. Lucas, *Philos. Trans. R. Soc. London, Ser. B*, 2002, **357**, 143–153.
7 A. Hagenau, M. H. Suhre and T. Scheibel, *Prog. Polym. Sci.*, 2014, **39**, 1564–1583.
8 X. Qin and J. H. Waite, *J. Exp. Biol.*, 1995, **198**, 633–644.
9 J. H. Waite, X. X. Qin and K. J. Coyne, *Matrix Biol.*, 1998, **17**, 93–106.
10 K. J. Coyne, X. X. Qin and J. H. Waite, *Science*, 1997, **277**, 1830–1832.
11 X. X. Qin, K. J. Coyne and J. H. Waite, *J. Biol. Chem.*, 1997, **272**, 32623–32627.
12 M. H. Suhre and T. Scheibel, *J. Struct. Biol.*, 2014, **186**, 75–85.
13 M. H. Suhre, M. Gertz, C. Steegborn and T. Scheibel, *Nat. Commun.*, 2014, **5**, 3392.
14 M. H. Suhre, T. Scheibel, C. Steegborn and M. Gertz, *Acta Crystallogr., Sect. F: Struct. Biol. Commun.*, 2014, **70**, 769–772.
15 A. Hagenau, P. Papadopoulos, F. Kremer and T. Scheibel, *J. Struct. Biol.*, 2011, **175**, 339–347.
16 T. Priemel, E. Degtyar, M. N. Dean and M. J. Harrington, *Nat. Commun.*, 2017, **8**, 14539.
17 M. J. Harrington, H. S. Gupta, P. Fratzl and J. H. Waite, *J. Struct. Biol.*, 2009, **167**, 47–54.
18 ppiczalpha_man.pdf, https://tools.thermofisher.com/content/sfs/manuals/ppiczalpha_man.pdf, accessed June 28, 2017.
19 D. R. Higgins and J. Cregg, *Pichia Protocols*, Humana Press, 2008.
20 J. M. Lucas, E. Vaccaro and J. H. Waite, *J. Exp. Biol.*, 2002, **205**, 1807–1817.
21 C. A. Scorer, J. J. Clare, W. R. McCombie, M. A. Romanos and K. Sreekrishna, *Biotechnology*, 1994, **12**, 181–184.
22 J. M. Cregg and K. A. Russell, *Methods Mol. Biol.*, 1998, **103**, 27–39.
23 K. Sreekrishna, R. H. Potenz, J. A. Cruze, W. R. McCombie, K. A. Parker, L. Nelles, P. K. Mazzaferro, K. A. Holden, R. G. Harrison and P. J. Wood, *J. Basic Microbiol.*, 1988, **28**, 265–278.
24 G. P. L. Cereghino, J. L. Cereghino, C. Ilgen and J. M. Cregg, *Curr. Opin. Biotechnol.*, 2002, **13**, 329–332.
25 J. Stratton, V. Chiruvolu and M. Meagher, *Methods Mol. Biol.*, 1998, **103**, 107–120.
26 B. Brodsky and J. A. M. Ramshaw, in *Fibrous Proteins: Structures and Mechanisms*, ed. D. A. D. Parry and J. M. Squire, Springer International Publishing, cham, 2017, vol. 82, pp. 601–629.
27 N. J. Greenfield, *Nat. Protoc.*, 2007, **1**, 2527–2535.
28 T. Hyashi, S. Curran-Patel and D. J. Prockop, *Biochemistry*, 1979, **18**, 4182–4187.
29 C. Louis-Jeune, M. A. Andrade-Navarro and C. Perez-Iratxeta, *Proteins: Struct., Funct., Bioinf.*, 2012, **80**, 374–381.

30 K. Spiess, A. Lammel and T. Scheibel, *Macromol. Biosci.*, 2010, **10**, 998–1007.
31 U. Slotta, S. Hess, K. Spieß, T. Stromer, L. Serpell and T. Scheibel, *Macromol. Biosci.*, 2007, **7**, 183–188.
32 S. Boudko, S. Frank, R. A. Kammerer, J. Stetefeld, T. Schulthess, R. Landwehr, A. Lustig, H. P. Bächinger and J. Engel, *J. Mol. Biol.*, 2002, **317**, 459–470.
33 M. J. Harrington and J. H. Waite, *Biomacromolecules*, 2008, **9**, 1480–1486.
34 F. Bauer and T. Scheibel, *Angew. Chem., Int. Ed. Engl.*, 2012, **51**, 6521–6524.
35 G. Lang, H. Herold and T. Scheibel, *Subcell. Biochem.*, 2017, **82**, 527–573.
36 D. Huemmerich, T. Scheibel, F. Vollrath, S. Cohen, U. Gat and S. Ittah, *Curr. Biol.*, 2004, **14**, 2070–2074.
37 A. Hagenau and T. Scheibel, *J. Adhes.*, 2010, **86**, 10–24.
38 A. Hagenau, H. A. Scheidt, L. Serpell, D. Huster and T. Scheibel, *Macromol. Biosci.*, 2009, **9**, 162–168.
39 J. P. Malone, K. Alvares and A. Veis, *Biochemistry*, 2005, **44**, 15269–15279.
40 Y. Xu, D. R. Keene, J. M. Bujnicki, M. Höök and S. Lukomski, *J. Biol. Chem.*, 2002, **277**, 27312–27318.
41 Z. Yu, O. Mirochnitchenko, C. Xu, A. Yoshizumi, B. Brodsky and M. Inouye, *Protein Sci.*, 2010, **19**, 775–785.
42 J. L. Fink and N. Hamilton, *In Silico Biol.*, 2007, **7**, 145–150.

Supplementary Information

Biotechnological Production of the Mussel byssus derived collagen preColD

Communication

Adrian V. Golser*, Thomas Scheibel*§

———

*Lehrstuhl Biomaterialien, Fakultät für Ingenieurwissenschaften
Universität Bayreuth, Universitätsstraße 30, 95440 Bayreuth, Germany

§Bayreuther Zentrum für Kolloide und Grenzflächen (BZKG);
§Bayerisches Polymerinstitut (BPI);
§Bayreuther Zentrum für Molekulare Biowissenschaften (BZMB);
§Bayreuther Materialzentrum (BayMAT)
Universität Bayreuth, Universitätsstraße 30, 95440 Bayreuth, Germany

E-mail: thomas.scheibel@uni-bayreuth.de

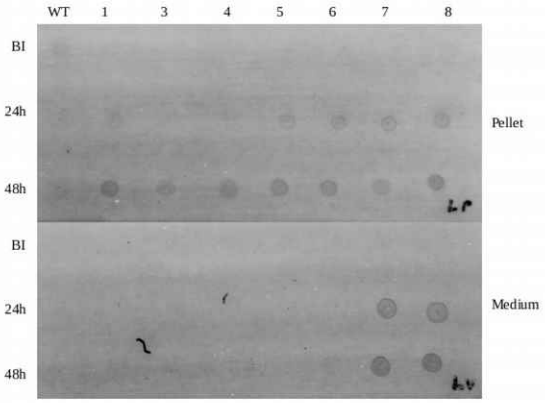

Supplementary Figure S1: Dot-Blot screening for a high preColD-expressing X33 strain. Selection was performed using a cMyc antibody. The selected strain used in this publication was #7. Samples were taken before induction (BI) and after 24 and 48 hours of induction.

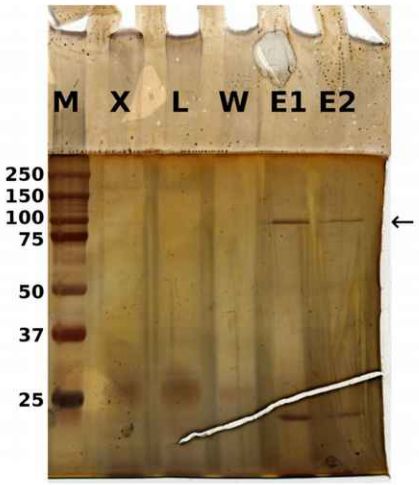

Supplementary Figure S2: Silver stained SDS-PAGE gel from the purification of preColD. M: PrecisionPlus(TM) prestained marker (BioRad, Hercules, CA USA). X: Extract before loading onto column. L: Flowthrough after column loading. W: Column wash. E1/E2 Eluted protein fractions. All samples were precipitated from the 4M Guanidinium HCl buffer with a 10x Volume of cold ethanol and resuspended in 2x Laemmli-buffer. The target protein can be seen eluting between the 75 and 100 kDa marker band (marked by arrow). A contaminating band, most likely a fragment upon unspecific proteolysis, can be seen eluting at < 25 kDa. When dialyzing the protein with a 30 kDa cutoff membrane, this contaminant was removed.

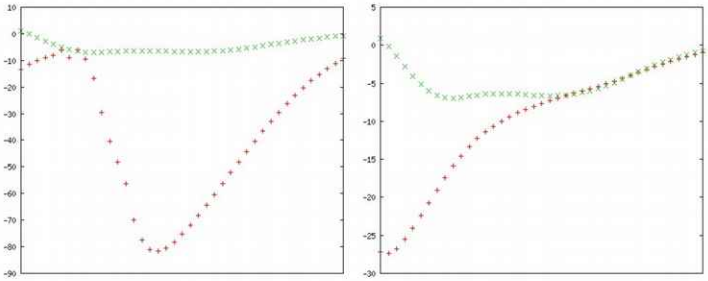

Supplementary Figure S3. Fit of the CD spectra of preColD in 4M urea buffer (left) and 0M urea buffer (right) to reference spectra using the K2D3 database (29). Input in red, prediction in green. The structure prediction determines a secondary structure content of 63.89% alpha helix / 12.28% beta sheet for the protein in 4M urea and 62.92% alpha-helix / 11.67% beta sheet for 0M urea. Both fits show a significant distance to the closest spectrum in the database, suggesting that the error of the structure prediction is large.

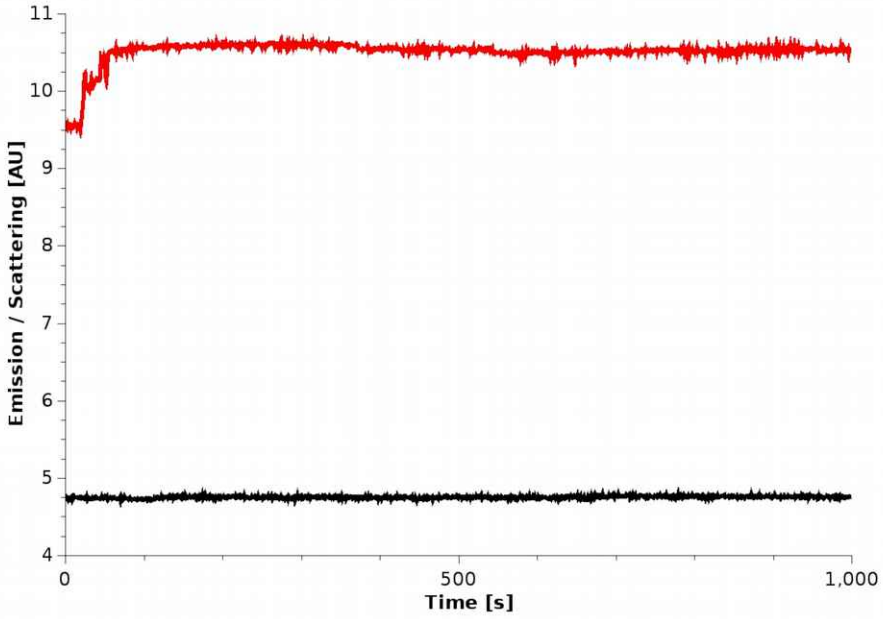

Supplementary Figure S4. Thioflavin T fluorescence (black; excitation: 450 nm, emission: 482 nm) and 90° light scattering (red; excitation: 350 nm, emission: 350 nm) of a preColD-solution diluted to a final concentration of 0.1 mg/ml from formic acid into PBS containing 50 µM Thioflavin T. While the increase of scattered light (red curve) suggests a 1st order formation of aggregates within 100 seconds of dilution, no increase in Thioflavin T fluorescence (black curve) can be seen. This indicates that the aggregates show no amyloid-like structure.

10 Engineered collagen - a redox switchable framework for tunable assembly and fabrication of biocompatible surfaces

Die genannte Teilarbeit wurde von mir als Erstautor verfasst. Das Manuskript wurde dankend mit der Hilfe von Prof. Dr. Scheibel unter Einbeziehung von Matthias Röber und Prof. Dr. Hans Börner (beide Laboratory for Organic Synthesis of Functional Systems, Department of Chemistry, Humboldt-Universität zu Berlin) erstellt.

Die Konzeptionierung fand zusammen mit allen Autoren statt und beruht auf Vorversuchen von mir, welche von Prof. Dr. Scheibel im Rahmen des Projektantrages konkretisiert wurden. Die praktische Arbeit und Datenauswertung dieses Projektes wurden von mir am Lehrstuhl Biomaterialen unter der Projektleitung von Prof. Dr. Thomas Scheibel durchgeführt. Die Messungen der CD-Spektren fand für die meisten Proben im Beisein von Matthias Röber statt. Die Peptidsynthese der Konstrukte $(GPP)_3$ und $(GPP)_7$ sowie Derivate davon wurde von Matthias Röber durchgeführt.

Während der Arbeit wurde dankend die Hilfe und Inspiration von anderen Mitgliedern des Lehrstuhls im Rahmen von Lehrstuhlseminaren und Gruppendiskussionen in Anspruch genommen.

Mein Eigenanteil an dieser Arbeit beträgt etwa 90%.

ACS Biomaterials SCIENCE & ENGINEERING
Article
Cite This: ACS Biomater. Sci. Eng. 2018, 4, 2106−2114

Engineered Collagen: A Redox Switchable Framework for Tunable Assembly and Fabrication of Biocompatible Surfaces

Adrian V. Golser,[†] Matthias Röber,[‡] Hans G. Börner,*[,‡] and Thomas Scheibel*[,†]

[†]Lehrstuhl Biomaterialien, Fakultät für Ingenieurwissenschaften Universität Bayreuth, Universitätsstraße 30, 95440 Bayreuth, Germany

[‡]Laboratory for Organic Synthesis of Functional Systems, Department of Chemistry Humboldt-Universität zu Berlin, Brook-Taylor-Strasse 2, 12489 Berlin, Germany

Supporting Information

ABSTRACT: Collagen, processed into several morphologies and originating from various sources, has long since been used as a biocompatible material that can assist wound healing and tissue regeneration. With the advent of biotechnology and solid-phase peptide synthesis, new possibilities arise to create rationally designed biomaterials based on collagen sequences incorporating new functionalities while maintaining the beneficial properties of natural collagen. In this study a new class of synthetic collagen materials is presented, defined by its simplistic core structure and its therefore predictable behavior. These so-called eCols (engineered collagens) consist of a varying number of Gly-Pro-Pro repeats, a redox-switchable aminoterminal nucleation site and an optional carboxyterminal cell adhesion motif. We show which of these proteins are able to self-assemble into triple helices and cross-linked gelatinous networks and provide insights into their cytocompatibility in vitro.

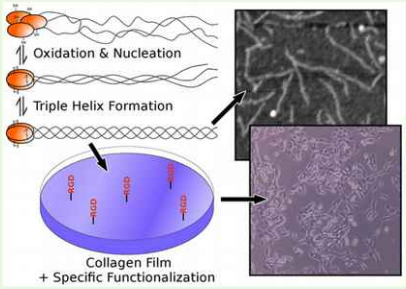

KEYWORDS: *collagen folding, synthetic peptides, cell adhesion, biopolymer self-assembly*

1. INTRODUCTION

Collagens are the most abundant class of proteins in the animal kingdom[1−3] and serve a major role in providing structural stability within the extracellular matrix (ECM), connective tissue and other supporting structures. By incorporating different functional domains, the several subclasses of collagen become fine-tuned to serve different purposes such as being mineralized (cartilage, tendon, bone),[4−6] providing specific mechanical properties for various tissues,[7−9] and interacting differently with specific other components of the ECM and cell types.[10,11]

Collagen is primarily defined by a triple-helical tertiary structure,[12,13] which has been shown to be masked from detection by the immune system regardless of the primary amino acid sequence or originating species. Therefore, collagen and collagen-derived substances have been used in medicine for centuries as biocompatible, nonimmunogenic grafts, scaffolds, dressings, etc.[14]

However, recent discoveries, such as the possible transfer of prion diseases by utilizing collagen from potentially infected sources,[15,16] have increased the demand of substituting animal products with synthetically or recombinantly produced alternatives. However, because of the extensive post-translational modification of collagen during and after biosynthesis, which involves the cleavage of pro-domains, the formation of heterotrimers, and the hydroxylation of proline to 4-hydroxyproline, the biotechnological production of collagen mimicking the natural counterparts have been shown to be challenging, and some attempts remain inefficient.[17−19]

The aim of this work was to establish a method for the production of engineered collagen-like peptides/proteins that can be easily produced in *E. coli*, to show comparable properties to naturally occurring collagen in terms of biocompatibility, with the additional feature to be biotechnologically or chemically modifiable or provide additional, specific functionalities, such as the incorporation of cell-adhesion motifs to be used in biomedical applications.

2. MATERIALS AND METHODS

2.1. Molecular Cloning and Biotechnological Protein Production. The $(GPP)_{50}$ encoding core sequence, including cloning sites at the 5′ and 3′ ends, was ordered from GeneArt (Thermo Fisher) and transferred into a pET28a vector already containing a gene encoding a SUMO tag[20] using standard molecular biology methods such as restriction enzyme digestion and PCR. The WC_2-sequence was later added using either long overhanging PCR-primers or by ligating short double stranded oligonucleotides complementing the overhangs left by restriction enzyme cleavage.

Protein production was first tested using the host strain BL21(DE3) in small volume shaker flasks and then scaled up to 5 L fermenters (Labfors 5; Infors HT Bottmingen, Switzerland) using complex medium. Expression was induced overnight with 0.1 mM IPTG (isopropyl β-D-1-thiogalactopyranoside) at 30 °C. After harvest and washing with

Received: August 17, 2017
Accepted: November 29, 2017
Published: November 29, 2017

DOI: 10.1021/acsbiomaterials.7b00583
ACS Biomater. Sci. Eng. 2018, 4, 2106−2114

PBS (phosphate buffered saline), the cells were resuspended in PBS + 4 M guanidinium hydrochloride, lysed using ultrasonication or a high pressure homogenizer, and loaded either onto a 200 mL Nickel-NTA column or free IMAC resin in suspension. After elution with imidazole, the soluble protein was dialyzed against buffer (PBS) in the presence of Ulp-protease. The eCol protein, which precipitates under nondenaturing conditions, could be centrifuged and redissolved in 6 M guanidinium thiocyanate (adjusted to pH 7 + - 0.5) and subsequently passed over a 20 mL Nickel-NTA column. The column flow through of this step contained the successfully cleaved eCol, because free SUMO tag, Ulp protease, and SUMO-eCol retained on the IMAC resin. The purified protein was dialyzed against 10 mM ammonium carbonate for subsequent lyophilization and storage.

2.2. Peptide Synthesis. Peptides were obtained by automated solid-phase peptide synthesis on an *ABI 433a* peptide synthesizer (Applied Biosystems, Darmstadt, Germany) following the standard *ABI-Fastmoc* protocol (single coupling until amino acid 15 followed by double couple, capping after all coupling steps) with *N*-Methyl-2-pyrrolidone (NMP) as solvent. 41 mL reaction vessels were used for a 0.25 mmol scale. Fmoc deprotection steps were monitored with an UV−vis detector (PerkinElmer LAS GmbH, Rodgau, Germany) at 301 nm. *Tentagel-SRAM* resin (Rapp Polymere, Tübingen, Germany) was used as solid support. After final Fmoc removal the resin was transferred to a 20 mL syringe reactor and subsequently washed with dichloromethane. Peptides were cleaved from the solid support by treatment with a mixture of 94% trifluoroacetic acid (TFA), 1% triethylsilane (TES), 2.5% 1,2-ethanedithiol (EDT) and 2.5% water at room temperature for 3 h resulting in fully deprotected peptides. The resin was filtered, washed with TFA and the collected supernatants were concentrated in vacuo. Afterward, peptides were precipitated in cold diethyl ether, centrifuged (20 min, 9000 rpm), and the supernatants were removed by decantation. The peptides were dissolved in TFA and precipitated again. Precipitates were dried in vacuo and dissolved in Milli-Q water/MeCN (2:1 v/v), followed by lyophilization.

Peptide purification was performed on a semipreparative high performance liquid chromatography (HPLC) System from Shimadzu (Shimadzu Deutschland GmbH, Duisburg, Germany) using a CBM-20A system controller, a DGU-14A online degasser, a LC-20AP liquid chromatograph pump unit, a SIL-20AHT autosampler, a FCV-200AL low-pressure gradient unit and a dual wavelength SPD-10A*vp* UV−vis detector with a preparative flow cell. Chromatographic separation was performed on a SynergiTM Fusion-RP column (80 Å, 4 μm, 250 × 21.20 mm ID, Phenomenex, Aschaffenburg, Germany) with a SecurityGuardTM PREP Cartridge (Fusion-RP 15 × 21.20 mm ID, Phenomenex) at a flow rate of 22.0 mL mL^{-1} at room temperature and monitored at 210 nm. As mobile phase a binary mixture of solvent A (Milli-Q water (MQH_2O) with 0.1% HCOOH) and B (MeCN with 0.1% HCOOH) and a linear gradient (from 10−30%, 15−30% or 10−50%) in 30 min was used. Separated fractions were collected with a Shimadzu FRC-10A fraction collector, followed by lyophilization.

Peptide Characterization. Peptides were characterized by MALDI-MS measured with a *5800 MALDI TOF/TOF* system (AB SIEX, Framingham, MA, USA) or an Autoflex III Smartbeam (Bruker Inc., Billerica, MA, USA) with matrix-assisted laser desorption/ionization and time-of-flight detector. One and a half milliliters of peptide solution was spotted on the MALDI plate together with 1.5 μL alpha-cyano-4-hydroxycinnamic acid (7 mg/mL) matrix in acetonitrile/Milli-Q water (1:1, v/v) + 0.1% TFA and dried by exposure to air. Measurements were performed in reflection positive mode or linear positive mode.

Analytical Ultra Performance Liquid Chromatography Mass Spectrometry (UPLC-MS). Analytical UPLC-MS was performed by using an Acquity-UPLC from Waters GmbH (Eschborn, Germany) with Waters Alliance systems consisting of: Waters Separations Module 2695, a Waters Diode Array detector 996, a LCT Premier XE mass spectrometer and a Waters Mass Detector ZQ 2000. The product purity was analyzed with a ACQUITY-UPLC BEH C18 column (110 Å, 1.7 μm, 50 × 2.1 mm ID Waters) and ACQUITY-UPLC BEH C18 VanGuardTM precolumns, (110 Å, 1.7 μm, 5 × 2.1 mm ID, Waters) using linear gradients in 4 min and a flow rate of 0.5 mL mL^{-1} at 40 °C and monitored at 210 nm.

2.3. Spectroscopy and Sample Preparation. Unless otherwise stated, measurements were performed in PBS at 20 °C. CD measurements were performed at a concentration of 0.1 mg/mL using a temperature controlled Jasco J-815 Spectrometer and 1 mm quartz cuvettes. FTIR was measured on a Bruker Tensor 27 using a contact mode gallium ATR crystal for films and an AquaSpec liquid cell for solutions of the water-soluble eCol-WC2-$(GPP)_{3/7}$ peptides.

SEC/MALS was performed using an Agilent 1100 series HPLC system, a Superdex 75 10/300 column followed by a Wyatt Technology DAWN EOS MALS detector. Peptide/protein concentration was determined by UV absorption at 280 nm using the calculated absorption coefficient.

Although it was noted that freshly prepared and/or dialyzed samples were typically fully oxidized, all samples were treated with 0.1% (v/v) H_2O_2 to guarantee full cystein linking before measuring "oxidized" samples. For reducing samples, a 1 M solution of TCEP (tris(2-carboxyethyl)-phosphine) in PBS was added to a final concentration of 10 mM before the measurement.

Solutions of eCol-WC_2-$(GPP)_{50}$, which was insoluble under all tested nondenaturing conditions, had to be prepared by either using the eluent directly after IMAC purification or by first dissolving the dried protein in formic acid or 6 M guanidinium thiocyanate. When used for solution-based measurements, the protein would typically be dialyzed against PBS containing 4 M guanidinium hydrochloride. AFM samples were prepared from these solutions by allowing the samples to adhere on mica for 5 min and then extensively washing with Milli-Q water.

2.4. Cell Culture. Cell culture experiments were performed according to previously described methods.[21] All films were based on eCol-WC_2-$(GPP)_{50}$ which was dissolved in formic acid at 1 mg/mL and cast into cell culture wells at a final concentration of 0.5 mg/mL. To introduce specific functionality, we introduced the short eCol-WC_2-$(GPP)_7$ peptides with various carboxyterminal tags (no tag, RDG negative control, RGD cell adhesion motif) at 10% (w/w) without additional treatment. After the films were fully dried, the plates were sterilized via UV treatment and seeded with the respective cell types (BALB Fibroblasts, RN22 and B50 Neuronal- and Schwann-Cells). These cell types were chosen to test for compatibility with cells that are known to be very responsive to the structure and composition of the ECM (Neuronal/Schwann-cells) and show the potential to remodel collagen-based substratum (Fibroblasts).

Live cell numbers were determined using CellTiter-Blue reagent (Promega, Madison, USA) according to the manufacturer's protocol.

3. RESULTS

3.1. Recombinant Protein Production and Peptide Synthesis. The eCol protein shown in Figure 1 (A) was obtained by producing a SUMO-coupled construct in *E. coli*. The eCol gene expression did not interfere with cell viability when growing under carbon-source-limiting conditions in a benchtop fermenter, which allowed overnight induction to yield maximum cell mass.

A: SWCGTTPGSWCGT-$[GPP]_{50}$

B: SWCGTTPGSWCGT-$[GPP]_{3/7}$

C: SWCGTTPGSWCGT-$[GPP]_7$-GRDGSPG

SWCGTTPGSWCGT-$[GPP]_7$-GRGDSPG

Figure 1. Constructs used in this work. (A) eCol-WC_2-$(GPP)_{50}$ was produced biotechnologically and purified after cleaving of a SUMO tag used for identification and early on purification steps. (B) Peptides eCol-WC_2-$(GPP)_7$ and eCol-WC_2-$(GPP)_3$, as well as (C) the peptides containing the motifs RGD and RDG (serving as a negative control), have been produced via solid phase peptide synthesis.

Cell lysis and all further purification steps were carried out under denaturing conditions, since the target protein was

DOI: 10.1021/acsbiomaterials.7b00583
ACS Biomater. Sci. Eng. 2018, 4, 2106−2114

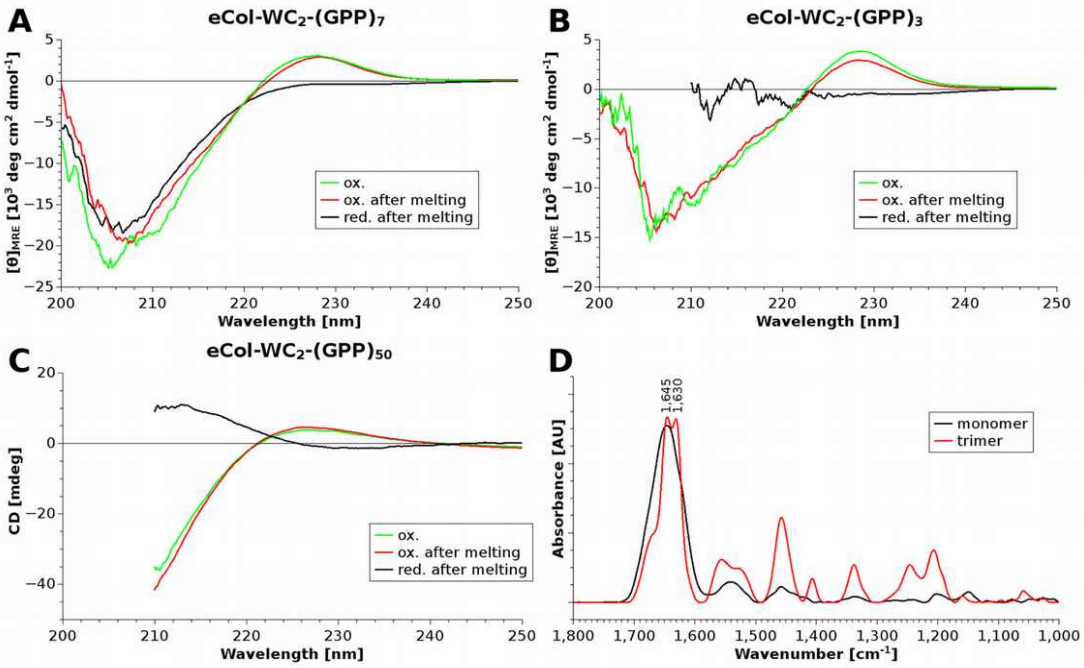

Figure 2. (A–C) Circular dichroism and (D)FTIR solution spectra of unstructured and assembled collagen proteins and peptides as indicated (FTIR: monomer = eCol-WC_2-$(GPP)_3$, trimer = eCol-WC_2-$(GPP)_7$; both samples were incubated under oxidizing conditions at 4 °C overnight). Although similar to random coil structures, the characteristic collagen triple helix can be identified by a positive peak around 227 nm in CD spectra and an additional peak in FTIR spectra at 1630 cm^{-1}. Ox.: cysteine residues are in an oxidized state; red.: cysteine residues have been reduced using TCEP (10 mM).

insoluble. Standard immobilized metal affinity chromatography (IMAC) could be performed only for very small sample volumes, as the local increase of SUMO-eCol on the chromatography column caused the protein to gel, thereby clogging the column and strongly increasing the back-pressure of the system. For preparative amounts of protein, a batch-purification with an IMAC-resin slurry in beaker flasks was performed, with several washing steps utilizing fritted glass Buechner funnels.

Cleavage of the SUMO-tag was carried out by adding Ulp-protease to the eluate and slowly removing the denaturant via dialysis. During this process, the free eCol precipitated and could be recovered via centrifugation. After redissolving the pellet in 4 M guanidinium hydrochloride, a final column-based IMAC-step was used to remove any residual SUMO-tag and Ulp-protease.

The typical yield using this method was in the range of 300–500 mg of free eCol per liter of fermentation medium.

The shorter constructs $(WC_2\text{-}(GPP)_n$ with $n = 3, 7)$ were produced using solid phase protein synthesis (see Materials & Methods).

3.2. Folding Studies. Far–UV circular dichroism (CD) spectroscopy is a well-established method for determining the secondary structure of collagen and soluble proteins in general. A distinct difference between triple helical and unstructured collagen has been shown previously for $(GPP)_n$ constructs[22,23] with the number of GPP-repeats ranging from $n = 3$ to $n = 10$. In general, a triplehelical collagen CD spectrum will have a positive Cotton effect at 220–230 nm with an $[\Theta]_{MRE}$ of around 5×10^3 (deg cm^2 $dmol^{-1}$) and a negative Cotton effect between 190–210 nm of -5 to -20×10^3 (deg cm^2 $dmol^{-1}$). When the collagen is unstructured, the positive peak will disappear, whereas the negative peak will remain mostly unchanged. Both of these values are highly dependent on external conditions, such as buffer components, concentrations and temperature, as well as the presence of folded domains within the protein, yielding overlaying signals corresponding to the typical canonical α-helical, beta-sheet and random coil secondary structures.

Figure 2 shows the spectra obtained for the constructs that were used in this study. As summarized in Figure 1, all proteins consist of an N-terminal 13 amino acid foldon ("WC_2") containing two cysteine residues, two tryptophan residues to facilitate spectroscopy and several hydrophilic amino acids as spacers, followed by a collagen-like sequence consisting of a variable number of GPP-repeats. When oxidized, the cysteines form intermolecular disulfide bridges which greatly facilitate the formation of triple helices. Under oxidizing conditions and after overnight incubation, all three constructs $(WC_2\text{-}(GPP)_n$ with $n = 3, 7, 50)$ show highly similar CD spectra corresponding to that of triple helical collagens.

Note that the construct with the highest molecular weight $(WC_2\text{-}(GPP)_{50})$ would only dissolve in buffers containing guanidinium hydrochloride (GdmCl) at concentrations exceeding 4 mol L^{-1}. Lowering the concentration of denaturant after dissolution induced aggregation and/or gelation of the protein, showing properties related to natural collagen. While it is assumed that solvents exist which allow the formation of soluble $WC_2\text{-}(GPP)_{50}$ trimers, such conditions were not found so far within the concentration range required for the measurements used herein.

DOI: 10.1021/acsbiomaterials.7b00583
ACS Biomater. Sci. Eng. 2018, 4, 2106–2114

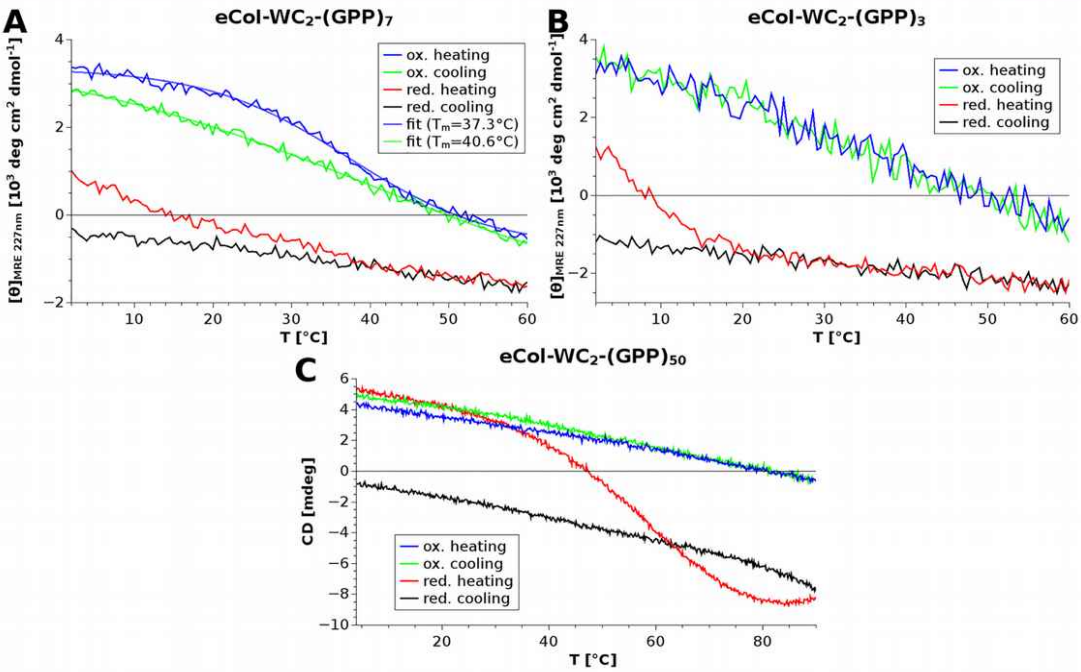

Figure 3. Thermal melting behavior of eCol-constructs under oxidizing and reducing conditions. The peptides (A, B) $(GPP)_{3/7}$ were tested under native conditions in PBS, whereas (C) the high MW $(GPP)_{50}$ construct was analyzed in the presence of 4 M guanidinium hydrochloride. Spontaneous trimerization at reducing conditions could be observed for all samples except eCol-WC_2-$(GPP)_3$ (B) when incubated for several hours at 4 °C. However, refolding of the triple helix was only observed after melting when the sample was oxidized before starting the heating. eCol-WC_2-$(GPP)_3$ only successfully trimerized when oxidatively linked via the WC_2-foldon (B, ox). Furthermore, it melted at temperatures above 40 °C in a noncooperative fashion even when oxidized.

Under reducing conditions, only the two larger constructs (WC_2-$(GPP)_n$ with $n = 7, 50$) slowly formed triple helices when incubated at 4 °C, whereas the short construct (WC_2-$(GPP)_3$) remained monomeric (see Figure 2D). However, all constructs remained triple helical at temperatures <4 °C after being oxidized and fully trimerized, even when treated with a 10-fold molar excess of TCEP or other reducing agents. Subsequent heat treatment, however, fully unfolded all samples when reduced, and the triple helical signal was not recovered during a fast (1 °C s^{-1}) cooling step.

Figure 3 shows the temperature dependent unfolding behavior of all three constructs. When unfolding is induced by heating, the cross-linked samples gradually lost the positive peak at 227 nm while transitioning toward the unstructured state. Subsequent cooling immediately restored the signal of the oxidized samples, suggesting that, while the triple helix was unfolded, the underlying network of cross-linked cystines remained intact throughout the experiment. For oxidized WC_2-$(GPP)_7$, a cooperative unfolding was observed, with a melting point of 37.3 °C as determined using a Boltzmann fit. The other peptide as well as the protein did not show this behavior, suggesting that the underlying quaternary structural features are different.

When the constructs were reduced, the initial positive signal at 227 nm was weakened but still present. Both of the peptide constructs (WC_2-$(GPP)_n$ with $n = 3, 7$) unfolded early at 8 °C ($n = 3$) and 14 °C ($n = 7$), respectively, as determined by the zero transitioning point for the ellipticity at 227 nm. The protein construct ($n = 50$) had a zero transition point of 47 °C and showed a cooperative unfolding with a melting point of 54.5 °C as determined using a Boltzmann fit. This suggests remarkable thermal stability comparable to that of natural collagens, considering that the construct is affected by the denaturing effect of 4 M GdmCl[24] in this experiment. This is especially surprising considering the absence of hydroxyproline, which is known to have a highly stabilizing effect on natural collagens and short collagen-like peptides.[25]

3.3. Oligomeric States Triggered by the WC_2 Folding.

The influence of the WC_2 cystein foldon domain on the stability of the $(GPP)_n$-domains could be shown by investigating the proteins under both oxidizing and reducing conditions. Further, it was determined whether the foldon-induced triple helical structures were single soluble trimers, higher order networks, fibrils or intermediate structures.

In order to investigate the direct influence of the WC_2 domain on the overall molecular structure of eCol-based polymers, SEC/MALS experiments were performed with WC_2-$(GPP)_3$ as shown in Figure 4. The short construct was chosen because the experiments shown in Figure 3 suggested that assembly at room temperature is manly driven by the WC_2 domain with no pronounced effect of the collagen domain.

Under reducing conditions, a single peak eluting at minute 28 could be observed showing a strong absorbance at 280 nm, which can be attributed to the two Tryptophan residues. Using MALS, a R_G corresponding to a molecular weight of approximately 2.5 kDa was observed, which corresponds well with the

DOI: 10.1021/acsbiomaterials.7b00583
ACS Biomater. Sci. Eng. 2018, 4, 2106−2114

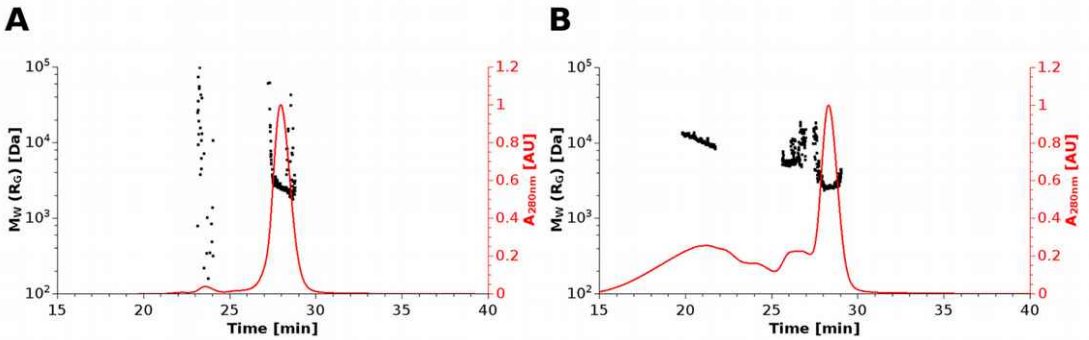

Figure 4. SEC-MALS-measurements of eCol-WC_2-$(GPP)_3$ under (A) reducing and (B) oxidizing conditions. Red line: UV-absorbance at 280 nm. Black dots: M_W as determined by MALS. The WC_2-motif has a strong influence on the ability of the peptide to form triple helices. While the reduced peptide is mainly monomeric, the oxidized form has several additional elution peaks showing calculated masses corresponding to dimers, trimers, and higher molecular weight oligomers.

calculated M_W of 2096 Da of the monomer. Additionally, a small peak with no clear MALS signal eluted around minute 23.5. The nature of this signal is unknown.

Under oxidizing conditions, the same peak could be observed with the corresponding M_W, however, additional earlier eluting peaks appeared with higher molecular weights. When averaging the MALS data of the shoulder eluting between minute 25.6 and 26.6, a mean M_W of 6.4 kDa was calculated. Considering the strong fluctuation of the signal in this range of the spectrum, it can be assumed that this is a mixed elution of both dimers and trimers. Additionally, a very broad peak eluted around minute 21, which showed an increase in molecular weight at earlier elution times, ranging from 8.2 up to 13.6 kDa. It can be assumed that this peak originates from oligomeric structures, ranging from trimers to higher-order oligomers.

This finding suggests that the WC2 domain, while forming predominantly dimers, also can induce the formation of oligomers rather than pure trimers in the longer constructs ($(GPP)_7$ and $(GPP)_{50}$). Given the strongly stabilizing effect of the oxidized foldon, the presence of "interwoven" structures with a high content of triple helices is reasonable.

This assumption could be verified using atomic force microscopy (AFM) (Figure 5A). Oxidized WC_2-$(GPP)_{50}$ led to sponge-like structures with sizes of several μm. It is assumed that, under oxidizing conditions, multiple cystein bridges form yielding dimers, trimers and oligomers. These knots bring unstructured GPP-repeats in spatial vicinity and function as nuclei for the formation of triple helices that further stabilize the network. For reduced GPP_{50}, instead of the observed spongy structures, we only found a clear mica surface. This suggests that, instead of small networked structures, big, highly dense aggregates had formed and were washed off due to limited interaction with the mica surface compared to the oxidized sample.

This observation was in contrast to the fibrillar structures seen for WC_2-$(GPP)_7$ when allowed to slowly assemble under reducing conditions, revealing single fibrils with lengths in the range of 25–30 nm up to 500 nm (Figure 5B). These fibrils show a diameter of about 2 nm in the AFM height profile (Figure 5D), which is similar to the dimension of a single tropocollagen helix (1.5 nm),[26] suggesting that the observed structures are indeed triplehelical collagen-like fibrils.

It is assumed that the supermolecular structure is similar to that described for functionalized collagen-like peptides,[27−30] albeit here these structures could be obtained without the use of active functional domains or heteromorphic fragments. Because no cross-linking is present, the structures are not interconnected beyond the triple-helix. It is important to note that the nonactivated WC_2-foldon did not sterically hinder the spontaneous formation of triple helices.

Oxidized WC_2-$(GPP)_7$ showed no distinctive fibrils in AFM (Figure 5C), but instead formed a granular surface coating with a surface roughness R_a of 0.143 nm, suggesting that covalently linked WC_2-foldons significantly influenced the assembly behavior of the peptide.

3.4. Cell Culture Experiments. Cell culture experiments were performed in order to determine the biocompatibility of eCol-based materials with various cell types. The adhesion of the cell lines BALB 3T3 (fibroblasts), B50 (neuronal cells) and RN22 (Schwann cells) to oxidized eCol films (WC_2-$(GPP)_{50}$) was assessed over 7 days as seen in Figure 6. As major cellular component of the extracellular matrix, fibroblasts are expected to show the strongest interaction with collagen and possibly partially digest and rearrange the collagen matrix after several days of incubation; however, this behavior could not be observed.

B50 and RN22-cells were tested for their compatibility with the novel material to assess the possible future applicability as a component within artificial nerve guide conduits.[31]

Protein films were prepared out of formic acid and washed extensively with PBS before being used for cell culture analysis. eCol showed no characteristic secondary structures after this procedure, as determined by FTIR (see Figure 2D and data not shown).

After 7 days of incubation, the integrity of the film was tested by scratching with a pipetting tip and was found to be intact for all samples. It is evident that all cell lines showed no adhesion to the unstructured collagen films. Microscopic studies showed that most cells had been washed off during cell medium exchange, and that any residual cells showed no strong interaction (i.e., spreading) with the protein film.

In contrast to the protein construct WC_2-$(GPP)_{50}$, the short peptides (WC_2-$(GPP)_3$ and WC_2-$(GPP)_7$) could be prepared in both oxidized and reduced states from aqueous solvents. When allowed to trimerize in solution, films cast from these solutions showed a triple helical signal using FTIR. The films prepared from triple-helical short peptides were stable in PBS for several days, but they could no longer be detected after completion of the cell culture experiment. Films of WC_2-$(GPP)_7$-RGD behaved

DOI: 10.1021/acsbiomaterials.7b00583
ACS Biomater. Sci. Eng. 2018, 4, 2106−2114

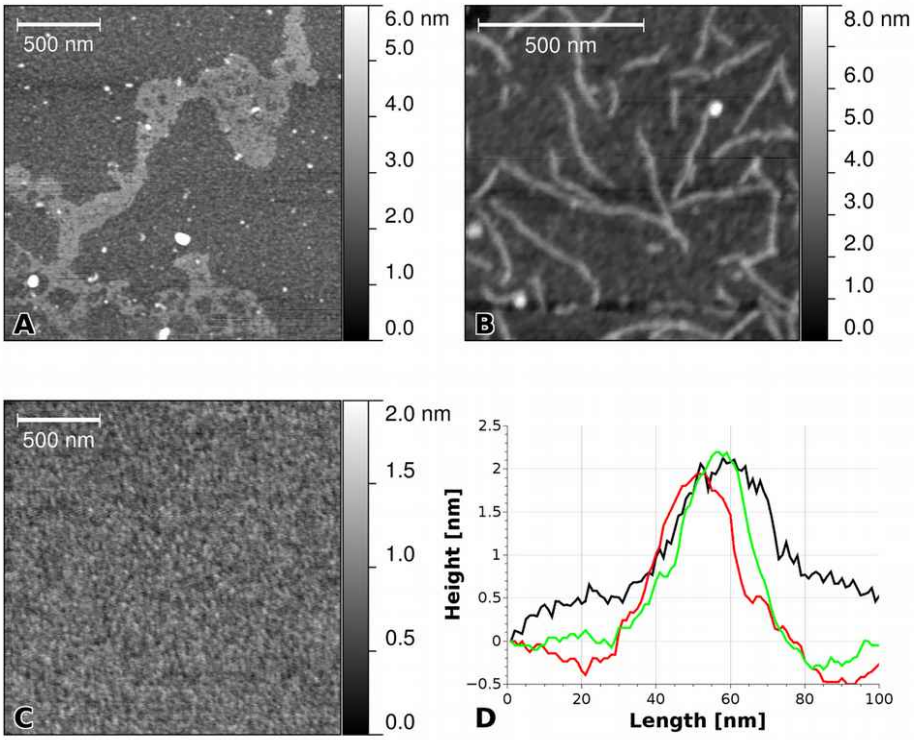

Figure 5. AFM images of (A) eCol-WC_2-$(GPP)_{50}$ and (B, C) eCol-WC_2-$(GPP)_7$. (A) was prepared in the presence of 4 M guanidinium hydrochloride under oxidizing conditions, following extensive washing to remove residual salt. No deposition could be observed under reducing conditions (not shown). (B) was prepared from a native solution of eCol-WC_2-$(GPP)_7$ under reducing conditions. Although the high-molecular-weight protein shows strongly interconnected long structures, the low MW peptide assembles into short fibrils showing rodlike morphologies (scale bars represent 500 nm). (C) was prepared like (B), but from oxidized peptide, showing a uniform granular surface coating. The observed granules have an average height of 0.841 nm, a maximum height of 1.779 nm, and a surface roughness Ra of 0.143 nm. (D) Height profile of a cross-ection of three of the fibrils in (B), demonstrating a height of around 2 nm, which is comparable to that of a natural tropocollagen triple helix.

similarly even upon cross-linking of the peptide using glutaraldehyde (Figure S1). It is unclear whether the peptides were redissolved or enzymatically digested. The cells showed weak adhesion and proliferation indistinguishable to that on non-treated tissue culture plates used as control.

On the basis of these results, WC_2-$(GPP)_{50}$ was blended with WC_2-$(GPP)_7$-RGD (9:1 w/w) and tested for adhesion with BALB Fibroblasts (Figure 6D).

As a control, WC_2-$(GPP)_{50}$ films blended 10% with WC_2-$(GPP)_7$ performed indistinguishably to nonblended WC_2-$(GPP)_{50}$ films. In contrast, a clear difference was seen upon blending WC_2-$(GPP)_{50}$ with WC_2-$(GPP)_7$-RGD, showing that the integrin binding motif RGD is readily presented on the surface of the film and serves to promote adhesion of fibroblasts. The RDG-motif, which consists of the same amino acids with a scrambled sequence and served as a negative control did not show this effect, which allowed the conclusion that the binding is specific and not a result of charge−charge interactions or changes in surface morphology. The cell morphology seen in Figure 6E is in agreement with these findings, because it is evident that the cells have multiple adhesion points yielding the typical spreading.

Because it is known that the surface density of RGD groups has a high influence on the ligand specificity of adhering cells,[32] it can be assumed that the selective blending of the WC_2-$(GPP)_{50}$ matrix with the RGD-carrying peptide offers a more suitable surface spacing to the fibroblasts than pure eCol-WC_2-$(GPP)_7$.

DISCUSSION

In this study, the biotechnological production of a highly repetitive GPP-multimer was demonstrated, and the effect of a simple aminoterminal, redox-responsive foldon on the ability of said multimer to adapt collagen-like properties, such as the formation of triple-helices in solution, was shown. Furthermore, it could be demonstrated that the material can be processed into films and modified to incorporate specific RGD-based integrin binding functionalities by incorporating short, synthetic peptides, which improved cell attachment in situ.

Several attempts have been previously made to biotechnologically produced collagen in a fashion which is feasible for potential biomedical applications.[19,33−36] Various challenges need to be overcome when attempting to produce animal-based collagen in hosts such as bacteria or yeast, the major ones being the hydroxylation of proline residues and the cleavage of pro-domains. Although some hosts such as *Pichia pastoris* have been successfully adapted to include the enzymatic activity necessary for some of these posttranslational modifications,[35,37−40] the yield of

DOI: 10.1021/acsbiomaterials.7b00583
ACS Biomater. Sci. Eng. 2018, 4, 2106−2114

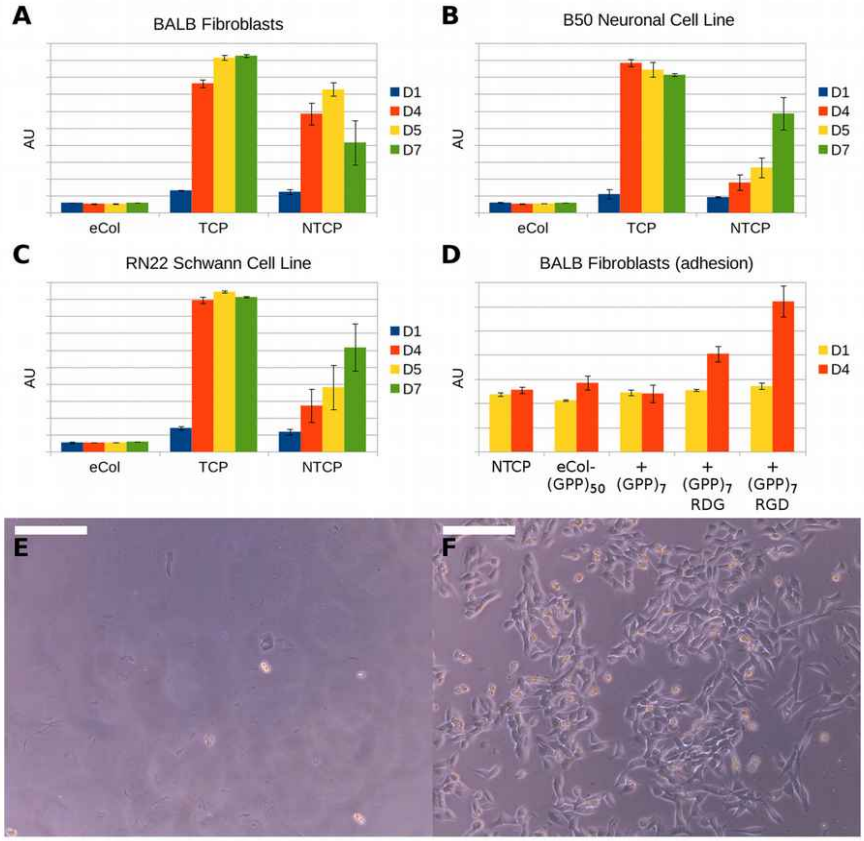

Figure 6. (A–C) Proliferation test of different cell lines (BALB Fibroblasts, RN22 and B50 Neuronal and Schwann cells) on oxidized eCol-WC_2-$(GPP)_{50}$. (TCP = treated culture plate; NTCP = nontreated culture plate). It is evident that none of the cell types showed adhesion to the eCol-based surface. (D) Cellular proliferation test showing the influence of introduced specific functionality by blending the eCol-solution with short eCol-peptides containing the RGD motif. When unmodified, eCol and eCol-based peptide films showed apparently no adhesion on day 4, whereas the incorporation of an RGD motif mediated attachment followed by proliferation. This effect is evident when comparing the morphology of cells grown on (E) eCol-WC_2-$(GPP)_{50}$ and (F) eCol-WC_2-$(GPP)_{50}$ blended with eCol$(GPP)_7$-RGD on day 3 (scale bars represent 200 μm).

correctly folded recombinant collagen is low in comparison to that of classically extracted collagen from animal tissue.

When secondary modification of the target protein is omitted, a wider variety of protein production systems can be used;[18,41] however, most of the resulting recombinant proteins do not show the desired properties: Nonhydroxylated animal collagen will only form trimers with very low melting points;[42,43] non-hydroxylated bacterial collagens require specific trimerization domains to induce correct folding[44,45] and several synthetic variants do not show the required stability for tissue engineering and other biomedical applications.

The engineered collagens presented in this publication overcome some of these obstacles. It could be shown that multimers of the (GPP)-motif are thermodynamically stable at body temperature, and that a simple aminoterminal redox-sensitive folding domain is sufficient to induce nucleation in a fashion that has since been shown to work only by incorporating noncanonical functional groups.[46]

So far, it is not clear how the supermolecular structure is affected by the WC_2-foldon. However, the propagation of the triple helix has previously been shown by other authors[24,47] to be purely entropically driven, and it can be approximated by a first-order kinetic once nucleation has succeeded, rather than a third-order kinetic without nucleation. It is therefore likely that the WC_2-foldon has no dramatic influence on the collagen structure other than providing a nucleation site that lowers the kinetic barrier of monomeric subunits "finding" each other at low concentrations.

This assumption has been confirmed for the shortest WC_2-$(GPP)_3$ construct using SEC/MALS. Without the oxidative cross-linking, only monomers can be detected at room temperature. When oxidized, dimers, trimers and higher order oligomers can be detected in a distribution that implies random cross-linking, suggesting that there is no driving force that specifically induces the formation of trimers above the melting point of the construct.

For WC_2-$(GPP)_7$, once the triple helical confirmation has been obtained for the oxidized sample, thermal unfolding of the cross-linked sample appears to be noncooperative with a nearly linear loss of signal at 227 nm, compared to the clear melting point being seen for the reduced samples (Figure 3). This suggests that for peptides, it is more likely for three monomers to

DOI: 10.1021/acsbiomaterials.7b00583
ACS Biomater. Sci. Eng. 2018, 4, 2106–2114

adapt into a distinct triple-helical trimer, rather than multiple monomers forming gelatin-like networks by spontaneous nucleation within the $(GPP)_n$-domain.

This hypothesis is supported by AFM images of reduced WC_2-$(GPP)_7$ (Figure 5B). The assumed length of a single GPP-repeat within a triple helix is around 8.6 Å,[48] so the observed fibrils with lengths of up to 500 nm cannot be obtained by a single WC_2-$(GPP)_7$ triplet and most likely are triple-helices consisting of overlapping $(GPP)_7$-monomers, with a thickness of around 2 nm (Figure 5D), which is slightly higher than the average thickness of a tropocollagen helix.[26]

This suggests that the WC2-domain does not sterically hinder the formation and growth of the collagen helix. Rather, it can be assumed that, once initiated via the oxidated WC_2-terminus, the growth of the observed WC_2-$(GPP)_{50}$ structures (AFM-data, Figure 5), as well as the soluble, triple helical fibrils of all the proteins/peptides observed in CD (Figure 2) is the result of successful nucleation and elongation of existing triple helices, and that the dimers and trimers observed in in SEC-MALS (Figure 4), have the ability to recruit monomers and other dimers, thereby promoting the growth of the fibril along an existing axis.

The protein construct WC_2-$(GPP)_{50}$ seems to be interconnected in a similar fashion, but suffers from the comparably long length of the collagen-like domain allowing branched propagation of the triple-helix nucleus across multiple $(GPP)_{50}$-chains. This interconnection occurs independently of the foldon-induced nucleation, given the tendency of the protein to assemble into hydrogels and denser aggregates under nondenaturing and even under reducing conditions.

Once the collagen has been assembled under partially denaturing conditions, applying aqueous buffers/media does not dissolve the films within 7 days, as shown in the cell culture experiments. Assuming the intended use of the biotechnologically produced engineered collagen as a novel biomaterial, a low solubility even under reducing conditions is highly desirable.

Because the most common collagen binding integrins, mainly $\alpha1\beta1$, $\alpha2\beta1$, $\alpha10\beta1$, and $\alpha11\beta1$,[49] all seem to bind specific adhesion motifs rather than general triple helical folds, it is not surprising that fibroblasts did not sufficiently adhere to the nonfunctionalized engineered collagen. However, it is also worth mentioning that the films did not show a clear triple helical structure directly after casting, but rather unfolded collagen, which might further contribute to the very weak cell adhesion at the early stages of the experiment.

Importantly, eCol itself is not cytotoxic, as shown upon incorporating the integrin specific RGD cell adhesion motif, since in these experiments, fibroblasts adhered and spread well on films made thereof. In contrast, films made solely of eCol-WC_2-$(GPP)_7$-RGD were unstable for the duration of the experiment, even when cross-linked with glutaraldehyde, and showed no better adhesion than the untreated tissue culture plate, highlighting the role of eCol-WC_2-$(GPP)_{50}$ as a biocompatible surface coating with variable functionalization.

Cells on the blended films showed good vitality and proliferation for the duration of the cell culture experiment, suggesting that engineered collagens are a viable framework for the development of designed biotechnologically produced biomaterials with controllable features.

■ ASSOCIATED CONTENT

Supporting Information

The Supporting Information is available free of charge on the ACS Publications website at DOI: 10.1021/acsbiomaterials.7b00583.

Cell culture microscopic images for films of eCol-WC_2-$(GPP)_7$-RGD (PDF)

■ AUTHOR INFORMATION

Corresponding Authors

*E-mail: h.boerner@hu-berlin.de.

*E-mail: thomas.scheibel@bm.uni-bayreuth.de.

ORCID

Thomas Scheibel: 0000-0002-0457-2423

Funding

This project was funded by the Deutsche Forschungsgemeinschaft (DFG), reference BO 1762/11-1 and SCHE 603/14-1. A.V.G. received support according to the Bayerische Eliteförderungsgesetz (BayEFG).

Notes

The authors declare no competing financial interest.

■ ACKNOWLEDGMENTS

We thank Claudia Stemmann and Alexandra Pellert for assistance with cell culture and Dr. Martin Humenik for assistance with SEC/MALS and AFM measurements.

■ REFERENCES

(1) Di Lullo, G. A.; Sweeney, S. M.; Korkko, J.; Ala-Kokko, L.; San Antonio, J. D. Mapping the Ligand-binding Sites and Disease-associated Mutations on the Most Abundant Protein in the Human, Type I Collagen. *J. Biol. Chem.* **2002**, *277* (6), 4223−4231.

(2) Claudio-Rizo, J. A.; Rangel-Argote, M.; Castellano, L. E.; Delgado, J.; Mata-Mata, J. L.; Mendoza-Novelo, B. Influence of residual composition on the structure and properties of extracellular matrix derived hydrogels. *Mater. Sci. Eng., C* **2017**, *79*, 793−801.

(3) Gartner, L. P. *Textbook of Histology*; Elsevier: Amsterdam, 2015; Vol. 4, pp 134−185.

(4) Yu, Y.; Fan, D. Characterization of the complex of human-like collagen with calcium. *Biol. Trace Elem. Res.* **2012**, *145* (1), 33−38.

(5) Tomoaia, G.; Pasca, R.-D. On the Collagen Mineralization. A Review. *Clujul Med.* **2015**, *88* (1), 15.

(6) Luo, Y.; Sinkeviciute, D.; He, Y.; Karsdal, M.; Henrotin, Y.; Mobasheri, A.; Önnerfjord, P.; Bay-Jensen, A. The minor collagens in articular cartilage. *Protein Cell* **2017**, *8*, 560.

(7) Wenger, M. P. E.; Bozec, L.; Horton, M. A.; Mesquida, P. Mechanical Properties of Collagen Fibrils. *Biophys. J.* **2007**, *93* (4), 1255−1263.

(8) Goh, K. L.; Holmes, D. F. Collagenous Extracellular Matrix Biomaterials for Tissue Engineering: Lessons from the Common Sea Urchin Tissue. *Int. J. Mol. Sci.* **2017**, *18* (5), 901.

(9) Vedadghavami, A.; Minooei, F.; Mohammadi, M. H.; Khetani, S.; Rezaei Kolahchi, A.; Mashayekhan, S.; Sanati-Nezhad, A. Manufacturing of hydrogel biomaterials with controlled mechanical properties for tissue engineering applications. *Acta Biomater.* **2017**, *62*, 42.

(10) Ricard-Blum, S. The Collagen Family. *Cold Spring Harbor Perspect. Biol.* **2011**, *3* (1), a004978−a004978.

(11) Sun, Z.; Guo, S. S.; Fässler, R. Integrin-mediated mechanotransduction. *J. Cell Biol.* **2016**, *215* (4), 445−456.

(12) Berisio, R.; Vitagliano, L.; Mazzarella, L.; Zagari, A. Crystal structure of the collagen triple helix model [(Pro-Pro-Gly)10]3. *Protein Sci.* **2002**, *11* (2), 262−270.

(13) Réty, S.; Salamitou, S.; Garcia-Verdugo, I.; Hulmes, D. J. S.; LeHégarat, F.; Chaby, R.; Lewit-Bentley, A. The crystal structure of the Bacillus anthracis spore surface protein BclA shows remarkable similarity to mammalian proteins. *J. Biol. Chem.* **2005**, *280* (52), 43073−43078.

(14) Kettle, C.; Dowswell, T.; Ismail, K. M. Absorbable suture materials for primary repair of episiotomy and second degree tears. In

Cochrane Database of Systematic Reviews; The Cochrane Collaboration, Ed.; John Wiley & Sons: Chichester, U.K., 2010.
(15) Centers for Disease Control and Prevention (CDC). Update: Creutzfeldt-Jakob disease associated with cadaveric dura mater grafts—Japan, 1978–2008. *MMWR Morb. Mortal. Wkly. Rep.* **2008**, *57* (42), 1152–1154.
(16) Raftery, R. M.; Woods, B.; Marques, A. L. P.; Moreira-Silva, J.; Silva, T. H.; Cryan, S.-A.; Reis, R. L.; O'Brien, F. J. Multifunctional biomaterials from the sea: Assessing the effects of chitosan incorporation into collagen scaffolds on mechanical and biological functionality. *Acta Biomater.* **2016**, *43*, 160–169.
(17) Buechter, D. D.; Paolella, D. N.; Leslie, B. S.; Brown, M. S.; Mehos, K. A.; Gruskin, E. A. Co-translational incorporation of trans-4-hydroxyproline into recombinant proteins in bacteria. *J. Biol. Chem.* **2003**, *278* (1), 645–650.
(18) Rutschmann, C.; Baumann, S.; Cabalzar, J.; Luther, K. B.; Hennet, T. Recombinant expression of hydroxylated human collagen in Escherichia coli. *Appl. Microbiol. Biotechnol.* **2014**, *98*, 4445.
(19) Brodsky, B.; Ramshaw, J. A. M. Bioengineered Collagens. In *Fibrous Proteins: Structures and Mechanisms*; Parry, D. A. D., Squire, J. M., Eds.; Springer International: Cham, Switzerland, 2017; Vol. 82, pp 601–629.
(20) Butt, T. R.; Edavettal, S. C.; Hall, J. P.; Mattern, M. R. SUMO fusion technology for difficult-to-express proteins. *Protein Expression Purif.* **2005**, *43* (1), 1–9.
(21) Wohlrab, S.; Müller, S.; Schmidt, A.; Neubauer, S.; Kessler, H.; Leal-Egaña, A.; Scheibel, T. Cell adhesion and proliferation on RGD-modified recombinant spider silk proteins. *Biomaterials* **2012**, *33* (28), 6650–6659.
(22) Cai, W.; Kwok, S. W.; Taulane, J. P.; Goodman, M. Metal-assisted assembly and stabilization of collagen-like triple helices. *J. Am. Chem. Soc.* **2004**, *126* (46), 15030–15031.
(23) Khew, S. T.; Tong, Y. W. Template-assembled triple-helical peptide molecules: mimicry of collagen by molecular architecture and integrin-specific cell adhesion. *Biochemistry* **2008**, *47* (2), 585–596.
(24) Bachmann, A.; Kiefhaber, T.; Boudko, S.; Engel, J.; Bächinger, H. P. Collagen triple-helix formation in all-trans chains proceeds by a nucleation/growth mechanism with a purely entropic barrier. *Proc. Natl. Acad. Sci. U. S. A.* **2005**, *102* (39), 13897–13902.
(25) Persikov, A. V.; Ramshaw, J. A. M.; Kirkpatrick, A.; Brodsky, B. Triple-helix propensity of hydroxyproline and fluoroproline: comparison of host-guest and repeating tripeptide collagen models. *J. Am. Chem. Soc.* **2003**, *125* (38), 11500–11501.
(26) Bhattacharjee, A.; Bansal, M. Collagen Structure: The Madras Triple Helix and the Current Scenario. *IUBMB Life* **2005**, *57* (3), 161–172.
(27) Paramonov, S. E.; Gauba, V.; Hartgerink, J. D. Synthesis of Collagen-like Peptide Polymers by Native Chemical Ligation. *Macromolecules* **2005**, *38* (18), 7555–7561.
(28) Kotch, F. W.; Raines, R. T. Self-assembly of synthetic collagen triple helices. *Proc. Natl. Acad. Sci. U. S. A.* **2006**, *103* (9), 3028–3033.
(29) Li, Y.; Yu, S. M. Targeting and mimicking collagens via triple helical peptide assembly. *Curr. Opin. Chem. Biol.* **2013**, *17* (6), 968–975.
(30) Malcor, J.-D.; Bax, D.; Hamaia, S. W.; Davidenko, N.; Best, S. M.; Cameron, R. E.; Farndale, R. W.; Bihan, D. The synthesis and coupling of photoreactive collagen-based peptides to restore integrin reactivity to an inert substrate, chemically-crosslinked collagen. *Biomaterials* **2016**, *85*, 65–77.
(31) Jiang, X.; Lim, S. H.; Mao, H.-Q.; Chew, S. Y. Current applications and future perspectives of artificial nerve conduits. *Exp. Neurol.* **2010**, *223* (1), 86–101.
(32) Sandrin, L.; Thakar, D.; Goyer, C.; Labbé, P.; Boturyn, D.; Coche-Guérente, L. Controlled surface density of RGD ligands for cell adhesion: evidence for ligand specificity by using QCM-D. *J. Mater. Chem. B* **2015**, *3* (27), 5577–5587.
(33) Schnicker, N. J.; Dey, M. *Bacillus anthracis* Prolyl 4-Hydroxylase Modifies Collagen-like Substrates in Asymmetric Patterns. *J. Biol. Chem.* **2016**, *291* (25), 13360–13374.
(34) Du, C.; Wang, M.; Liu, J.; Pan, M.; Cai, Y.; Yao, J. Improvement of thermostability of recombinant collagen-like protein by incorporating a foldon sequence. *Appl. Microbiol. Biotechnol.* **2008**, *79* (2), 195–202.
(35) Pakkanen, O.; Pirskanen, A.; Myllyharju, J. Selective expression of nonsecreted triple-helical and secreted single-chain recombinant collagen fragments in the yeast Pichia pastoris. *J. Biotechnol.* **2006**, *123* (2), 248–256.
(36) Peng, Y. Y.; Howell, L.; Stoichevska, V.; Werkmeister, J. A.; Dumsday, G. J.; Ramshaw, J. A. M. Towards scalable production of a collagen-like protein from Streptococcus pyogenes for biomedical applications. *Microb. Cell Fact.* **2012**, *11*, 146.
(37) Werten, M. W. T.; Teles, H.; Moers, A. P. H. A.; Wolbert, E. J. H.; Sprakel, J.; Eggink, G.; de Wolf, F. A. Precision gels from collagen-inspired triblock copolymers. *Biomacromolecules* **2009**, *10* (5), 1106–1113.
(38) Peng, Y. Y.; Stoichevska, V.; Schacht, K.; Werkmeister, J. A.; Ramshaw, J. A. M. Engineering multiple biological functional motifs into a blank collagen-like protein template from Streptococcus pyogenes. *J. Biomed. Mater. Res., Part A* **2014**, *102*, 2189.
(39) Pozzolini, M.; Scarfì, S.; Mussino, F.; Salis, A.; Damonte, G.; Benatti, U.; Giovine, M. Pichia pastoris production of a prolyl 4-hydroxylase derived from Chondrosia reniformis sponge: A new biotechnological tool for the recombinant production of marine collagen. *J. Biotechnol.* **2015**, *208*, 28–36.
(40) Silva, C. I. F.; Teles, H.; Moers, A. P. H. A.; Eggink, G.; de Wolf, F. A.; Werten, M. W. T. Secreted production of collagen-inspired gel-forming polymers with high thermal stability in Pichia pastoris. *Biotechnol. Bioeng.* **2011**, *108* (11), 2517–2525.
(41) Leski, T. A.; Caswell, C. C.; Pawlowski, M.; Klinke, D. J.; Bujnicki, J. M.; Hart, S. J.; Lukomski, S. Identification and classification of bcl genes and proteins of Bacillus cereus group organisms and their application in Bacillus anthracis detection and fingerprinting. *Appl. Environ. Microbiol.* **2009**, *75* (22), 7163–7172.
(42) Engel, J.; Chen, H. T.; Prockop, D. J.; Klump, H. The triple helix in equilibrium with coil conversion of collagen-like polytripeptides in aqueous and nonaqueous solvents. Comparison of the thermodynamic parameters and the binding of water to (L-Pro-L-Pro-Gly)n and (L-Pro-L-Hyp-Gly)n. *Biopolymers* **1977**, *16* (3), 601–622.
(43) Hayashi, T.; Curran-Patel, S.; Prockop, D. J. Thermal stability of the triple helix of type I procollagen and collagen. Precautions for minimizing ultraviolet damage to proteins during circular dichroism studies. *Biochemistry* **1979**, *18* (19), 4182–4187.
(44) Lukomski, S.; Bachert, B. A.; Squeglia, F.; Berisio, R. Collagen-like proteins of pathogenic streptococci: Streptococcal collagen-like proteins. *Mol. Microbiol.* **2017**, *103*, 919.
(45) Yu, Z.; Mirochnitchenko, O.; Xu, C.; Yoshizumi, A.; Brodsky, B.; Inouye, M. Noncollagenous region of the streptococcal collagen-like protein is a trimerization domain that supports refolding of adjacent homologous and heterologous collagenous domains. *Protein Sci. Publ. Protein Soc.* **2010**, *19* (4), 775–785.
(46) Frank, S.; Boudko, S.; Mizuno, K.; Schulthess, T.; Engel, J.; Bächinger, H. P. Collagen triple helix formation can be nucleated at either end. *J. Biol. Chem.* **2003**, *278* (10), 7747–7750.
(47) Areida, S. K.; Reinhardt, D. P.; Muller, P. K.; Fietzek, P. P.; Kowitz, J.; Marinkovich, M. P.; Notbohm, H. Properties of the collagen type XVII ectodomain. Evidence for n- to c-terminal triple helix folding. *J. Biol. Chem.* **2001**, *276* (2), 1594–1601.
(48) Kramer, R. Z.; Vitagliano, L.; Bella, J.; Berisio, R.; Mazzarella, L.; Brodsky, B.; Zagari, A.; Berman, H. M. X-ray crystallographic determination of a collagen-like peptide with the repeating sequence (Pro-Pro-Gly). *J. Mol. Biol.* **1998**, *280* (4), 623–638.
(49) Elangbam, C. S.; Qualls, C. W.; Dahlgren, R. R. Cell Adhesion Molecules—Update. *Vet. Pathol.* **1997**, *34* (1), 61–73.

DOI: 10.1021/acsbiomaterials.7b00583
ACS Biomater. Sci. Eng. 2018, 4, 2106–2114

Supporting Information

Engineered collagen - a redox switchable framework for tunable assembly and fabrication of biocompatible surfaces

Adrian V. Golser, Matthias Röber, Hans G. Börner, Thomas Scheibel

1 page, 1 figure

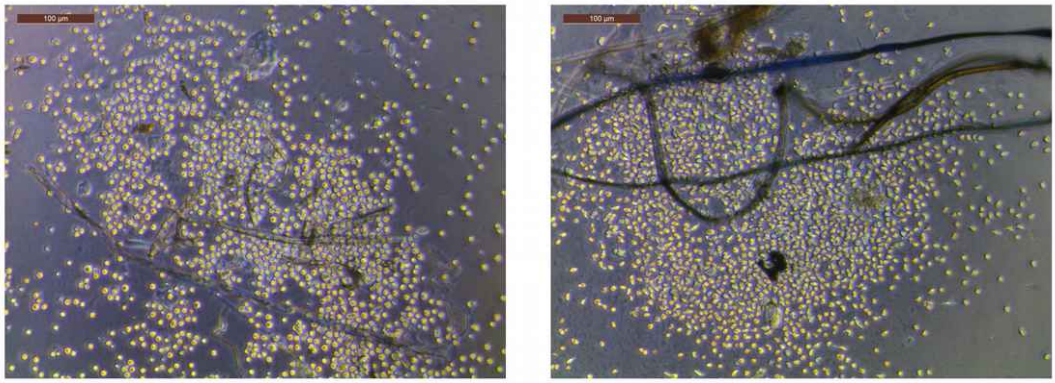

Supporting Figure S1: Films of eCol-WC_2-$(GPP)_7$-RGD (left) and eCol-WC_2-$(GPP)_7$-RGD crosslinked with glutaraldehyde (right) after 1 day of cell culture. The film had partially dissolved from the surface and formed long, unstable fibrillar structures, which were lost during the following culture medium exchange. The round morphology of the fibroblasts suggests poor adhesion.

11 Routes towards Novel Collagen-Like Biomaterials

Bei der genannten Publikation handelt es sich um eine Übersichtsarbeit. Die genannte Teilarbeit wurde von mir als Erstautor verfasst. Das Manuskript wurde dankend mit der Hilfe von Prof. Dr. Scheibel erstellt.

Die Konzeptionierung dieser Publikation wurden von mir am Lehrstuhl Biomaterialen unter der Projektleitung von Prof. Dr. Thomas Scheibel durchgeführt.

[65] – Published by MDPI.

fibers

MDPI

Review

Routes towards Novel Collagen-Like Biomaterials

Adrian V. Golser [1] and Thomas Scheibel [2,*]

[1] Lehrstuhl Biomaterialien, Fakultät für Ingenieurwissenschaften, Universität Bayreuth, Universitätsstraße 30, 95440 Bayreuth, Germany; adrian.golser@bm.uni-bayreuth.de

[2] Bayreuther Zentrum für Kolloide und Grenzflächen (BZKG), Bayerisches Polymerinstitut (BPI), Bayreuther Zentrum für Molekulare Biowissenschaften (BZMB), Bayreuther Materialzentrum (BayMAT), Universität Bayreuth, Universitätsstraße 30, 95440 Bayreuth, Germany

* Correspondence: thomas.scheibel@bm.uni-bayreuth.de; Tel.: +49-921-557-361

Received: 22 December 2017; Accepted: 11 February 2018; Published: 3 April 2018

check for updates

Abstract: Collagen plays a major role in providing mechanical support within the extracellular matrix and thus has long been used for various biomedical purposes. Exemplary, it is able to replace damaged tissues without causing adverse reactions in the receiving patient. Today's collagen grafts mostly are made of decellularized and otherwise processed animal tissue and therefore carry the risk of unwanted side effects and limited mechanical strength, which makes them unsuitable for some applications e.g., within tissue engineering. In order to improve collagen-based biomaterials, recent advances have been made to process soluble collagen through nature-inspired silk-like spinning processes and to overcome the difficulties in providing adequate amounts of source material by manufacturing collagen-like proteins through biotechnological methods and peptide synthesis. Since these methods also open up possibilities to incorporate additional functional domains into the collagen, we discuss one of the best-performing collagen-like type of proteins, which already have additional functional domains in the natural blueprint, the marine mussel byssus collagens, providing inspiration for novel biomaterials based on collagen-silk hybrid proteins.

Keywords: collagen; silk; byssus; tissue replacement; biomaterials; preCol

1. Introduction

Collagens are extracellular, fibrous structural proteins fulfilling a variety of functions related to providing mechanical support. Collagen is historically defined to be a component of the extracellular matrix (ECM) and further characterized by its primary and secondary structure, as well as the potential for hierarchical self-arrangement that can lead to large, complex assemblies. However, several collagens have been described that do not constitute a component of an ECM; for this review, as a simplification, all proteins that contain collagen-like structural elements will be regarded as collagens.

As often in biology, most definitions tend to become blurred around the edges: Since a highly diverse class of collagens is used by mollusks as major load-bearing structures within threads (i.e., mussel byssus [1]), and even another class of natural protein fibers, namely silk, sometimes contain collagen-like motifs [2], it can, depending on the context, be worthwhile to look at collagen as a "sibling" of silk. Both collagen and silk have long been used as suture materials, confirming their suitability for biomedical applications, and have since been developed into a vast variety of biomaterials with remarkable properties. In this review, we try to give an insight into the current approaches of collagen research for use in medicine and try to show recent advances utilizing knowledge gained from the examination of different silk-like structures to yield novel collagen-based materials.

1.1. Molecular Structure of Collagen

Collagen is typically found in all animals, occurring early in evolution in several simple multicellular organisms such as sponges (*Poriferae*) [3] and *Cnidariae* [4]; however it is not present in plants and fungi, where its role has been taken over by polysaccharides such as cellulose and chitin. While it has been shown that collagen plays a crucial role in the formation of the animal extracellular matrix [5], collagen-like proteins have also been identified in several bacteria [6], where they mask the bacterial cell from animals' immune receptors and facilitate the formation of biofilms as well as the adhesion to host tissue.

Not taking into account several exceptions from the rule, such as collagen-based insect silks which are spun from specialized glands [2], collagens in higher eukaryotes are generally not secreted outside the respective tissue and contribute to and often largely define its mechanical and biochemical characteristics. While several classes of collagens are fibrous, especially those abundantly found in bone, skin, tendon, cartilage and connective tissues (types I, II, III, V, XI, XXIV and XXVII) [7], most people associate collagen with gelatin (made from type I collagen).

While the extraction of gelatin from collagen-rich tissues involves partial hydrolysis of the protein, as well as the partial or complete unfolding of the triple helix due to thermal denaturation, some mild extraction methods for triple helical collagen exist (see below) [8,9].

Although based on the same polypeptide, gelatin and collagen have vastly different properties, which largely stem from the fact that mature collagen has lost its ability to self-assemble into discrete fibrils, and therefore, once the triple helix has been denatured, restructures into an amorphous gelatin network.

Recent advances in both the recombinant production of synthetic collagen-like proteins and new, mild extraction and purification techniques out of natural sources, as well as the advanced processing of these extracts have opened a range of possibilities allowing the production of collagen-based materials with remarkable mechanical and biological properties. Many new methods to process collagen are biomimetic and some are inspired by the natural fiber spinning process of silk-producing animals [10–12].

Collagen fibers are hierarchically assembled structures that can be readily identified by their amino acid sequence [13]. A specific consensus sequence has been identified for collagen which follows the pattern $(GXY)_n$, with the *X*-position often being proline residues and the *Y*-position often being 4-hydroxyproline residues. On a genetic level the high glycine and proline content of collagen-encoding genes creates GC-rich patches, which makes the identification of such genes from genomic sequences difficult, so that most known collagen sequences were obtained by cross-referencing cDNA-libraries with Edman-based peptide sequencing [14,15].

The $(GXY)_n$ consensus sequence can be explained by the spatial requirements for the formation of the triplehelical collagen tropomolecule [16]: Being a right-handed triple-helix with one turn every three amino acids and a very narrow diameter of 1.6 nm, in order for the molecule to fold, steric hindrances due to bulky amino acid side chains must be omitted on every position pointing said residue inwards, explaining the occurrence of glycine as every third residue. This glycine is essential, and mutations or deletions of the consensus motif have been shown to have a strong destabilizing effect on the collagen molecule, often described as "nicks" due to the localized breaking of the rigid helix and the resulting angular flexibility [17,18].

The amino acid distribution of the X- and Y-position is less stringent but, for most animal collagen, contain a comparably high amount of proline and 3- or 4-hydroxyproline, since these residues are slightly more stable than other amino acids in their cis-configuration, which is closer to the ideally required angle within the helix and thereby increases the thermodynamic stability of the fibril. The hydroxyl group of hydroxyproline, which is added post-translationally by specific enzymes (e.g., proline-4-hydroxylase, P4H), further increases the helical stability by allowing the formation of intermolecular hydrogen bonds between the α-chains involved in helix formation. Insufficiently hydroxylated collagen helices tend to partially unfold, thereby destabilizing the collagen fibrils and

tissues based thereon, resulting in the pathological condition known as scurvy [19]. Some collagen-like proteins, such as streptococcal bacterial collagens [6,20–23] and sawfly cocoon silk [2], do not contain hydroxyproline and instead stabilize the triple helix via the formation of intermolecular salt-bridges between charged amino acids.

Since collagen is a highly abundant class of proteins that fulfills a variety of roles, it also contains a highly diverse group of subclasses. The main variances between collagen subtypes are not necessarily large differences in the collagen helix, but the presence of non-collagenous functional domains flanking the collagen core domain, which provide additional functionalities and physicochemical properties to the molecule.

The mollusk byssus threads, produced by the mussels *Pinnidae*, *Mytilidae* and the *Dreissenidae*, serve as a holdfast structure and have extraordinary mechanical and chemical properties being able to resist the harsh environment of the intertidal zone in which these species reside, and combine features of structured, collagen-based block copolymers, as well as the concept of crystalline silk-like domains within an amorphous matrix. The byssus thread is produced in a specific secretory organ, the so-called mussel foot, which, in addition to its main anchoring function, serves as the main sensory and locomotive organ in the young mussel. The soluble byssus precursor proteins are excreted into a groove within this gland, where they are believed to be mixed and molded into the required shape by the flexible mussel foot and, after successful attachment via the formation of an adhesive plaque to a suitable surface has been achieved, quickly form an insoluble fiber upon opening of the groove as they come in contact with the seawater [24].

The "sibling" material silk typically comprises distinct, specialized proteins (fibroins) [25], and they strongly differ from fibers within the ECM in that they have usually been spun by the animal, i.e., processed from a highly-concentrated precursor solution within dedicated glands that can very tightly control the necessary parameters influencing fiber formation, such as drawing speed, pH and the concentration of salts and metal ions [26].

1.2. Motivation

The aim of this review is to give an insight into the current state of natural and synthetic fibrous collagens regarding their use as surgical sutures in wound repair and tissue engineering. Applying an understanding of the established processing of silk towards processing of collagen and collagen-like materials might be a way to overcome the shortcomings of current manufacturing collagen-based biomaterials.

2. Collagen as a Biomaterial

Due to the similarity of the collagen sequence and content within the extracellular matrix of different vertebrate species, animal-derived collagen is an attractive material for biomedical applications, because it is often compatible with the existing extracellular matrix of a receiving patient regardless of source or processing. Since the triple-helical fold typically does not induce an immune response, collagen is non-antigenic, as well as non-toxic, biodegradable (the rate of degradation is controllable via chemical crosslinking), can be formulated in a variety of shapes and forms, and is chemically modifiable to fulfill many specific purposes [27].

Collagen-based biomaterials are used as bacteriostatic shields and barriers, as sponges and pellets for tissue regeneration and accelerated blood coagulation, as gels for sustained drug delivery, as absorbable surgical sutures (catgut), as well as grafts for tissue engineering and replacement of tendons, bones, blood vessels and skin [28].

Most of the collagen used for these purposes has been extracted from animal sources and consists largely of the most abundant type I collagen. During the natural aging of collagen, intermolecular crosslinks with other molecules inside the ECM are formed, which makes the extraction of high-purity single molecule fibrils difficult especially from adult animals, and increases the cost of products that require pure, soluble tropocollagen in its non-hydrolyzed triple helical form. Therefore, many

formulations allow for a variable degree of crosslinking or hydrolysis and proteolytic degradation, although both of these processes increase the complexity and variability of the handling and processing of extracted collagen between batches.

Having access to a source of collagen-like materials allowing the same kind of biocompatibility but show no batch-to-batch variability in their biophysical and chemical properties would immensely support the establishment of collagen-based products.

2.1. Towards Spun Collagen Fibers

Surgical sutures, historically known as catgut [29], have been a major utilization for collagen fibers in biomedical applications, since they get readily resorbed into the surrounding tissue over time and thereby promote wound healing and tissue regeneration. While catgut collagen is prepared from the decellularized small intestine of sheep and is therefore a fully matured and cross-linked collagen network that has been reshaped into fibers by cutting and stripping, its mechanical properties, although poor compared to that of silks and synthetic polymers in terms of toughness and ultimate stress, are still well suited for its purpose: Given that the catgut suture closely resembles the original structure of the intestinal endothelium, the elastic modulus is very similar to that of most internal soft-tissue ECMs and therefore will show comparable deformation when stressed, which in turn reduces the strain on the suture itself.

Nevertheless, the biomechanical properties of living tissue in the human body span several orders of magnitude both in elasticity and toughness [30], with, for instance, an aorta valve having a low ultimate stress of 0.3–0.8 MPa, compared to that of skin (1–20 MPa) or tendon (50–100 MPa). Ruptured cartilage, tendon and bone, even though they mostly consist of type I collagen, cannot typically be sutured with catgut, since the material does not have the required tensile strength and toughness, and instead require the use of synthetic materials with lower biocompatibility and no biodegradability [31].

Researchers have therefore begun to investigate processing methods in order to improve the mechanical properties of collagen-based fibers and thereby tailor the material to the requirements of the tissue it is intended to be used in. One major improvement was the wet-spinning of extracted or recombinantly produced, soluble collagen [10,12,32], which demonstrated the possibility of producing fibers from this source material outside of a biological system. Since the mechanical properties were still poor, these materials were mostly used to demonstrate their applicability for in vitro tissue engineering. However, due to the high cost of soluble full-length collagen, no commercial products have been made available so far.

Another recent approach [11] used a microfluidic system to produce mechanically highly stable fibers from acid-soluble type 1 collagen (Figure 1). The authors suggest that the small diameter and the directional laminar shear forces in the spinning channel help in axially aligning the collagen fibrils in a fashion comparable to the fibril formation from tropocollagen during biosynthesis, thereby yielding a product with similar mechanical characteristics as tendon.

All of these approaches use the intrinsic property of collagen triple helices to be soluble but still folded in dilute acetic acid and therefore require an independent first step inducing the folding of the collagen triplehelix from the α-chain precursors. As a result of this limitation, no conditions such as high temperature or denaturing solvents, which would melt the triple helix, can be used during production, processing and sterilization. It is, therefore, highly desirable to find collagen-like proteins that intrinsically possess the ability to form soluble triple helices without requiring complex biological systems and mild conditions for their manufacture.

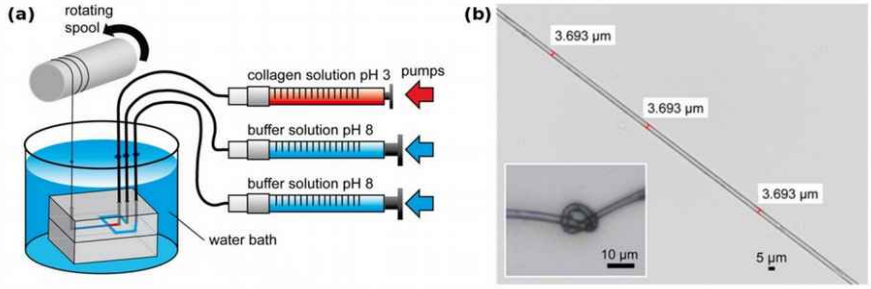

Figure 1. (**a**) Collagen microfibers are produced within a PDMS microfluidic chip from a soluble precursor solution (pH 3 in dilute acetic acid). Thread formation takes place at the junction that brings the spinning solution in contact with the pH 8 buffer solution. The flowrate of each solution is tightly controlled by independent syringe pumps; (**b**) the resulting collagen fiber is highly homogeneous and has remarkable mechanical properties comparable to that of tendon, while still being flexible enough for downstream processing. Modified with permission from [11] (ACS, 2016).

2.2. Collagen-Analogues as Basis for Future Biomaterials

As mentioned above, biomaterials based on natural collagens today are still mostly decellularized animal tissues that have been mechanically or chemically processed into the desired morphologies. This approach carries the intrinsic risk of adverse immunological reactions in the receiving patient due to allergies towards the graft [33], as well as the spreading of viral or prion-based contaminants [34].

The currently used methods for the extraction of soluble collagen from tissue include the use of mild solvents (phosphate buffered salt solution; dilute acetic acid) [9], which yield full length triple helices that still contain the terminal telopeptides. The best yields are gained when collagen is extracted from young tissues, such as calf skin and rat tail. Another option employs proteases such as pepsin, which utilizes the enzyme's unspecific activity to digest all non-collagen-like domains and therefore removes telopeptides, which results in higher yields even from more strongly cross-linked tissues [35].

Recently, collagen-based scaffolds for tissue engineering have been produced from solubilized and purified collagen that often has been blended with other polymers due to the limited availability of the soluble collagen source material [36,37].

When purified collagen is required for the production of mechanically stable biomaterials such as grafts for tendon replacement, the trade-off between batch-to-batch homogeneity and yield will always be a restricting factor. While large amounts of animal tissue are available for the extraction of collagen not intended for clinical use, the current sources of human collagen are limited to scarcely available extractable tissues (such as dermis) [8] and biotechnologically produced collagen made from human fibroblast cell culture (e.g., CosmoDerm) [38].

To overcome these limitations, different approaches have been made to find substitutes for natural vertebrate collagen which have adequate properties for tissue engineering, regenerative medicine and other biomedical applications.

Collagen mimetic peptides were originally used in determining the structure, stability and folding kinetics of collagen and collagen-like sequences [39–41], which provided remarkable insight into the role of each amino acid within the $(GXY)_n$-repetitive sequence and led to attempts at stabilizing short triplehelical peptides by incorporating non-canonical amino acids, such as 4-fluoroproline [42] or N-isobutylglycine [43]. Furthermore, these experiments identified the reason for the comparably slow folding of nucleated triplehelices to be based upon the slow cis/trans-isomerization rates of residues in the X- and Y-positions [44–46].

Using these peptides, researchers also noted that the formation of gelatin-like networks could be largely avoided by incorporating amino- or carboxyterminal nucleation sites that would

promote helix formation within the cross-linked trimer at a much higher rate than between non-nucleated single-chain constructs [44,46]. Possible nucleation sites can be TRIS-scaffolds [47,48], 1,2,3-propan-tricarboxylic-acid scaffolds [49], collagen III derived cystine knots [50] and bacterial or bacteriophage-derived protein domains [20,51].

All of these approaches use peptide synthesis, which is typically limited to a maximal peptide length of 30–50 amino acids. Since most collagen sequences are strictly water soluble but tend to form gels at higher molecular weights, peptide synthesis suffers from problems with limited solubility and aggregation as the molecular weight (MW) increases. Native chemical ligation has been used to increase the chain length after synthesis [52], which increased the thermal stability of the product but reduced the MW homogeneity of the resulting proteins.

Biotechnological collagen production is non-trivial and suffers from the complex requirements of collagen synthesis (Figure 2a). In vivo, human type I collagen is assembled within fibroblasts from two pro-α1(I) and one pro-α2(I) protocollagen chains, both around 1400 amino acids long, to form a procollagen triplehelix. Both the α-collagens as well as the procollagen get enzymatically modified by prolyl-3-, prolyl-4- and lysyl-oxidase, after which the N- and C-terminal telopeptides are cleaved by specific proteases to yield the 300 nm long tropocollagen triplehelix. These tropocollagen trimers can then assemble into collagen fibrils during secretion and further form macroscopic collagen fibers with varying degrees of chemical crosslinking [53,54].

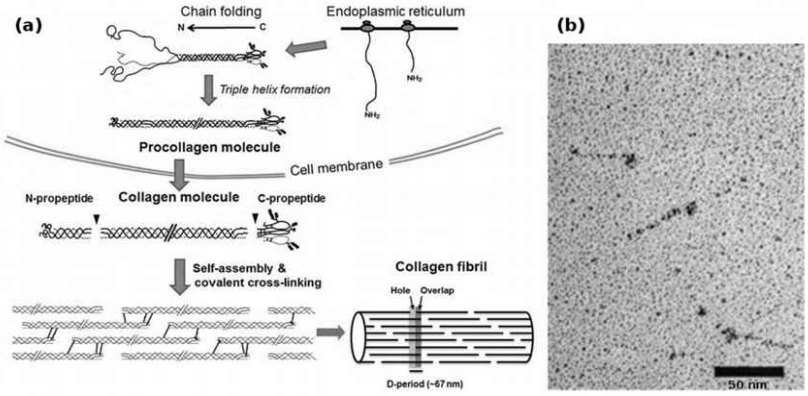

Figure 2. (**a**) Biosynthesis of fibrillar collagens within the ECM. After translation, the nascent α-chains assemble into procollagen within the endoplasmic reticulum. During and after secretion, the propeptides are cleaved by specific enzymes, yielding the soluble tropocollagen molecule, which quickly self-assembles into collagen fibrils. These fibrils can then form collagen fibers; (**b**) transmission electron micrograph of recombinantly produced bacterial Scl1 collagen, showing the globular terminal V-domain and the rod-like collagen helix. Bacterial collagen does not assemble into fibrils. Modified with permission from [53] (**a**) (Portland Press 2012) and [21] (**b**) (American Society for Biochemistry and Molecular Biology, 2002).

The most common bacterial production host, *E. coli*, is unable to produce full-length collagens due to size constraints, but has successfully been utilized in the production of "collagen-like proteins" [55], which are truncated proteins derived from human collagen. Nevertheless, *E. coli* has no intrinsic apparatus to catalyze the aforementioned secondary modifications, which therefore result in unstable products, mostly due to the lack of 4-hydroxyproline. A newly discovered bacterial P4H found in *Bacillus anthracis* [56,57], might be able to overcome this limitation in future experiments. In addition, recent advances have been made in coexpressing eukaryotic proline-4-hydroxylase in origami-type *E. coli* [58], which provides conditions similar to that of the endoplasmic reticulum (ER) within

its cytosol and therefore allow the activity of the transgenic P4H-complex, as well as the yeast *P. pastoris* [59,60] which, being an eukaryote, has the necessary organelles for early-stage collagen assembly and the ability to produce high MW proteins, although only with poor yields and varying degrees of hydroxylation [61,62].

Interestingly, bacterial collagen-like proteins have been identified [21], which function as a virulence factor in *Streptococcus pyogenes*: The Scl1 and Scl2 proteins are secreted and carboxyterminally anchored within the cell wall of the bacterium, where a terminal domain induces trimerization and, thereby, nucleation resulting in the formation of stable triple helical collagen rods (Figure 2b). The proteins then attach to collagen-binding proteins in the extracellular matrix and shield the bacterium from the immune system of e.g. vertebrates. On a structural basis, these proteins are remarkable, because they contain no non-canonical amino acids, and instead of utilizing hydroxyproline, stabilize the collagen helix by forming salt bridges via charged amino acids between the α-chains [22]. In addition, the trimerizing V-domain has been shown to be an effective collagen nucleation inducer, even for non-streptococcal collagens and collagen-mimetic peptides [20].

These bacterial collagen-like proteins can be recombinantly produced in high yields in common bacteria such as *E. coli*. When the immunogenic V-domain is proteolytically cleaved and the remaining collagen cross-linked to increase the thermal stability, they have been shown to be non-immunogenic when implanted into mice for up to 6 weeks [63].

However, it is unclear whether long-term presence and degradation of bacterial collagen-like proteins exposes the host to short, immunogenic peptides, since several examples are known that show different immunogenity between triplehelical and denatured collagen [64–67].

Nevertheless, since these proteins circumvent all the problems associated with the production of eukaryotic collagens in bacterial hosts mentioned earlier, they are strong candidates for future materials based thereon; however, their low melting point of 36–38 °C requires the presence of a non-collagenous folding domain which has been shown to be strongly immunogenic [63] and necessitates other means of stabilization, such as glutaraldehyde crosslinking, once this domain has been removed. Increasing the stability of the Scl2 protein by multimerization does not significantly increase its melting point [68]. Therefore, while the low temperature stability of the Scl proteins is of no consequence for the production of three-dimensional scaffolds [69–71], it hinders the spinning of stable collagen fibers.

The three collagen-like proteins found in sawfly silk (SfC A-C) [2] have been recombinantly produced in a similarly successful fashion, but so far they have not been investigated as potential future biomaterials.

Engineered collagens (eCols) are closely related to collagen mimetic peptides but are produced biotechnologically in *E. coli*. A model collagen consisting of $(GPP)_{50}$ produced at high yields, was found to be sufficiently stable to be used in common applications even without containing hydroxyproline, and, when an aminoterminal nucleation site was introduced, demonstrated the ability to form collagen triple helices rather than gelatin networks [72]. The mentioned eCol has been successfully used as a matrix for the fixation of collagen-mimetic peptides without the use of crosslinking agents, and could be used as a substratum in cell culture, showing its applicability for tissue engineering.

In addition, fully synthetic genes also allow the direct incorporation of integrin-specific cell adhesion sites, such as the RGD motif and more collagen-typical adhesion sites such as GFOGER-like sequences [73]. When processed into more tightly packed structures such as fibrils and fibers, direct integrin mediated cell adhesion has been shown to be impaired [74], and thus will possibly require more complex solutions to mediate the adhesion between eCol-fibrils and the cells within the ECM. One recently described group of proteins, the so-called COLIBRIs (COLlagen INtegrin BRIdging proteins) [75,76], which form a bridge between natural fibrillar collagen and integrin including the well-known proteins fibronectin and von Willebrand factor, might be able to fulfill this role. Thus, despite the promising results, the development of eCols is still in its early stages.

Synthetic collagen-based block copolymers are artificially designed constructs and combine some of the approaches mentioned so far. When short collagen-like $(GPP)_n$-peptides are positioned around

a hydrophilic unstructured core domain and expressed in *P. pastoris*, a stable gelatin-like hydrogel can be produced with high yields [77,78]. Since these structures, like engineered collagens, are based on synthetic genes, the addition of short peptide sequences such as cell adhesion motifs or calcification sites is trivial. When the same authors replaced the randomized central sequence with a *B. mori*-inspired silk sequence and the $(GPP)_n$-motif with a hydrophilic $(GXY)_n$-polymer containing a large amount of charged amino acids in the X and Y position, they obtained a hybrid material that formed micelles and fibrils depending on pH, thereby confirming that rational design on the basis of silk and collagen is possible [79].

However, the most successful example for a collagen-based block copolymer is provided by nature: The class of collagens, so-called preCols, found in the byssus produced by marine mussels as a hold-fast structure.

3. Mussel Byssus-Silk, Collagen or Both?

Among the byssus-producing mussels, the blue mussel, *Mytilus edulis* and the closely related mediterranean mussel *Mytilus galloprovincialis* are the best characterized. These species produce a bundle of threads which connects the soft mussel to the substrate, and the threads show a mechanical gradient with increasing stiffness from the proximal to the distal portion of the fiber. This allows the byssus to dissipate high amounts of mechanical energy without causing radial stress between the parts with highly different elastic moduli, thereby withstanding the mechanical challenges caused by the tidal currents without damaging the soft mollusk's organs and tissues.

The byssus thread itself is rather complex and contains a large set of matrix proteins, called mussel foot proteins (mfp's), which, in addition to contributing to the chemical and physical properties of the fibrous portion of the thread, form an adhesive plaque that is just as remarkable as the rest of the byssus, since it provides strong and durable underwater adhesion to a variety of substrates with different chemical compositions. These somewhat amorphous matrix proteins interact with the main load bearing structure of the byssus, which are called preCols because of their collagen-like structure.

The three known preCols of *M. edulis* are block-copolymers which consist of a central collagen-like core domain that is surrounded by flanking domains [80].

Even though the preCols differ strongly from vertebrate collagens in that they are homotrimers and do not undergo the same kind of propeptide processing, their central collagen-like core domain has been described to be most closely related to that of fibrillar collagens (type I–III) [81]. It has to be noted, however, that most of the mechanical properties of the preCols are attributed to the flanking domains, which make up a significant portion of every preCol [14,81,82].

Depending on the type of preCol, these flanking domains contain motifs that are similar to other structural proteins: preColD contains silk-fibroin-like flanks, the flanks of preColP shows similarity to elastin and preColNG contains plant cell wall-like sequences, which include features of alanine-rich β-sheets as well as glycine-rich helices (Figure 3a,b). While the macroscopic byssus threads of *M. edulis* and *M. galloprovincialis* differ slightly in size and in their mechanical properties, the preCols are closely related on a molecular level and only differ in short inserts/deletions and point mutations [83].

In addition to the flanking domains, the preCols all contain terminal domains which are rich in histidine and 3,4-dihydroxyphenylalanine (DOPA, post-translationally oxidized tyrosine) which form sacrificial metal ion mediated complexes that can absorb mechanical stress and reassemble over time without taking damage [84]. In addition, they undergo a slow quinone-based tanning, thereby forming irreversible crosslinks with other proteins in the byssus and providing a redox-dependent mechanism further stabilizing the byssus [85,86].

One remarkable observation is the fact that the previously mentioned mechanical gradient corresponds to the abundance of preColP and preColD within the respective section of the byssus thread. The proximal section of the byssus, which connects to the stem within the mussel and has a Young's modulus of around 50–80 MPa, is rich in preColP; while the distal portion with a stiffness of

E_i = 500–600 MPa contains high amounts of preColD [83]. The third mussel byssus collagen, preColNG, has a constant concentration throughout the thread (Figure 4).

With the preCols making up between 70% and 90% of the protein fraction of the byssus thread, it stands to reason that these flanking domains have a high influence on the mechanical properties of the fiber, and for biotechnologically produced preColD it could be shown that β-sheet crystals could be induced within the protein by ethanol treatment in a similar fashion as with materials made of silk fibroin or biotechnologically produced spider silk proteins [87].

Investigation of the biotechnologically produced cwCT-domain derived from the carboxyterminal flank of preColNG showed that this protein undergoes reversible structural transitions between random-coil and β-hairpin structures when in contact with lipid vesicles, suggesting that the flanking domains of this preCol can be triggered by external stimuli during byssus formation and thereby greatly influence the overall properties of the thread in a switchable fashion [88].

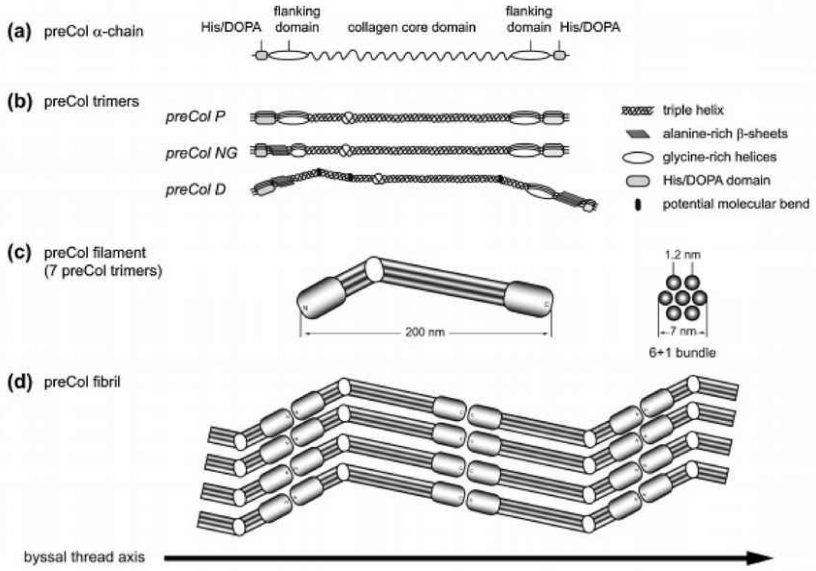

Figure 3. Model of the molecular structure of preColD, P and NG trimers and preCol arrangement. (**a**) preCol α-chains comprise a collagen core domain, flanking domains and terminal His/DOPA-enriched regions; (**b**) Proposed structure of the preCol homotrimers folding into a rod-like triple helical central domain. Perturbations of the regular collagen motif $(GXY)_n$ result in either an unwinding of the triple helix, increasing the molecular flexibility (glycine deletions), or in putative molecular bends (glycine substitutions in preColD); (**c**) The preCol filaments consist of 7 preCol trimers forming a 6 + 1-bundle; (**d**) Linear arrangement of the preCol filaments in head-to-head and tail-to-tail orientation parallel to the thread axis. Figure and caption used with permission from [89] (Elsevier, 2014).

As other authors have noted [89], this suggests that the distal portion of the mussel byssus is likely a β-sheet crystalline particle reinforced polymer matrix, providing a nearly 10-fold increase in stiffness and a threefold increase in breaking stress and toughness compared to that of the proximal portion of the fiber, which can be viewed as a fiber reinforced polymer with dedicated elastic domains.

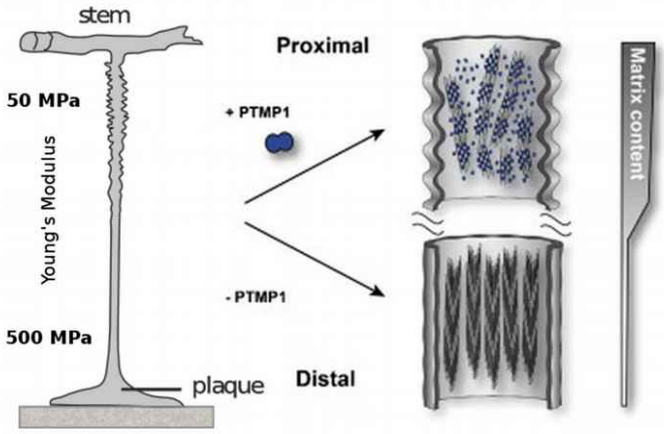

Figure 4. The proximal part of the mussel byssus is elastic and contains fibrils of preColP embedded in a matrix of PTMP1 (proximal thread matrix protein 1). This matrix protein allows the fibrils to slide freely and act as within a fiber-reinforced composite material. The distal portion of the mussel byssus has a much higher stiffness, in addition to the ability to dissipate large amounts of mechanical energy without taking irreversible damage. The content of matrix protein in the distal thread is much lower and the collagen domains, instead of reinforcing an amorphous matrix, are tightly packed around silk-like crystalline β-sheets. Modified with permission from [89] (Elsevier 2014).

3.1. Hierarchical Assembly and Structure of preCols in the Byssus

During biosynthesis, the preCol monomers form homotrimers of their unfolded α-chains before being transported into storage vesicles. During this stage, the rod-like trimers further assemble into hexagonal higher-order 7 + 1 structures, in which they are stored until the byssus neogenesis triggers secretion (Figure 3) [90,91]. The morphology of these pre-secreted structures suggest that the collagen domain has a large influence on the early stages of assembly, whereas the other functional groups, such as the flanking domains and the His/DOPA-rich termini are kept inactive until they get molded into the final byssus thread within the mussel foot groove. This activation is most likely a result of the preCols coming into contact with a different chemical environment (oxidizing, high pH), the sudden presence of matrix proteins which have been shown to interact with preCols [92], and the influence of mechanical stimuli introduced by contractions within the mussel foot.

As mentioned above, the proximal section of the mussel byssus differs from classical silk in that it comprises a dedicated mix of matrix proteins which embed the load-bearing, fibrous preCols. In this portion of the byssus, matrix proteins, in particular the proximal thread matrix protein (PTMP)1 with two von Willebrand factor-like domains (which makes up about 30% of the proximal byssus), strongly interact with the preCol-assemblates and is thought to have a great influence on the higher order assembly of preColP and NG [93]. The current understanding is that PTMP1 builds a soft matrix with the ability to bind and lubricate the rod-like preCol during deformation, thereby forming a classical fiber-reinforced polymer with the ability to mitigate shear-induced damage to the comparably stiff collagen fibrils, while still allowing enough movement for the flanking domains to exercise their elastic behavior (Figure 4).

Given that the distal portion of the fiber contains more than 90% (*w*/*w*) preCols, however, many of the physical attributes of the distal byssus must stem from the intrinsic ability of preColD to form stable assemblies without requiring the interaction with other mussel foot proteins. Most of its properties can therefore be explained by the hierarchical arrangement of preCols, which is a result of the block-like character of the protein. Instead of being a fiber reinforced matrix, the distal byssus thread is more

like a particle reinforced block-copolymer, with the β-sheet crystals formed by the preColD-flanks embedded in a densely packed collagen matrix (Figure 3).

This would explain the threefold higher prevalence of defects in the collagen sequence ("nicks") of preColD compared to preColP: Instead of being the ultimate load-bearing structure within a soft matrix (proximal byssus thread), the distal collagen domain of preColD is the flexible component in a particle reinforced system during low-stress situations and therefore absorbs small amounts of force before stronger mechanical loads result in the gradual unfolding of sacrificial bonds within the His/DOPA-termini and, subsequently, the β-crystalline flanks [94].

3.2. Chemical Modifications of Byssus Proteins

The mussel byssus collagens are based on the canonical amino acids but, after being secreted into the ER, undergo two kinds of chemical modification that have a strong influence on the stability of the resulting material.

Like most kinds of collagen, the repetitive sequence (GXY) often contains 4-hydroxyproline at the Y position because of the stabilizing effect of the resulting hydrogen bond with adjacent collagen chains. The chemical reaction is catalyzed within the ER by a mussel prolyl-4-hydroxylase (P4H) [95], which, due to the low solubility of the α-subunit, has not been well characterized [96]. Like in other collagens, the absence of hydroxyproline manifests itself in a lower stability of the collagen helix and thereby a lower melting point, a less compact collagen assembly and a higher tendency to unfold under destabilizing conditions.

The second preCol-modification is the oxidation of tyrosine by a tyrosinase, an ER-resident oxidase that produces DOPA from tyrosine within the His/DOPA-rich termini of the protein. When oxidized, these residues, in addition to the metal-chelation and tanning mentioned earlier, are also responsible for many of the covalent connections to other mussel foot proteins via crosslinks based on lysine, cysteine and histidine residues [80]. Although not yet observed for the preCols, many of the adhesive properties of the adhesive plaque can be attributed to the presence of DOPA within mfp-3 [97], which gets modified by the same enzyme.

These secondary protein modifications make it hard to investigate byssus proteins, mostly because of the inability to extract these highly cross-linked proteins from the thread and the difficulty to biotechnologically produce preCols and preCol-analoga with high levels of proline hydroxylation.

3.3. preCol-Based Biomaterials

Extraction of preCols without partial hydrolysis is not possible from the byssus because of the high degree of crosslinking, while the extraction of soluble proteins from the mussel foot is not feasible due to low yields [24]. While efforts have been made to use reconstituted mussel byssus as functional biocompatible matrices that retain some of the properties of the natural threads, mainly the ability to modify their mechanical behavior upon metal-ion binding, the overall mechanical performance is not comparable to that of pristine byssus threads [98].

The length of >1000 amino acids as well as the collagen-typical posttranslational processing challenges the biotechnological production in the same fashion that other full-length collagens do. Furthermore, it was shown that the expression of the isolated flanking domains [88] of most preCols is only possible in *E. coli* when they are combined with stabilizing tags, such as SUMO (small ubiquitin-like modifier) [99].

Despite these challenges, it was recently possible to express and purify non-hydroxylated preColD in the yeast *P. pastoris*, which showed the ability to form fibrils and which could be post-treated to selectively convert the unstructured flanking domains into β-sheets [87]. While it is unlikely that biotechnologically produced, full-length mussel byssus collagens will directly be used as biomaterials for tissue engineering due to concerns regarding possible immunogenic properties, their block-like assembly could add a variety of functional domains to the toolkit of synthetic biology towards the design of tailored collagen-like materials for biomedical applications. Furthermore, it might be possible

to rationally design block-copolymers which resemble the overall structure of preColD, but consist of domains that have independently been shown to be fully biocompatible.

4. Conclusions

The major drawback in creating collagen-based fibers from soluble precursors is the limited availability of extractable source material: While an abundance of cheap, collagen-rich animal tissues is available that can readily dismiss the low yields of some methods such as acetic acid extraction, the scarcity of human tissue for collagen production often justifies the use of pepsinization to improve extraction yield but simultaneously reduce product homogeneity. Even though several biomaterials can be manufactured from partially degraded tropocollagen or even gelatin-like polypeptides, the production of high-performance materials, such as fibers spun using a microfluidic technology showing tendon-like mechanical properties, has only been possible with highly homogeneous, soluble collagen containing intact, non-cross-linked telopeptides.

The biotechnological production of natural collagens is currently limited by the large size of the proteins and the high level of posttranslational modification (e.g., cleavage of prepeptides, proline and lysine hydroxylation, prearrangement into nanofibrils) that often cannot be emulated by most production hosts, while collagen-mimetic peptides produced by solid phase synthesis are even more constrained regarding the size of the resulting product.

Future collagen-like proteins used in biomedical applications will most likely overcome these problems by incorporating a variety of strategies to simplify the requirement of post-translational modification, or omit them completely, such as nature does in bacterial and insect silk collagen. Other possible strategies might be to modify the collagen protein sequence to not require non-canonical amino acids and still be structurally stable, as well as utilizing stabilizing domains inspired by a variety of hosts, such as flanking domains derived from the mussel byssus preCols, which will likely be incorporated in a block-copolymer-like fashion and provide specifically engineered functionalities.

In conclusion, examples are presented for the successful use of synthetic biology and *ab initio* design, combined with biotechnological protein production, as well as the applicability of processing methods inspired by the processing of natural and artificial silks, to create novel types of high-performance, biocompatible, collagen-based materials.

Acknowledgments: This work was funded by the Deutsche Forschungsgemeinschaft (DFG), reference SCHE 603/14-1. Adrian Golser received support according to the Bayerische Eliteförderungsgesetz (BayEFG).

Conflicts of Interest: The authors declare no conflict of interest. The founding sponsors had no role in the design of the study; in the collection, analyses, or interpretation of data; in the writing of the manuscript, and in the decision to publish the results.

References

1. Bouhlel, Z.; Genard, B.; Ibrahim, N.; Carrington, E.; Babarro, J.M.F.; Lok, A.; Flores, A.A.V.; Pellerin, C.; Tremblay, R.; Marcotte, I. Interspecies comparison of the mechanical properties and biochemical composition of byssal threads. *J. Exp. Biol.* **2017**, *220*, 984–994. [CrossRef] [PubMed]
2. Sutherland, T.D.; Peng, Y.Y.; Trueman, H.E.; Weisman, S.; Okada, S.; Walker, A.A.; Sriskantha, A.; White, J.F.; Huson, M.G.; Werkmeister, J.A.; et al. A new class of animal collagen masquerading as an insect silk. *Sci. Rep.* **2013**, *3*. [CrossRef] [PubMed]
3. Fidler, A.L.; Vanacore, R.M.; Chetyrkin, S.V.; Pedchenko, V.K.; Bhave, G.; Yin, V.P.; Stothers, C.L.; Rose, K.L.; McDonald, W.H.; Clark, T.A.; et al. A unique covalent bond in basement membrane is a primordial innovation for tissue evolution. *Proc. Natl. Acad. Sci. USA* **2014**, *111*, 331–336. [CrossRef] [PubMed]
4. Holland, J.W.; Okamura, B.; Hartikainen, H.; Secombes, C.J. A novel minicollagen gene links cnidarians and myxozoans. *Proc. R. Soc. B* **2011**, *278*, 546–553. [CrossRef] [PubMed]
5. Exposito, J.-Y.; Cluzel, C.; Garrone, R.; Lethias, C. Evolution of collagens. *Anat. Rec.* **2002**, *268*, 302–316. [CrossRef] [PubMed]

6. Lukomski, S.; Bachert, B.A.; Squeglia, F.; Berisio, R. Collagen-like proteins of pathogenic streptococci: Streptococcal collagen-like proteins. *Mol. Microbiol.* **2017**, *103*, 919–930. [CrossRef] [PubMed]
7. Bella, J.; Hulmes, D.J.S. Fibrillar Collagens. In *Fibrous Proteins: Structures and Mechanisms*; Parry, D.A.D., Squire, J.M., Eds.; Springer International Publishing: Cham, Switzerland, 2017.
8. Pacak, C.A.; MacKay, A.A.; Cowan, D.B. An improved method for the preparation of type I collagen from skin. *J. Vis. Exp. JoVE* **2014**. [CrossRef] [PubMed]
9. Mocan, E.; Tagadiuc, O.; Nacu, V. Aspects of collagen isolation procedure. *Curiecul Med.* **2011**, *2*, 320.
10. Yaari, A.; Schilt, Y.; Tamburu, C.; Raviv, U.; Shoseyov, O. Wet spinning and drawing of human recombinant collagen. *ACS Biomater. Sci. Eng.* **2016**, *2*, 349–360. [CrossRef]
11. Haynl, C.; Hofmann, E.; Pawar, K.; Förster, S.; Scheibel, T. Microfluidics-produced collagen fibers show extraordinary mechanical properties. *Nano Lett.* **2016**, *16*, 5917–5922. [CrossRef] [PubMed]
12. Zeugolis, D.I.; Paul, R.G.; Attenburrow, G. Post-self-assembly experimentation on extruded collagen fibres for tissue engineering applications. *Acta Biomater.* **2008**, *4*, 1646–1656. [CrossRef] [PubMed]
13. Gautieri, A.; Vesentini, S.; Redaelli, A.; Buehler, M.J. Hierarchical structure and nanomechanics of collagen microfibrils from the atomistic scale up. *Nano Lett.* **2011**, *11*, 757–766. [CrossRef] [PubMed]
14. Qin, X.X.; Coyne, K.J.; Waite, J.H. Tough tendons. Mussel byssus has collagen with silk-like domains. *J. Biol. Chem.* **1997**, *272*, 32623–32627. [CrossRef]
15. Tromp, G.; Kuivaniemi, H.; Stacey, A.; Shikata, H.; Baldwin, C.T.; Jaenisch, R.; Prockop, D.J. Structure of a full-length cDNA clone for the prepro alpha 1(I) chain of human type I procollagen. *Biochem. J.* **1988**, *253*, 919–922. [CrossRef] [PubMed]
16. Bhattacharjee, A.; Bansal, M. Collagen structure: The madras triple helix and the current scenario. *IUBMB Life* **2005**, *57*, 161–172. [CrossRef]
17. Long, C.G.; Braswell, E.; Zhu, D.; Apigo, J.; Baum, J.; Brodsky, B. Characterization of collagen-like peptides containing interruptions in the repeating Gly-X-Y sequence. *Biochemistry* **1993**, *32*, 11688–11695. [CrossRef] [PubMed]
18. Beck, K.; Chan, V.C.; Shenoy, N.; Kirkpatrick, A.; Ramshaw, J.A.M.; Brodsky, B. Destabilization of osteogenesis imperfecta collagen-like model peptides correlates with the identity of the residue replacing glycine. *Proc. Natl. Acad. Sci. USA* **2000**, *97*, 4273–4278. [CrossRef] [PubMed]
19. Van Robertson, W.B. The effect of ascorbic acid deficiency on the collagen concentration of newly induced fibrous tissue. *J. Biol. Chem.* **1952**, *196*, 403–408. [PubMed]
20. Yu, Z.; Mirochnitchenko, O.; Xu, C.; Yoshizumi, A.; Brodsky, B.; Inouye, M. Noncollagenous region of the streptococcal collagen-like protein is a trimerization domain that supports refolding of adjacent homologous and heterologous collagenous domains. *Protein Sci.* **2010**, *19*, 775–785. [CrossRef] [PubMed]
21. Xu, Y.; Keene, D.R.; Bujnicki, J.M.; Höök, M.; Lukomski, S. Streptococcal Scl1 and Scl2 proteins form collagen-like triple helices. *J. Biol. Chem.* **2002**, *277*, 27312–27318. [CrossRef] [PubMed]
22. Han, R.; Zwiefka, A.; Caswell, C.C.; Xu, Y.; Keene, D.R.; Lukomska, E.; Zhao, Z.; Höök, M.; Lukomski, S. Assessment of prokaryotic collagen-like sequences derived from streptococcal Scl1 and Scl2 proteins as a source of recombinant GXY polymers. *Appl. Microbiol. Biotechnol.* **2006**, *72*, 109–115. [CrossRef] [PubMed]
23. Lukomski, S.; Nakashima, K.; Abdi, I.; Cipriano, V.J.; Shelvin, B.J.; Graviss, E.A.; Musser, J.M. Identification and characterization of a second extracellular collagen-like protein made by group A Streptococcus: Control of production at the level of translation. *Infect. Immun.* **2001**, *69*, 1729–1738. [CrossRef] [PubMed]
24. Harrington, M.J.; Waite, J.H. PH-dependent locking of giant mesogens in fibers drawn from mussel byssal collagens. *Biomacromolecules* **2008**, *9*, 1480–1486. [CrossRef] [PubMed]
25. Bittencourt, D.; Oliveira, P.F.; Prosdocimi, F.; Rech, E.L. Review protein families, natural history and biotechnological aspects of spider silk. *Genet. Mol. Res.* **2012**, *11*, 2360–2380. [CrossRef] [PubMed]
26. Vollrath, F.; Knight, D.P. Liquid crystalline spinning of spider silk. *Nature* **2001**, *410*, 541–548. [CrossRef] [PubMed]
27. Lee, C.H.; Singla, A.; Lee, Y. Biomedical applications of collagen. *Int. J. Pharm.* **2001**, *221*, 1–22. [CrossRef]
28. Chattopadhyay, S.; Raines, R.T. Review collagen-based biomaterials for wound healing: Collagen-based biomaterials. *Biopolymers* **2014**, *101*, 821–833. [CrossRef] [PubMed]
29. Gibson, T. Evolution of catgut ligatures: The endeavours and success of Joseph Lister and William Macewen. *Br. J. Surg.* **1990**, *77*, 824–825. [CrossRef] [PubMed]
30. Fung, Y.-C. *Biomechanics*; Springer: New York, NY, USA, 1993.

31. Lee, S.; Hailey, D.M.; Lea, A.R. Tensile strength requirements for sutures. *J. Pharm. Pharmacol.* **1983**, *35*, 65–69. [CrossRef] [PubMed]
32. Siriwardane, M.L.; DeRosa, K.; Collins, G.; Pfister, B.J. Controlled formation of cross-linked collagen fibers for neural tissue engineering applications. *Biofabrication* **2014**, *6*, 015012. [CrossRef] [PubMed]
33. Zeide, D.A. Adverse reactions to collagen implants. *Clin. Dermatol.* **1986**, *4*, 176–182. [CrossRef]
34. Liscic, R.; Brinar, V.; Miklic, P.; Barsić, B.; Himbele, J. Creutzfeldt-Jakob disease in a patient with a lyophilized dura mater graft. *Acta Med. Croatica* **1999**, *53*, 93–96. [PubMed]
35. Sabeh, F.; Shimizu-Hirota, R.; Weiss, S.J. Protease-dependent versus -independent cancer cell invasion programs: Three-dimensional amoeboid movement revisited. *J. Cell Biol.* **2009**, *185*, 11–19. [CrossRef] [PubMed]
36. Piez, K.A.; Reddi, A.H. *Extracellular Matrix Biochemistry*; Elsevier Science Ltd.: New York, NY, USA, 1984.
37. Wu, X.; Black, L.; Santacana-Laffitte, G.; Patrick, C.W. Preparation and assessment of glutaraldehyde-crosslinked collagen–chitosan hydrogels for adipose tissue engineering. *J. Biomed. Mater. Res. A* **2007**, *81A*, 59–65. [CrossRef] [PubMed]
38. Bauman, L. CosmoDerm/CosmoPlast (human bioengineered collagen) for the aging face. *Facial Plast. Surg.* **2004**, *20*, 125–128. [CrossRef] [PubMed]
39. Fields, C.G.; Lovdahl, C.M.; Miles, A.J.; Hagen, V.L.; Fields, G.B. Solid-phase synthesis and stability of triple-helical peptides incorporating native collagen sequences. *Biopolymers* **1993**, *33*, 1695–1707. [CrossRef] [PubMed]
40. Li, M.H.; Fan, P.; Brodsky, B.; Baum, J. Two-dimensional NMR assignments and conformation of (Pro-Hyp-Gly)10 and a designed collagen triple-helical peptide. *Biochemistry* **1993**, *32*, 7377–7387. [CrossRef] [PubMed]
41. Cejas, M.A.; Kinney, W.A.; Chen, C.; Leo, G.C.; Tounge, B.A.; Vinter, J.G.; Joshi, P.P.; Maryanoff, B.E. Collagen-related peptides: Self-assembly of short, single strands into a functional biomaterial of micrometer scale. *J. Am. Chem. Soc.* **2007**, *129*, 2202–2203. [CrossRef] [PubMed]
42. Holmgren, S.K.; Taylor, K.M.; Bretscher, L.E.; Raines, R.T. Code for collagen's stability deciphered. *Nature* **1998**, *392*, 666–667. [CrossRef] [PubMed]
43. Goodman, M.; Bhumralkar, M.; Jefferson, E.A.; Kwak, J.; Locardi, E. Collagen mimetics. *Biopolymers* **1998**, *47*, 127–142. [CrossRef]
44. Bachmann, A.; Kiefhaber, T.; Boudko, S.; Engel, J.; Bächinger, H.P. Collagen triple-helix formation in all-trans chains proceeds by a nucleation/growth mechanism with a purely entropic barrier. *Proc. Natl. Acad. Sci. USA* **2005**, *102*, 13897–13902. [CrossRef] [PubMed]
45. Boudko, S.; Frank, S.; Kammerer, R.A.; Stetefeld, J.; Schulthess, T.; Landwehr, R.; Lustig, A.; Bächinger, H.P.; Engel, J. Nucleation and propagation of the collagen triple helix in single-chain and trimerized peptides: Transition from third to first order kinetics. *J. Mol. Biol.* **2002**, *317*, 459–470. [CrossRef] [PubMed]
46. Frank, S.; Boudko, S.; Mizuno, K.; Schulthess, T.; Engel, J.; Bächinger, H.P. Collagen triple helix formation can be nucleated at either end. *J. Biol. Chem.* **2003**, *278*, 7747–7750. [CrossRef] [PubMed]
47. Cai, W.; Wong, D.; Kinberger, G.A.; Kwok, S.W.; Taulane, J.P.; Goodman, M. Facile and efficient assembly of collagen-like triple helices on a TRIS scaffold. *Bioorg. Chem.* **2007**, *35*, 327–337. [CrossRef] [PubMed]
48. Kwak, J.; De Capua, A.; Locardi, E.; Goodman, M. TREN (Tris(2-aminoethyl)amine): An effective scaffold for the assembly of triple helical collagen mimetic structures. *J. Am. Chem. Soc.* **2002**, *124*, 14085–14091. [CrossRef] [PubMed]
49. Greiche, Y.; Heidemann, E. Collagen model peptides with antiparallel structure. *Biopolymers* **1979**, *18*, 2359–2361. [CrossRef]
50. Barth, D.; Kyrieleis, O.; Frank, S.; Renner, C.; Moroder, L. The role of cystine knots in collagen folding and stability, Part II. conformational properties of (pro-hyp-gly)n model trimers with N- and C-terminal collagen type III cystine knots. *Chem. Eur. J.* **2003**, *9*, 3703–3714. [CrossRef] [PubMed]
51. Boudko, S.P.; Engel, J.; Bächinger, H.P. The crucial role of trimerization domains in collagen folding. *Int. J. Biochem. Cell Biol.* **2012**, *44*, 21–32. [CrossRef] [PubMed]
52. Paramonov, S.E.; Gauba, V.; Hartgerink, J.D. Synthesis of collagen-like peptide polymers by native chemical ligation. *Macromolecules* **2005**, *38*, 7555–7561. [CrossRef]
53. Yamauchi, M.; Sricholpech, M. Lysine post-translational modifications of collagen. *Essays Biochem.* **2012**, *52*, 113–133. [CrossRef] [PubMed]

54. Hagenau, A.; Scheibel, T. Towards the recombinant production of mussel byssal collagens. *J. Adhes.* **2010**, *86*, 10–24. [CrossRef]
55. Fan, D. Proteine du Type Collagene Humain et Son Procede de Production. Patent WO2003106494A1, 24 December 2003.
56. Schnicker, N.J.; Dey, M. Bacillus anthracis prolyl 4-Hydroxylase modifies collagen-like substrates in asymmetric patterns. *J. Biol. Chem.* **2016**, *291*, 13360–13374. [CrossRef] [PubMed]
57. Schnicker, N.J.; Razzaghi, M.; Thakurta, S.G.; Chakravarthy, S.; Dey, M. Bacillus anthracis prolyl 4-hydroxylase interacts with and modifies elongation factor Tu. *Biochemistry* **2017**, *56*, 5771–5785. [CrossRef] [PubMed]
58. Tang, Y.; Yang, X.; Hang, B.; Li, J.; Huang, L.; Huang, F.; Xu, Z. efficient production of hydroxylated human-like collagen via the co-expression of three key genes in escherichia coli origami (DE3). *Appl. Biochem. Biotechnol.* **2016**, *178*, 1458–1470. [CrossRef] [PubMed]
59. Pozzolini, M.; Scarfì, S.; Mussino, F.; Salis, A.; Damonte, G.; Benatti, U.; Giovine, M. Pichia pastoris production of a prolyl 4-hydroxylase derived from Chondrosia reniformis sponge: A new biotechnological tool for the recombinant production of marine collagen. *J. Biotechnol.* **2015**, *208*, 28–36. [CrossRef] [PubMed]
60. Vuorela, A.; Myllyharju, J.; Nissi, R.; Pihlajaniemi, T.; Kivirikko, K.I. Assembly of human prolyl 4-hydroxylase and type III collagen in the yeast pichia pastoris: Formation of a stable enzyme tetramer requires coexpression with collagen and assembly of a stable collagen requires coexpression with prolyl 4-hydroxylase. *EMBO J.* **1997**, *16*, 6702–6712. [CrossRef] [PubMed]
61. Xu, J.; Wang, L.N.; Zhu, C.H.; Fan, D.D.; Ma, X.X.; Mi, Y.; Xing, J.Y. Co-expression of recombinant human prolyl with human collagen α1 (III) chains in two yeast systems. *Lett. Appl. Microbiol.* **2015**, *61*, 259–266. [CrossRef] [PubMed]
62. Báez, J.; Olsen, D.; Polarek, J.W. Recombinant microbial systems for the production of human collagen and gelatin. *Appl. Microbiol. Biotechnol.* **2005**, *69*, 245–252. [CrossRef] [PubMed]
63. Peng, Y.Y.; Yoshizumi, A.; Danon, S.J.; Glattauer, V.; Prokopenko, O.; Mirochnitchenko, O.; Yu, Z.; Inouye, M.; Werkmeister, J.A.; Brodsky, B.; et al. A Streptococcus pyogenes derived collagen-like protein as a non-cytotoxic and non-immunogenic cross-linkable biomaterial. *Biomaterials* **2010**, *31*, 2755–2761. [CrossRef] [PubMed]
64. Nowack, H.; Hahn, E.; Timpl, R. Specificity of the antibody response in inbred mice to bovine type I and type II collagen. *Immunology* **1975**, *29*, 621–628. [PubMed]
65. Kim, H.Y.; Kim, W.U.; Cho, M.L.; Lee, S.K.; Youn, J.; Kim, S.I.; Yoo, W.H.; Park, J.H.; Min, J.K.; Lee, S.H.; et al. Enhanced T cell proliferative response to type II collagen and synthetic peptide CII (255–274) in patients with rheumatoid arthritis. *Arthritis Rheum.* **1999**, *42*, 2085–2093. [CrossRef]
66. Davison, P.F.; Levine, L.; Drake, M.P.; Rubin, A.; Bump, S. The serologic specificity of tropocollagen telopeptides. *J. Exp. Med.* **1967**, *126*, 331–346. [CrossRef] [PubMed]
67. Bentkover, S. The biology of facial fillers. *Facial Plast. Surg.* **2009**, *25*, 73–85. [CrossRef] [PubMed]
68. Peng, Y.Y.; Stoichevska, V.; Howell, L.; Madsen, S.; Werkmeister, J.A.; Dumsday, G.J.; Ramshaw, J.A.M. Preparation and characterization of monomers to tetramers of a collagen-like domain from Streptococcus pyogenes. *Bioengineered* **2014**, *5*, 378–385. [CrossRef] [PubMed]
69. Parmar, P.A.; St-Pierre, J.-P.; Chow, L.W.; Puetzer, J.L.; Stoichevska, V.; Peng, Y.Y.; Werkmeister, J.A.; Ramshaw, J.A.M.; Stevens, M.M. Harnessing the versatility of bacterial collagen to improve the chondrogenic potential of porous collagen scaffolds. *Adv. Healthc. Mater.* **2016**, *5*, 1656–1666. [CrossRef] [PubMed]
70. Peng, Y.Y.; Stoichevska, V.; Vashi, A.; Howell, L.; Fehr, F.; Dumsday, G.J.; Werkmeister, J.A.; Ramshaw, J.A.M. Non-animal collagens as new options for cosmetic formulation. *Int. J. Cosmet. Sci.* **2015**, *37*, 636–641. [CrossRef] [PubMed]
71. Peng, Y.Y.; Glattauer, V.; Ramshaw, J.A.M. Stabilisation of collagen sponges by glutaraldehyde vapour crosslinking. *Int. J. Biomater.* **2017**, *2017*. [CrossRef] [PubMed]
72. Golser, A.; Roeber, M.; Boerner, H.; Scheibel, T. Engineered collagen—A redox switchable framework for tunable assembly and fabrication of biocompatible surfaces. *ACS Biomater. Sci. Eng.* **2017**. [CrossRef]
73. Hamaia, S.; Farndale, R.W. Integrin recognition motifs in the human collagens. *Adv. Exp. Med. Biol.* **2014**, *819*, 127–142. [PubMed]

74. Woltersdorf, C.; Bonk, M.; Leitinger, B.; Huhtala, M.; Käpylä, J.; Heino, J.; Gil Girol, C.; Niland, S.; Eble, J.A.; Bruckner, P.; et al. The binding capacity of α1β1-, α2β1- and α10β1-integrins depends on non-collagenous surface macromolecules rather than the collagens in cartilage fibrils. *Matrix Biol. J. Int. Soc. Matrix Biol.* **2017**, *63*, 91–105. [CrossRef] [PubMed]
75. Zeltz, C.; Orgel, J.; Gullberg, D. Molecular composition and function of integrin-based collagen glues-introducing COLINBRIs. *Biochim. Biophys. Acta* **2014**, *1840*, 2533–2548. [CrossRef] [PubMed]
76. Zeltz, C.; Gullberg, D. The integrin-collagen connection—A glue for tissue repair? *J. Cell Sci.* **2016**, *129*, 653–664. [CrossRef] [PubMed]
77. Werten, M.W.T.; Teles, H.; Moers, A.P.H.A.; Wolbert, E.J.H.; Sprakel, J.; Eggink, G.; de Wolf, F.A. Precision gels from collagen-inspired triblock copolymers. *Biomacromolecules* **2009**, *10*, 1106–1113. [CrossRef] [PubMed]
78. Silva, C.I.F.; Teles, H.; Moers, A.P.H.A.; Eggink, G.; de Wolf, F.A.; Werten, M.W.T. Secreted production of collagen-inspired gel-forming polymers with high thermal stability in Pichia pastoris. *Biotechnol. Bioeng.* **2011**, *108*, 2517–2525. [CrossRef] [PubMed]
79. Beun, L.H.; Storm, I.M.; Werten, M.W.T.; de Wolf, F.A.; Cohen Stuart, M.A.; de Vries, R. From micelles to fibers: balancing self-assembling and random coiling domains in ph-responsive silk-collagen-like protein-based polymers. *Biomacromolecules* **2014**, *15*, 3349–3357. [CrossRef] [PubMed]
80. Waite, J.H.; Qin, X.X.; Coyne, K.J. The peculiar collagens of mussel byssus. *Matrix Biol. J. Int. Soc. Matrix Biol.* **1998**, *17*, 93–106. [CrossRef]
81. Qin, X.-X.; Waite, J.H. A potential mediator of collagenous block copolymer gradients in mussel byssal threads. *Proc. Natl. Acad. Sci. USA* **1998**, *95*, 10517–10522. [CrossRef] [PubMed]
82. Coyne, K.J.; Qin, X.X.; Waite, J.H. Extensible collagen in mussel byssus: A natural block copolymer. *Science* **1997**, *277*, 1830–1832. [CrossRef] [PubMed]
83. Lucas, J.M.; Vaccaro, E.; Waite, J.H. A molecular, morphometric and mechanical comparison of the structural elements of byssus from Mytilus edulis and Mytilus galloprovincialis. *J. Exp. Biol.* **2002**, *205*, 1807–1817. [PubMed]
84. Schmidt, S.; Reinecke, A.; Wojcik, F.; Pussak, D.; Hartmann, L.; Harrington, M.J. Metal-mediated molecular self-healing in histidine-rich mussel peptides. *Biomacromolecules* **2014**, *15*, 1644–1652. [CrossRef] [PubMed]
85. Ravindranath, M.H.; Ramalingam, K. Histochemical identification of dopa, dopamine and catechol in the phenol gland and the mode of tanning of byssus threads of Mytilus edulis. *Acta Histochem.* **1972**, *42*, 87–94. [PubMed]
86. Waite, J.H. The phylogeny and chemical diversity of quinone-tanned glues and varnishes. *Comp. Biochem. Physiol. Part B* **1990**, *97*, 19–29. [CrossRef]
87. Golser, A.V.; Scheibel, T. Biotechnological production of the mussel byssus derived collagen preColD. *RSC Adv.* **2017**, *7*, 38273–38278. [CrossRef]
88. Heim, M.; Elsner, M.B.; Scheibel, T. Lipid-specific β-sheet formation in a mussel byssus protein domain. *Biomacromolecules* **2013**, *14*, 3238–3245. [CrossRef] [PubMed]
89. Hagenau, A.; Suhre, M.H.; Scheibel, T.R. Nature as a blueprint for polymer material concepts: Protein fiber-reinforced composites as holdfasts of mussels. *Prog. Polym. Sci.* **2014**, *39*, 1564–1583. [CrossRef]
90. Bairati, A.; Vitellaro Zuccarello, L. The ultrastructure of the byssal apparatus of Mytilus galloprovincialis: IV. Observations by transmission electron microscopy. *Cell Tissue Res.* **1976**, *166*. [CrossRef]
91. Zuccarello, L.V. The collagen gland of mytilus galloprovincialis: An ultrastructural and cytochemical study on secretory granules. *J. Ultrastruct. Res.* **1980**, *73*, 135–147. [CrossRef]
92. Suhre, M.H.; Scheibel, T. Structural diversity of a collagen-binding matrix protein from the byssus of blue mussels upon refolding. *J. Struct. Biol.* **2014**, *186*, 75–85. [CrossRef] [PubMed]
93. Suhre, M.H.; Gertz, M.; Steegborn, C.; Scheibel, T. Structural and functional features of a collagen-binding matrix protein from the mussel byssus. *Nat. Commun.* **2014**, *5*, 3392. [CrossRef] [PubMed]
94. Hagenau, A.; Papadopoulos, P.; Kremer, F.; Scheibel, T. Mussel collagen molecules with silk-like domains as load-bearing elements in distal byssal threads. *J. Struct. Biol.* **2011**, *175*, 339–347. [CrossRef] [PubMed]
95. Koski, M.K.; Anantharajan, J.; Kursula, P.; Dhavala, P.; Murthy, A.V.; Bergmann, U.; Myllyharju, J.; Wierenga, R.K. Assembly of the elongated collagen prolyl 4-hydroxylase α2β2 heterotetramer around a central α2 dimer. *Biochem. J.* **2017**, *474*, 751–769. [CrossRef] [PubMed]
96. Marumo, K.; Waite, J.H. Prolyl 4-hydroxylase in the foot of the marine mussel Mytilus edulis L.: purification and characterization. *J. Exp. Zool.* **1987**, *244*, 365–374. [CrossRef] [PubMed]

97. Wei, W.; Yu, J.; Broomell, C.; Israelachvili, J.N.; Waite, J.H. Hydrophobic enhancement of dopa-mediated adhesion in a mussel foot protein. *J. Am. Chem. Soc.* **2013**, *135*, 377–383. [CrossRef] [PubMed]
98. Montroni, D.; Valle, F.; Rapino, S.; Fermani, S.; Calvaresi, M.; Harrington, M.J.; Falini, G. Functional biocompatible matrices from mussel byssus waste. *ACS Biomater. Sci. Eng.* **2017**. [CrossRef]
99. Butt, T.R.; Edavettal, S.C.; Hall, J.P.; Mattern, M.R. SUMO fusion technology for difficult-to-express proteins. *Protein Exp. Purif.* **2005**, *43*, 1–9. [CrossRef] [PubMed]

12 Versicherungen und Erklärungen

(§ 9 Satz 2 Nr. 3 PromO BayNAT)

Hiermit versichere ich eidesstattlich, dass ich die Arbeit selbstständig verfasst und keine anderen als die von mir angegebenen Quellen und Hilfsmittel benutzt habe (vgl. Art. 64 Abs. 1 Satz 6 BayHSchG).

(§ 9 Satz 2 Nr. 3 PromO BayNAT)

Hiermit erkläre ich, dass ich die Dissertation nicht bereits zur Erlangung eines akademischen Grades eingereicht habe und dass ich nicht bereits diese oder eine gleichartige Doktorprüfung endgültig nicht bestanden habe.

(§ 9 Satz 2 Nr. 4 PromO BayNAT)

Hiermit erkläre ich, dass ich Hilfe von gewerblichen Promotionsberatern bzw. -vermittlern oder ähnlichen Dienstleistern weder bisher in Anspruch genommen habe noch künftig in Anspruch nehmen werde.

(§ 9 Satz 2 Nr. 7 PromO BayNAT)

Hiermit erkläre ich mein Einverständnis, dass die elektronische Fassung meiner Dissertation unter Wahrung meiner Urheberrechte und des Datenschutzes einer gesonderten Überprüfung unterzogen werden kann.

(§ 9 Satz 2 Nr. 8 PromO BayNAT)

Hiermit erkläre ich mein Einverständnis, dass bei Verdacht wissenschaftlichen Fehlverhaltens Ermittlungen durch universitätsinterne Organe der wissenschaftlichen Selbstkontrolle stattfinden können.

……
Ort, Datum, Unterschrift